The role of Adenylate Kinase 2 in thymic epithelial cell development and function

Inauguraldissertation
zur
Erlangung der Würde eines Doktors der Philosophie
vorgelegt der
Philosophisch-Naturwissenschaftlichen Fakultät
der Universität Basel

von

Lucas Musette

Basel 2022

Genehmigt von der Philosophisch-Naturwissenschaftlichen Fakultät

auf Antrag von

Prof. Dr. Georg Andreas Holländer

Prof. Dr. Christoph Hess

Dr. Klaus Schwarz

Basel, den 20. September 2022

Prof. Dr. Marcel Mayor
Dekan

"We shall come to regard the presence of lymphocytes in the thymus as an evolutionary accident of no very great significance"

Peter Medawar, 1960 Nobel Laureate in Physiology or Medecine

Table of Contents

Acknowledgements

"A tout Seigneur tout honneur", I would like to express my deepest gratitude to Professor Georg Holländer without whom this thesis would not exist. I could never thank him enough for putting his trust in me to take care of this nice and challenging project. His time and energy to shape a more global, logical and critical thinking will be precious tools that I will use for rest of my life. Furthermore, his diligence and his encyclopaedic knowledge regarding immunology are inspiring qualities for the scientist I would like to be. Being a member of his lab during the last 4 years has been an honour and a privilege.

A special gratitude goes to Doctor Saulius Žuklys for its supervision all along my PhD. Many of my improvements can be attributed to him, his kindness and our conversations regarding this or that project. I hope his eyesight did not deteriorate too much from reading all my reports in "franglais"! But it has been a pleasure to work with him.

I would like also to thank Doctor Thomas Barthlott and Doctor Irene Calvo for their inputs on my projects, nice moments we could share together between 2 gipfelis and a piece of boo-boo cake. Another big thanks to Katrin Hafen and Elli Christen for their manual and emotional support during the three years we could share together.

As a thesis without co-PhD would be like long stay at monastery, I would like to thank Doctor Veysel Kaya (a.k.a the goat) for being such a good friend during all my time here in Basel. I enjoyed to be "your dad" and to make you discover the supremacy of Belgian zythology. Thanks also to my comrades Anja Kusch and Julian Behr for their help and friendship, and for supporting my puns (in both senses).

I would also like to acknowledge my PaC committee members: Professor Christoph Hess and Doctor Klaus Schwarz. Thank you for your valuable inputs throug my thesis and your opinion as experts of the field.

Among people who helped me directly or indirectly with this project, I would like to thanks Doctor Gaël Auray for the help with the FACS; Blanco Ilda and Rees Sylvie for their

support with the lab material and solutions; Angelika Offinger and Emilia Terszowska for their work at animal facility.

And then, I would like to thank any member of my family, especially my mum, as well as friends in and outside of Basel, for all their support throughout this journey. A special thought for Lilia, Hayley, Madhuri, Adelin, Natalia, Mali, Julia, Alois, my former colleagues of the DBM PhD club, we did a good job and I had a great pleasure to do it with you !

This doctoral thesis is dedicated to Pan-pan.

List of abbreviations

2-DG	2-deoxyglucose
AAO	Amino acid oxidation
ADP	Adenosine diphosphate
AIRE	Autoimmune regulator
AK2	Adenylate Kinase 2
AMP	Adenosine monophosphate
AMPK	AMP-activated protein kinase
APC	Antigen presenting cell
ATP	Adenosine triphosphate
BCR	B cell receptor
BrdU	Bromodeoxyuridine
CCR#	C-C chemokine receptor #
CCL#	Chemokine (C-C motif) ligand #
CD#	Cluster of differentiation #
cFbs	Capsular fibroblasts
CK#	Cytokeratin #
CMJ	Cortico-medullary junction
cTEC	Cortical TEC
DC	Dendritic cell
DLL4	Delta-like 4
DN#	Double negative #
DNA	Deoxyribonucleic acid
DP	Double positive
ECM	Extra-cellular matrix
EMT	Epithelial-mesenchymal transition
ETC	Electron transport chain
ETP	Early thymic progenitor
FACS	Fluorescent activated cell sorting
FAO	Fatty acid oxidation
FCCP	carbonyl cyanide 4-(trifluoromethoxy)phenylhydrazone
FoxN1	Forkhead Box N1
FSC-W	Forward scatter width
FTOC	Foetal thymic organ cultures
IFN-γ	Interferon gamma
Ig#	Immunoglobulin #
iPSCs	Induced pluripotent stem cells
GSH	Glutathione in reduced state
M#	Mature #
MedFI	Median fluorescence intensity
mFbs	Medullary fibroblasts
MHC#	Major histocompatibility complex #
mtDNA	Mitochondrial DNA
mTEC	Medullary TEC
NAC	N-acetyl-L-cystein
NCC	Neural crest cells
OLI	Oligomycin A

OXPHOS	Oxidative phosphorylation
PAMP	Pathogen-associated molecular pattern
pAMPK	Phosphorylated AMPK
PCR	Polymerase chain reaction
PD-1	Programmed cell death protein
PI	Puromycin incorporation
PRR	Pattern recognition receptor
PS	Protein synthesis
RAG	Recombination activating gene
RANK	Receptor activator of nuclear factor κB
RANK-L	RANK-ligand
RD	Reticular Dysgenesis
RNA	Ribonucleic acid
RNAseq	RNA sequencing
ROS	Reactive oxygen species
RTOC	Reaggregate thymic organ culture
RT-qPCR	Quantitative reverse transcription PCR
SA	Streptavidin
scRNAseq	Single-cell RNAseq
SIRT1	Silent mating-type information regulation 2 homolog 1
SM	Semi-mature
SP4	Single positive CD4
SP8	Single positive CD8
TCA	Tricarboxylic acid
TCR	T-cell receptor
TEC	Thymic epithelial cell
TFAM	Transcriptional Factor A Mitochondrial
Th#	Helper T cell #
TNF	Tumor necrosis factor
TRA	Tissue-restricted antigens
UEA-1	Ulex Europaeus Agglutinin 1

Abstract

Reticular Dysgenesis (RD) is a genetic immunodeficiency characterised by severe neutropenia, lymphopenia, thymic and secondary lymphoid organ hypoplasia associated with a high risk for fatal septicaemia within days after birth. RD is caused by a loss of function of the Adenylate Kinase 2 (*AK2*), an enzyme mainly localised in the mitochondrial intermembrane space that generates ADP via the transfer of a phosphate from ATP to AMP. The only treatment of RD's haematological pathology is a bone marrow transplant that results in generation of donor-derived peripheral T cells. However, the functional capacity of these cells and the thymopoïetic competence of AK2-deficient stromal cells have never been investigated in detail.

The thymus provides a highly organised environment where hematopoietic early thymic progenitors (ETP) differentiate into naïve T-cells. Thymic epithelial cells (TEC) which constitute the major stroma cell type, are essential for this function. Based on morphological, gene expression and functional characteristics, TEC are differentiated into cortical (c) and a medullary (m) epithelial cells. cTEC attract blood-borne ETP, induce their specification to the T-cell lineage, foster their early development and survival and shape their T-cell receptor (TCR) repertoire, together with mTEC thus eliminating thymocytes with a high receptor specificity to self- antigens. To investigate the role of AK2 in TEC function and development, a mouse model lacking *Ak2* in a TEC-restricted fashion has been generated.

AK2-deficient mice displayed hypoplastic thymi that correlated with a lower cellularity. Within TEC population, mTEC of knockout mice were severely decreased, resulting in a centrally positioned medulla containing keratin-free zones filled with fibroblasts. Mutant mice also displayed an abundant subpopulation of TEC lacking classical cortical and medullary markers that showed molecular features of immature cTEC. Loss of AK2 affected the energy metabolism of TEC and resulted in an enhanced mitochondrial superoxide content. The augmentation of reactive oxygen species (ROS) contributed to the reduction of mTEC in mutant mice and was likely involved in the increase of number of mitochondria in AK2-deficient cTEC and immature mTEC subpopulations. Thymopoïetic function is negatively affected by the loss of AK2: lower recruitment of T cell progenitors, decreased progression across beta-selection, reduced positive and negative selection and diminished post-selection maturation. Impairment of thymopoïesis resulted in T cell lymphopenia but did not induce overt autoimmunity in mutant mice. Taken together, this work demonstrates that AK2 plays a crucial role in TEC development and function.

1. Introduction

1.1 Immunity

Immunity is one of the greatest tools that evolution provides to living organisms to defend themselves against pathogens. Improved by hundreds of millions of years of natural selection[1], immune system protects from threats as small as adeno-associated virus (±25 nm)[1] to parasites as large as *Ascaris lumbricoides* (females reaching 20-35 cm in length)[2]. The diversity of pathogens requires a collection of mechanisms to recognize and eliminate potential threats. For that purpose, a sophisticated network of cells, molecules and pathways were selected and kept over generations. This system of defence is called immune system and is highly regulated. Indeed, an excessive inflammatory response can cause systemic or regional damages to the host sometimes leading to the death[3]. On the other hand, organisms with a low immune system response are more susceptible to infectious diseases which are fought with less efficiency[4]. Individuals with such health conditions are then more prone to premature death.

The immune system can be divided into 2 different branches: adaptive and innate immunity.

The innate immune system is the body's first line of defence against germs entering the body. It responds to foreign substances (e.g. bee stinger, toxin...) and germs (e.g. bacteria, yeast...) but doesn't necessitate previous exposition to get efficiently triggered. The innate immune system is composed of the protection offered by mechanical and chemical barriers, antimicrobial proteins and immune cells such as mast cells, neutrophils, eosinophils, basophils, monocytes and macrophages.

The adaptative immune system is the second line of defence that generates immune memory from encounters with pathogens, enabling a faster and more robust response in case of re-exposure later on. This mechanism is at the basis of vaccination and is mediated by bursa-derived lymphocytes (B cells) and thymus-derived lymphocytes (T cells).

1.1.1 *Innate immunity*

Anatomic (e.g. skin, mucous membranes...) and chemical barriers (e.g. acidity of the stomach content,...) are the initial defences to prevent the entrance of pathogens into the

organism. Additional resistance mechanisms can be generated at anatomic barriers such as production of antimicrobial peptides (e.g. defensins) to strengthen host defence.

If these barriers are ruptured or evaded, pathogen will encounter the immune cells of innate immunity such as eosinophils, neutrophils, natural killer cells (NK cells), macrophages and dendritic cells (DC). Innate immune cells possess extra and intracellular pattern recognition receptors (PRRs) that detect components of foreign pathogens referred as pathogen-associated molecular patterns (PAMPs) and initiate cellular immune response. PAMPs that trigger PRRs include lipopolysaccharides from bacterial walls, double-stranded RNA (dsRNA) from viruses or molecules such as adenosine trisphosphate (ATP), which is not normally found in the extracellular space. Triggered, innate immune cells initiate phagocytosis of pathogens and their following elimination, or start to produce and release pro-inflammatory signalling proteins to propagate and enhance inflammatory response[5].

In addition, a non-cellular mechanism of defence supports the innate immunity. Known as "complement system", this system is a group of plasmatic and membrane-associated serum proteins which activate a cascade of proteolytic reactions which result in the end to the lysis or phagocytosis of pathogen or the production of proinflammatory molecules[6].

Although the innate immune system can rapidly detect and effect the elimination of a wide range of pathogens, the array of PAMPs it can recognize is limited. The overwhelming variability of antigenic structures, as well as the ability of pathogens to mutate to avoid host detection, has driven the evolution of the adaptive immune system[7].

1.1.2 *Adaptive immunity*

In contrast to PRR of the innate immune system, which are all encoded fully functional in the genome, receptors of adaptive immune system developed in jawed vertebrates are custom tailored[7]. Receptors result from a process of somatic recombination of a large array of gene segments that generate unique antigen recognition receptor. After exposure to pathogens, cells expressing immune receptors recognizing antigens of this pathogen will proliferate, clear the pathogen and for some persist in the host for a certain time, generating immunologic memory and the capacity for a faster response in case of re-exposure.

Adaptive immunity is carried out by two lymphocyte subsets: B cells and T cells. Both arise from a common haematopoietic stem cell population localised is the bone marrow but their antigen receptors, their role in the immune system as well as their organs of maturation

differ. Stem cells released in the circulatory system can enter the thymus and develop into mature T cells while stem cells remaining in the bone marrow can initiate their differentiation into B cells which is then terminated in the spleen. After maturation, lymphocytes T traffic to secondary lymphoid organs, including lymph nodes and the spleen, which serve to capture circulating antigens from lymph and blood, respectively, and consequently generate an immune response[7].

In case of encounter with the cognate antigen of the B cell receptor (BCR), B cells proliferate and differentiate into plasma cells. These generate and secrete antibodies that will recognise the same antigen as BCR since the genes encoding BCR are the same than those encoding antibodies. Antibodies are Y-shaped molecules that can neutralize viruses or mark pathogens or their product to eliminate them by phagocytosis or complement system.

While B cells are responsible of the humoral part of the immunity (humoral immunity), with the secretion of antibodies in the plasma of blood, T cells mediate the immunity based on cell-cell interactions (cell-mediated immunity). The receptor responsible of these interactions is the T cell receptor (TCR), a protein complex composed of an αß or γδ heterodimer, two CD3 dimers and a ζζ dimer[8]. TCR do not bind antigens themselves but to their shorter fragments presented at the surface of cells by proteins known as major histocompatibility complex (MHC). TCR:MHC interactions in αß T cells are stabilized by additional co-receptors which separate them into two functionally different subsets: T helper cells expressing CD4 (SP4) and cytotoxic T cells expressing CD8 (SP8). While CD8 binds to a region of MHC class I (MHCI), CD4 recognizes a region of MHC class II (MHCII).

SP8 kill cells infected with viruses. Infected cells present antigens derived from the virus via MHCI. Then, SP8 recognizing foreign antigen displayed by MHCI release perforin to generate holes in the cells and granzyme to induce apoptosis. Like this, SP8 can limit the spread of infection by directly killing the infected cell before the release of virions. Because MHCI are expressed on most cells of the body, with the exception of red blood cells, this mechanism represents an important system of defence against infections. SP8 can also release pro-inflammatory cytokines such as interferon gamma (IFN-γ) or tumour necrosis factor (TNF).

SP4 aid or repress immune response through a myriad of different subpopulations. After recognition of foreign antigen presented by MHCII expressed by antigen presenting cells (APC) of immune system (e.g. macrophages, dendritic cells, B cells), SP4 can differentiate into 3 main supporting subsets of helper T cells (Th) expressing each different cytokines: Th1, Th2

and Th17. Th1 express IFN-γ and TNF-α to activate macrophages and eliminate intracellular pathogens (bacteria, viruses or protozoans). Th2 express chemokines such as IL-4, IL-5 or IL-13 to attract and activate basophiles, eosinophils and mast cells to protect organism against extracellular parasites (e.g. helminths) but also mediate allergies through the production of immunoglobulin E (IgE) by B cells. TH17 express IL-17 to induce nearby stromal and epithelial cells to release chemokines that recruit neutrophils and IL-22 to stimulate along with IL-17 the production of antimicrobial peptides by epithelial cells. SP4 can also differentiate into 2 additional subtypes: T follicular helper (Tfh) and T regulatory (Treg). Tfh recognize foreign antigen presented by MHCII of B cells and induce their proliferation and differentiation into antibody-producing plasma cells. Tregs are inhibitory cells that supress innate immune cells and T cells activity to prevent the risk of autoimmunity and damages caused to the organism by a too strong immune response.

1.2 Thymus

The thymus is the primary lymphoid organ where lymphoid progenitors develop into mature T cells.

The thymus is constituted of 2 lobes and is located above the heart in the upper chest (Figure **1**). In human, rat and rabbit but not in mouse, connective tissue from capsule invaginates in the lobes to form lobules. Lobes or lobules display 2 main distinct areas: the cortex, an outer lymphocyte-rich region where thymocytes, developing T cells when they are in the thymus, begin their maturation[9], and the medulla, the inner and less dense region where thymocytes finish their maturation. Cortex and medulla are separated by a region known as cortico-medullary junction (CMJ) which is enriched in blood vessels from which progenitors enter and seed the thymus. In human, thymus grows from birth until it reaches its highest weight and then begins to shrink in the period of adolescence[10].

Development of thymocytes into mature T cells depend on interactions with several types of stromal cells such as epithelial cells, fibroblasts, macrophages, and dendritic cells. Cortical and medullary thymic epithelial cells (cTEC and mTEC respectively) and fibroblasts form a highly organized three-dimensional network to allow lymphocyte trafficking and interactions[11,12]. Communication between thymocytes and TECs is bi-directional since these interactions also mediate the development of cTEC[13] and mTEC[14,15].

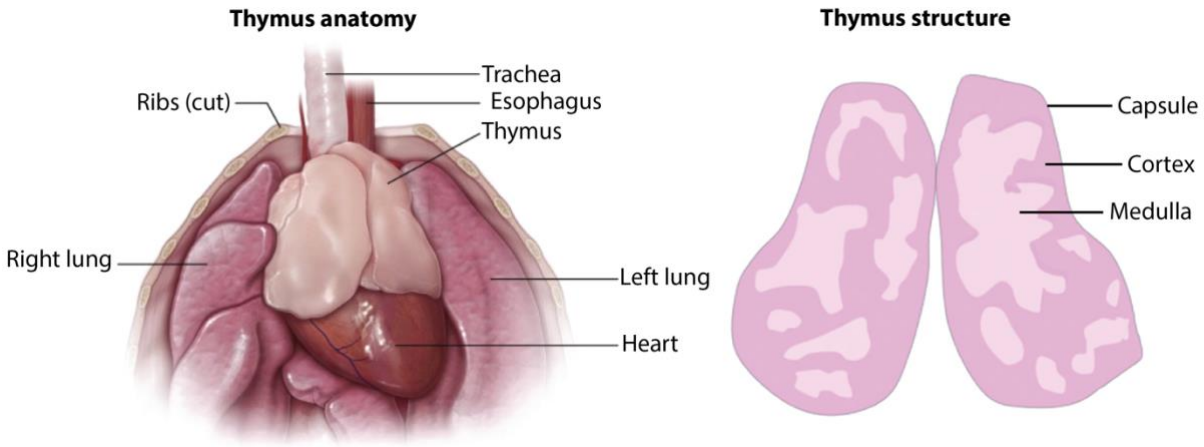

Figure 1: Schematic representation of murine thymus anatomy and structure.

Murine thymus is anatomically localized in central compartment of thorax cavity, above the heart and behind the sternum of thoracic cage. Thymus from mouse is bilobed and each of this lobe is divided into an outer region known as cortex (dark pink) and an inner layer known as medulla (light pink). Cortex is limited by a fibroblastic capsule.

Schemes adapted from Linden et al.[16] and Nitta et al.[17]

1.2.1 *Murine thymus ontogeny and TEC heterogeneity*

The thymus and the parathyroid glands are derived from a common primordium (earliest stage of development of an organ). At E9.5, the common primordium evaginates from the pharyngeal endoderm in the third pharyngeal pouch[18]. Twelve hours later, the ventral domain of the common rudiment starts to express Forkhead Box N1 (Foxn1), while future parathyroid cells expression Glial cells missing homolog 2 (Gcm2). FOXN1 is a transcription factor expressed by thymic epithelial cells (TEC) and epithelial cells from skin. FOXN1 regulates the proliferation and the differentiation of TEC and so the maintenance of thymus, its reduction of expression has been coupled with the thymic involution. From embryonic day 11.5 (E11.5), common rudiment is gradually separated from the pharynx with the support of surrounding neural crest cells (NCC) until its complete detachment the day after. From E12.5, thymic tissue separates from parathyroid glands and thymic lobes descent to the midline (Figure **2**).

The next phase of thymic organogenesis depends on the interplay between different cell types which involves NCC, endothelial cells, mesenchymal cells, TEC but also hematopoietic cells, first and foremost maturing thymocytes. The first lymphoid progenitors enter the thymus

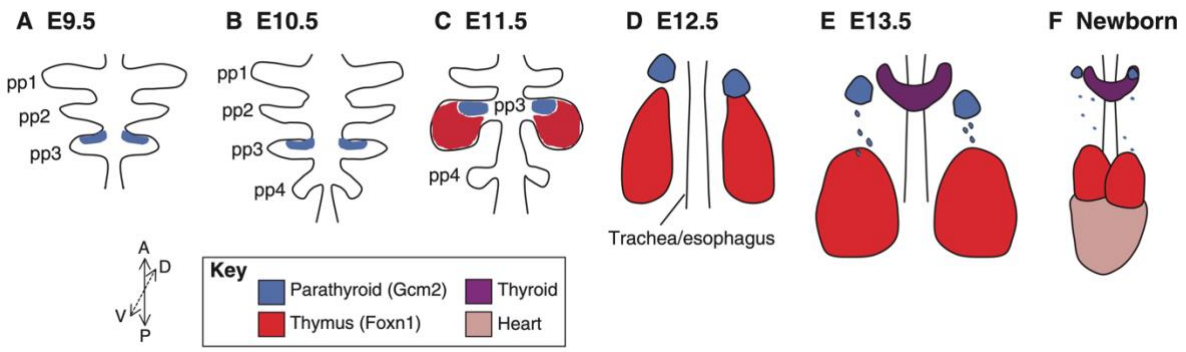

Figure 2: Schematic of thymus development from E9.5 to birth.

Third pharyngeal pouch (3PP) evaginates from endodermal gut tube at embryonic day 9.5 (E9.5). Gcm2 expression (blue) marks the future parathyroid glands. From E11.5, future thymic lobes express FOXN1 (red) and start their detachment. At E12.5, thymic primordia have detached from trachea/oesophagus and parathyroid glands have started to detach from thymic lobes to join the thyroid (purple) and be adjacent to it by E13.5. At birth, the two thymic lobes are joined and are positioned above the heart (pink).

Schema adapted from Gordon and Manley[18].

primordium around E11.5 via the capsule of developing organ as thymus anlage is still avascular at this age[19]. Another major input of new T cell precursors with higher efficiency for T cell generation occurs between day 12 and 14 post coitus[20]. These precursors are crucial for further thymus growth since thymocyte-TEC crosstalk supports cTEC development[13] and their three-dimensional organization[21], a prerequisite for the development of the thymic medulla. In absence of these progenitors, thymus remain small, without medulla and develop cysts. Interactions with thymocytes are also essential for the generation and maturation of mTEC that are confidently detected around E13.5[22,23]. Among molecules involved in these interactions, we find multiple members of tumour necrosis factor receptor superfamily (TNFRSF) including receptor activator of nuclear factor κB (RANK), CD40 and lymphotoxin ß receptor (LTßR)[24–26]. Stimulation *ex vivo* of these receptors with their respective ligands (e.g. RANK-L) or with antibody, even in absence of thymocytes, induce mTEC development[24].

After the formation of a primordial epithelial scaffold, TEC differentiate into 2 functionally and anatomically separate lineages: cTEC and mTEC.

cTEC are localised in the cortical region of the thymic lobe and can be phenotypically distinguished using several extra-and intracellular markers such as glutamyl aminopeptidase (Ly51 a.k.a CD249), cytokeratin 8 (CK8) or lymphocyte antigen 75 (Ly75 a.k.a CD205 or DEC-205). In addition, 2 main subpopulations of cTEC can be phenotypically identified based

on their level of expression for Sca-1 and MHCII: cTEC^{lo} (cTEC Sca-1^{pos} MHCII^{low}) and cTEC^{hi} (cTEC Sca-1^{neg} MHCII^{high}). Besides that, Shakib et al.[27] identified an embryonic developmental progression of cTEC that can be followed using CD40 and CD205: from a progenitor expressing none of these markers (CD40^{neg} CD205^{neg}), cTEC then express CD205 (CD40^{neg} CD205^{pos}) prior upregulation of CD40 (CD40^{pos} CD205^{pos}). Developmental block at double negative stage (CD40^{neg} CD205^{neg}) observed in nude mice demonstrated that this maturation program is mediated by FOXN1 expression.

Thymic cortex attracts progenitors and mediates their commitment to T cell fate through Notch signalling via Delta-like 4 (DLL4). Cortical epithelium also mediates ß-selection, a process which selects CD4^{neg}CD8^{neg} thymocytes (DN thymocytes) that successfully rearranged their TCRß chain which then undergo a proliferative burst and continue their developmental progression[28]. cTEC are also responsible for inducing TCR-mediated positive selection through presentation of self-antigen by MHCI or MHCII. During this step of development, immature CD4^{pos}CD8^{pos} thymocytes (DP thymocytes) expressing a sufficient level of affinity/avidity for self-peptide-MHC complexes receive a survival signal and then follow their maturational development while others die by "neglect"[29]. Recent work[30] showed that cTEC^{hi} are more stringent in positive selection in comparison to cTEC^{lo}. The predominance of cTEC^{hi} subset in juvenile mice limit the generation of auto-reactive T cells clones with a competitive advantage against T cell with lower TCR avidity at an age when T cell pool is still fully expanding[31]. Moreover, cortical epithelium participates to the negative selection, also known as clonal deletion, a process eliminating thymocytes with too high affinity/avidity for self-antigens[29].

mTEC are localised in the medullary region of the thymic lobe and can be identified by different markers such as cytokeratin 14 (CK14), mouse thymic stroma 10 (MTS10) or the binding of Ulex Europaeus Agglutinin 1 (UEA1). Immature, mature and terminally differentiated mTEC can be distinct using markers such as Sca-1, MHCII and CD80[32,33]: Immature mTEC are CD80^{neg} MHCII^{low} Sca-1^{pos}, mature mTEC are CD80^{pos} MHCII^{high} Sca-1^{neg} and terminally differentiated mTEC are CD80^{neg} MHCII^{low} Sca-1^{neg}. Mature mTEC can be further divided based on CD86 or autoimmune regulator (AIRE) expression.

Medullary epithelium is responsible for the second wave of negative selection and the last steps of thymocyte maturation. Diversity of the body's self-antigens is mainly presented by a subset mTEC expressing AIRE[34]. AIRE is a transcriptional regulator binding to specific marks of inactive chromatin[35,36], enabling the expression of tissue-restricted antigens (TRA) normally not expressed in thymic epithelial cells. Lack of this transcription factor in human

and mouse results in the development of autoimmune disorders[34]. In addition to mTEC, additional cell types such as dendritic cells or fibroblasts support the negative selection[26,27]. By convention, negative selection occurring earlier in the cortex and is designated as "wave 1" in comparison to cells undergoing negative selection in the medulla designated as "wave 2". Thymocytes subjected to wave 1 upregulate the programmed cell death protein 1 (PD-1) and transcription factor Helios whereas SP4 subjected to wave 2 upregulate Helios but hardly induce PD-1[37]. SP8 are also subjected to negative selection[38] but markers that would identify SP8 undergoing negative selection, similarly to Helios/PD-1, have not been reported so far. Apoptosis of thymocytes is induced by upregulation of the pro-apoptotic molecule BCL-2-interacting mediator of cell death (Bim) through TCR:MHC interactions[29].

Despite substantial progresses, the identities and developmental dynamics of pre and postnatal TEC progenitors remains unclear[39]. Several lineage-tracing studies demonstrated that embryonic and postnatal mTEC originate from a TEC population expressing cTEC features[40–42]. However, mTEC may originate from different populations of progenitors that change over time. The development of high-throughput single-cell sequencing and sequencing-based lineage-tracing technologies may uncover more precisely the developmental history of TEC[43]. Recently, a study combining RNA sequencing (RNAseq) and cellular barcoding with CRISPR-Cas9 system claimed that cTEC and mTEC originate from two bipotent progenitor populations[44]: an early progenitor population mainly present prenatally with a bias towards cTEC development, and a postnatal population with a mTEC bias. This last is closely related to intertypical TEC subtype previously identified by Baran-Garan et al[33].

1.2.2 *Intrathymic thymocyte development*

Maturational development of T cells can be separated into distinct stages based on expression of cell-surface markers. Lymphoid progenitors migrate from the foetal liver[20,45] to the thymus through the capsule when thymus is avascular (prenatal) then from the bone marrow via blood after the establishment of intrathymic blood circulation (between E14.5 and E15.5)[46]. Key signal for the recruitment of progenitors is given by chemokines, cytokines that drive the attraction of cells possessing receptors (chemoattraction). Among them, C-C motif chemokine ligand 19 (CCL19), 21 (CCL21) and 25 (CCL25) were shown to orchestrate the thymus seeding by T-lymphoid progenitors at pre- and post-vascular stage[47,48]. Indeed, the knocking-out of C-C chemokine receptor 7 (CCR7), receptor of CCL19 and CCL21, the knocking-out

CCR9, receptor of CCL25, or antibody neutralization of CCL21 or CCL25 flaw thymus colonization[47–49].

Upon entry, lymphoid progenitors become qualified as early thymic progenitors (ETPs). The subsequential developmental progression can be followed using CD117 (a.k.a c-kit), CD44, CD25 and CD71 markers[50,51]. Because thymocytes express neither CD4 nor CD8 coreceptors of TCR in the first steps of their development, they are referred as DN (double negative) thymocytes. The most immature population DN1 (also sometimes referred as ETP) can be identified by the co-expression of c-kit and CD44. After specification to the T cell lineage upon engagement of Notch 1 with DLL4 on cTEC[52], they upregulate CD25 and become DN2. Afterwards, cells begin to express recombination activating genes 1 or 2 (Rag1 and Rag2) to rearrange the ß locus of their TCR if following αβ lineage or γ and δ loci if following γδ lineage. Transition from DN2 to DN3a is observed by the downregulation of CD44 and c-kit. Then occur a crucial developmental checkpoint named ß-selection that allows only for thymocytes that successfully rearranged their ß-chain to develop further. Indeed, during the "VDJ recombination" mediated by RAG nucleases, genome is randomly and irremediably shortened to generate a unique combination of variable (V), diversity (D) and joining (J) segments[53]. Randomness of this process can generate thymocytes with unfunctional TCR sequences (e.g. out-of-frame or early stop codon) that are purged by ß-selection. DN3a that successfully passed ß-selection undergo a proliferative expansion and start to express CD71 to become DN3b. Then, thymocytes continue their maturation by downregulation of CD25 to develop into DN4. Subsequently, these cells continue their maturational progression with first the expression CD8 (CD8 immature single positive, CD8ISP) and then expression of CD4 to become double positive (DP) thymocytes.

The newly generated DP thymocytes rearrange the α-chain of the TCR to generate at the surface of the cell a heterodimeric αβTCR which forms a complex with two CD3 dimers and a ζζ dimer[8]. To select future T cells possessing an appropriate avidity/affinity for MHC:peptide complexes, DP thymocytes have to pass through selection processes mediated by APCs. The first of them is the positive selection, a process during which DP thymocytes with a TCR binding to self-antigen presented by MHCI or MHCII with a sufficient strength receive a survival signal while others die by neglect. Majority of DP thymocytes (±85%) do not receive survival signal and undergo apoptosis[54]. At the opposite, thymocyte binding to antigen:MHC complexes too strongly will also be eliminated to limit the risk of developing self-reactive T cells[55]. This second process, known as negative selection, is continued and

terminated in the medulla. Positively selected thymocytes gradually transition from DP to single positive (SP) with various intermediate stages and the physical migration from cortex to the medulla. In more detail, DP thymocytes start to express CD69[56], increase TCR expression but decrease CD4 and CD8 expression[57] before upregulation of CD4 (intermediate $CD4^{high}$ $CD8^{low}$ stage)[58]. After this stage, thymocytes will be separated into two lineages: whether they become SP4 ($CD4^{high}$ $CD8^{neg}$) or they become SP8 ($CD4^{neg}$ $CD8^{high}$). Although processes deciphering the lineage remain debated, the model encompassing them the best is the "kinetic signalling model". After downregulation of CD8, thymocytes with a remaining TCR signal through CD4:MHCII interactions will follow the differentiation program of SP4. Otherwise, if the TCR signal ceases, they will follow the SP8 differentiation.

First SP4 (designated semi-mature; SP4 SM) are localised in the cortex since they lack the expression of CCR7 to get attracted to the medulla by CCL19 and CCL21 expressed by mTEC. By flow cytometry, SP4 SM are identified as SP4 $CD24^{pos}$ $CCR7^{neg}$. In the medulla, first mature SP4 (SP4 M1) competent for cytokine production and proliferation are positive for CCR7, CD24 and CD69[59]. Thereafter, these cells downregulate CD24 and CD69 to progress further in maturation (SP4 M2) with an improved cytokine production and proliferation capacity. Similarly to SP4, the different stages of development of SP8 (SM, M1 and M2) can also be identified based on the expression CD24, CD69 and CCR7. But at the opposite of SP4, SP8 are exclusively localised in the medulla[60].

During their journey in the medulla, thymocytes pass through a second wave of negative selection initiated in the cortex. SP cells encounter mTEC expressing and presenting a variety of peripheral tissue self-antigens and those with a too high affinity/avidity for the antigen are eliminated. Thymic dendritic cells also participate to the negative selection by cross-presentation of mTEC-derived self-antigens[61] or innocuous peripheral self-antigens[62]. In addition to mTEC and dendritic cells, B cells also contribute to negative selection[63]. Another mechanism of protection against the production of over-reactive T cells is the generation of Treg, a subset of CD4 T cells with an immuno-suppressive function generated in the thymus from thymocyte with a higher avidity/affinity for self-antigens than conventional positively selected cells[64].

After completion of developmental process, mature thymocytes escape the thymus to join the peripheral T cell pool as naïve but functional T cells (Figure **3**).

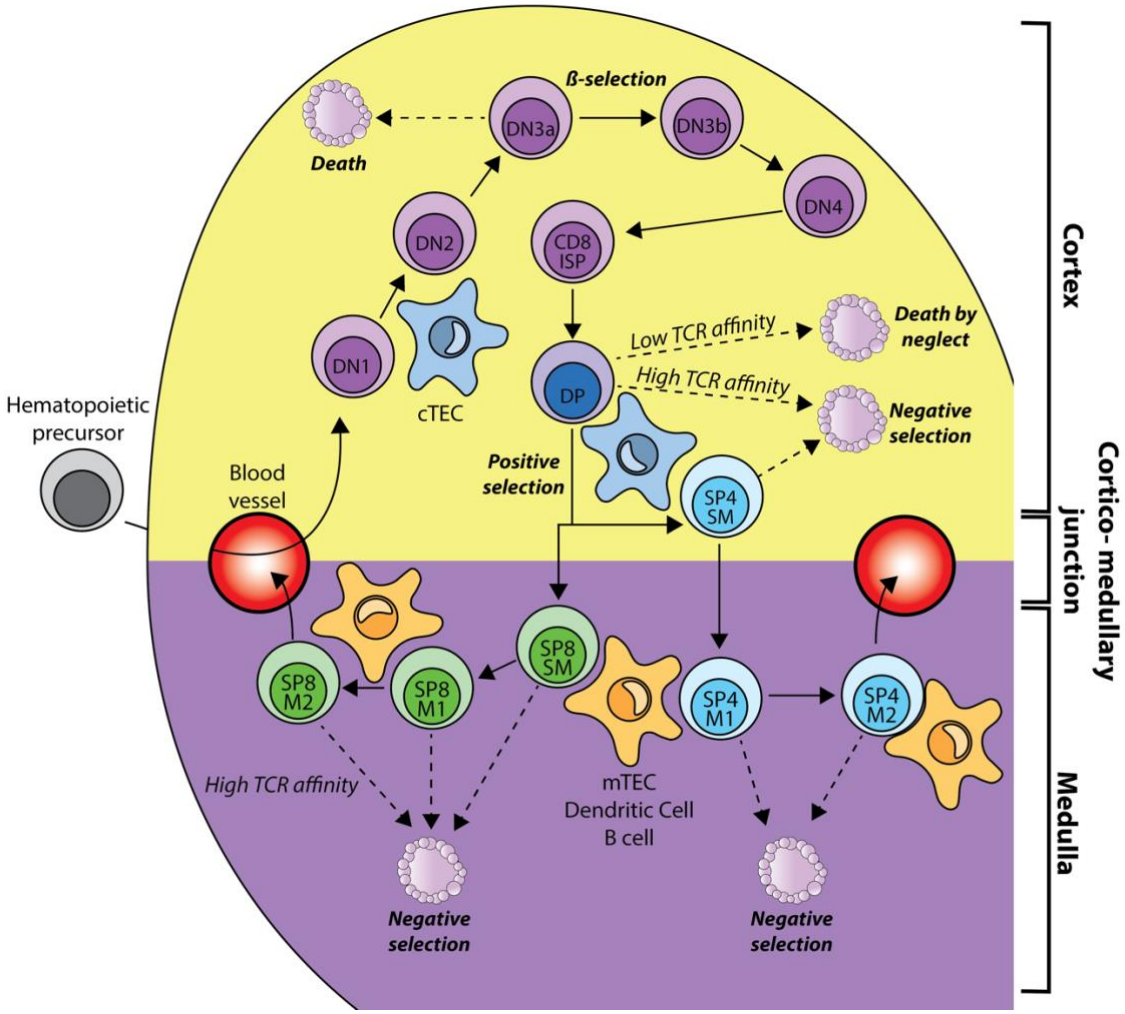

Figure 3: Intrathymic thymocyte maturation.

Hematopoietic progenitors migrate from the periphery to the thymus through the blood vessels of the cortico-medullary junction guided by chemokines. To develop into fully mature T cells, precursors have to pass through several steps of selection during which cells expressing a potential deleterious or useless TCR are eliminated. Most immature stage of thymocyte is identified by the absence of co-receptor CD4 and CD8 at the surface (termed as double negative, DN). During this stage, thymocytes that successfully rearranged the ß-chain of the TCR will develop from DN3a to DN3b (**ß-selection**). Later, co-receptors start to be expressed, first CD8 (CD8ISP; CD8 immature single positive) then CD4 (DP; double positive) and pre-TCR α-chain is replaced with a newly rearranged TCR α-chain, which yields a complete αβ TCR. At this stage, fate of DP thymocytes depends on signalling that is mediated by interactions between TCR complex (TCR+co-receptors) and MHC of cTEC presenting self-antigens. Thymocytes with a sufficient avidity/affinity for antigen:MHC complexes receive a survival signal allowing further maturational progression (positive selection) while others are eliminated (**death by neglect**). In parallel, thymocytes displaying a too high affinity/avidity are eliminated from TCR repertoire to avoid the development of auto-reactive T cells (**negative selection**). Then, thymocytes downregulate one of the co-receptor (SP4 or SP8; single positive CD4 or CD8), specify into CD4 and CD8 lineage and migrate to the medulla where another step of negative selection is mediated by mTECs, B cells and dendritic cells. After a semi-mature stage (SM), SP thymocytes become fully mature and competent (M1-M2) prior escaping the thymus to join the periphery via blood vessels.

1.3 Reticular dysgenesis

Reticular dysgenesis (RD) is an autosomal recessive disorder caused by an absence of functional adenylate kinase 2 (AK2) due to a variety of mutations that all manifest themselves as a severe combined immunodeficiency[65,66].

Thymic hypoplasia correlating with profound T lymphopenia and absence of significant lymphoid or tonsillar tissue together with agranulocytosis constitute the typical immunological hallmarks of RD and provide a cellular explanation for the disease's characteristic clinical presentation of e.g. sepsis[67,68]. In addition to these typical features, RD patients can also develop autoimmunity: two patients have been reported to present clinical features of Omenn Syndrome[68,69] and another one developed autoimmune haemolytic anaemia[70]. The immunodeficiencies can lead to premature death within weeks after birth. The only curative treatment for the immunological aspects of RD is an allogeneic haematopoietic stem cells transplantation (HSCT) with an overall survival of 68%[68]. The donor-derived de novo generation of T cells following HSCT is robust and grants patients to get an immune system responsive to vaccination[68]. However, HSCT do not cure non-haematological defects such as sensorineural hearing defects and the formation of keloid during wound healing[71,72]. A bone marrow transplant is not necessary when a partial preservation of AK2 enzyme activity remains (e.g. hypomorphic variants) to maintain sufficient T cell proliferation and differentiation capacities to fight opportunistic infections[70].

1.3.1 *Adenylate kinase 2*

Adenine nucleotide homeostasis is essential to assure diverse biological processes including cellular proliferation, differentiation or apoptosis. As constituents of RNA and DNA first, but also as donors of phosphate groups in living organisms[73]. Indeed, chemical energy is transmitted through high-energy phosphate groups primarily carried by ATP. ATP synthesis occurs either through oxidative phosphorylation (OXPHOS) or substrate-level phosphorylation (glycolysis)[74]. Glycolysis is a cytoplasmic pathway that generates 2 ATP per molecule of glucose while OXPHOS takes place in the mitochondria and generates 15 times more ATP than glycolysis[75]. If OXPHOS is much more efficient in terms of amount of ATP produced per molecule of glucose, glycolysis produces ATP at a faster rate[76].

Adenylate kinase 2 (AK2) is a phosphotransferase located in the mitochondrial intermembrane space and that regulates intracellular ATP levels by catalysing the reversible transfer of a phosphate group in the reaction of ATP + AMP ↔ 2 ADP[77,78]. AK2 is constituted of 3 essential domains: the phosphate-binding loop (P-loop), a nucleoside monophosphate binding domain (NMP-binding site) and a LID-domain[79]. P-loop is attributed to ATP binding, the NMP-binding site to AMP binding while the LID domain moves towards the NMP-binding site and initiates the transfer of the phosphate group[65] (Figure **4**). Human AK2 exists in two splicing variants: isoform A consisting of 239 amino acids and isoform B consisting of 232 amino acids, shorter at the C-terminal region[65]. Whether variants differ in enzymatic activity, subcellular localization or additional cellular function remains unknown[65].

In addition to its kinase activity, AK2 can directly regulate apoptosis and proliferation. AK2 bound to Fas-Associated protein with Death Domain (FADD) can get associated with caspase-10 to mediate an amplification of apoptotic signal in Hela and Jurkat cells[80]. On the other hand, AK2 is a co-activator of DUSP26 (Dual-specificity phosphatase 26) which regulates cell proliferation by dephosphorylation of FADD[81]. Authors of both studies suggest that the nucleotide kinase activity of AK2 is unlikely involved in the process but rather suppose that AK2 favours interactions with other co-factors/substrates.

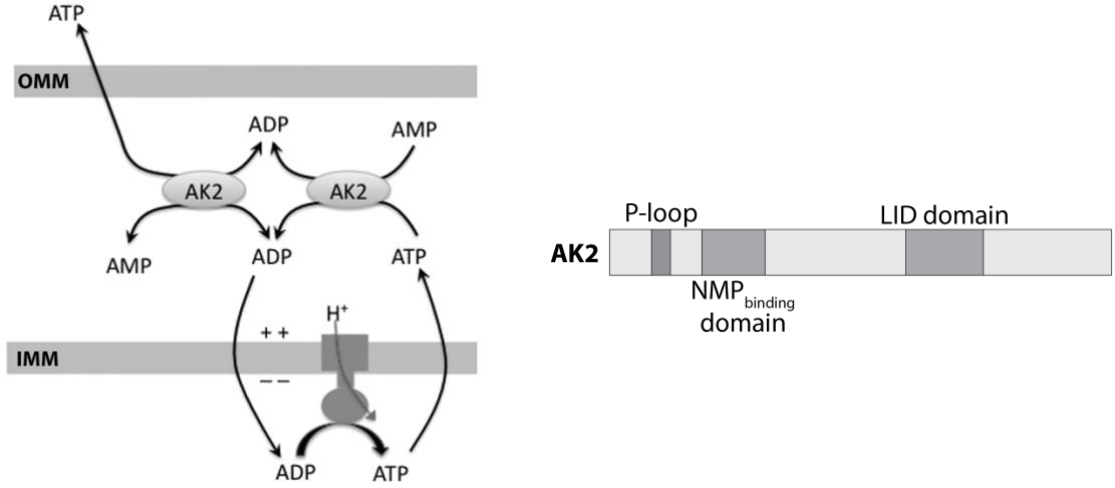

Figure 4: Adenylate kinase 2 cellular localization and structure.

Left: Adenylate kinase 2 (AK2) is localized in the intermembrane membrane of the mitochondria. AK2 catalyses the reversible reaction ATP+AMP ↔ 2 ADP. Afterwards, generated ADP molecules serve as substrate for ATP synthase of electron transport chain. OMM: outer mitochondrial membrane; IMM: inner mitochondrial membrane. Right: AK2 is composed of 3 essential domains. The phosphate-binding loop (P-loop), the nucleoside monophosphate binding domain (NMP-binding site) and the LID domain (dark grey regions). While ATP binds to P-loop and AMP binds to NMP-binding site, LID domain moves towards the NMP-binding site to initiate the transfer of phosphate group between ATP and AMP.

Figure at left is adapted from Burkart et al.[78]

1.3.2 *Pathophysiology of AK2-deficiency in vivo and in vitro*

AK2 is essential for the growth of some insects. Fruit fly (*D.melanogaster*) with genetic homozygous deficiency of *Dak2* (orthologous *AK2* in fruit fly) arrests development at third instar larva stage[82]. AK2 knockdown in larvae of *H.armigera* by RNA interference represses larval growth and development through downregulation of growth and developmental genes while its epidermal cell line (HaEpi) supplemented with AK2 display promoted cell growth and viability[83].

Overall early embryonic development of zebrafish (*D.rerio*) is not altered by knockdown of *ak2* by morpholinos[67]. But developing lymphocytes were absent in *ak2* morphants despite immature hematopoietic cells nor erythropoiesis remaining unaffected, indicating a specific leukocyte developmental defect. Analysis of hematopoietic tissue also revealed a block of myeloid development attributed to an enhanced cell death consecutive to increased reactive oxygen species (ROS) levels, possibly as a consequence of impaired ADP/ATP recycling[67,84]. The phenotype can be partially rescued in embryos by antioxidant treatment with N-acetyl-L-cystein (NAC), glutathione at reduced state (GSH) or its derivate. GSH treatment also rescues partially hair cell numbers in the inner ear of *ak2* mutant zebrafishes[85].

Similarly to observations made in zebrafish, fibroblasts from RD patients reveal an increased level of ROS and apoptosis[67]. Directed myeloid differentiation of induced pluripotent stem cells (iPSCs) derived from RD patients recapitulate the promyelocyte maturation attested in zebrafish and in RD patients[84]. However, antioxidant treatment with GSH partially rescues the differentiation. Because quantification of nucleotide content of these derived myeloid cells revealed an decreased amount of ADP skewed towards AMP[84], authors concluded that ADP shortage, substrate for ATP synthase, impairs cellular respiration, leading to a rise of membrane potential followed by an increased oxidative stress.

Bone marrow progenitors from RD patients display impaired capacity of T and NK lymphoid differentiation[77]. AK2 knocked-down progenitors from cord blood (CBP) reveal an defective T cell and NK cell-directed differentiation capacity and a decreased membrane potential 3 days after initiation differentiation[77]. Similarly, granulocyte-directed differentiation is impaired by AK2-deficiency[77]. More, AK2-deficient HL60 cells (promyelocytic leukemia cells) show a decreased capacity of neutrophile differentiation associated to a compromised energy metabolism[77]. This last result agreed with the decreased expression of transcripts related to mitochondrial function in AK2-deficient CBP undergoing T cell differentiation. Regarding

energy metabolism, fibroblasts from RD patient displayed an impaired respiration associated with an increased mitochondrial mass, membrane potential and mitochondrial superoxide production[86]. In addition, B cells expressing hypomorphic AK2 variants also show impaired maximal mitochondrial respiration with a decreased mitochondrial quality after stimulation of oxidative phosphorylation metabolism with anti-CD40 +IL-21 or by infection by Epstein-Barr virus[70].

The constitutive absence of AK2 in mice (*M.musculus*) results in embryonic lethality at about embryonic day 7[81,87]. Hematopoietic-specific (Vav-Cre) AK2-deficient mouse model recently generated at Ulm University[88] displayed embryonic mortality between E13 and E15 due to severe anaemia, confirming similar markedly reduced potential of AK2-deficient iPSCs to give rise to erythrocyte colonies[84]. Moreover, foetal liver cells isolated from AK2-knockout embryos cannot differentiate into pre-B-cells after IL-7 stimulation.

The diversity of consequences among AK2-deficient systems, leading sometimes to contradictory results[67,80], suggests species- and tissue-specific differences as to the enzyme's essential role in multiple functions.

2. Overall objective of the thesis

RD patients with successful bone marrow transplant can mount immune responses to pathogens or vaccination. However, the quantity and quality of these T cells, generated in a microenvironment where thymic epithelial cells remain AK2-deficient, has never been tested in detail. The *de novo* generation of T cells indicates that thymopoïetic function is maintained to a certain degree but the process' efficiency and quality remain to be investigated.

In addition to the clinical interest of this research, there is a growing body of literature that recognises the importance of energy metabolism in cell development and function, a field of research that has been poorly explored for TEC.

The experimental work presented here addresses the objective to delineate the role of AK2 in TEC function and development.

For that purpose, we generated a mouse model lacking functional *Ak2* in a TEC-restricted fashion.

3. Material and methods

3.1 Mouse model and manipulation

3.1.1 *Mouse model*

The generation of mice expressing Cre recombinase in thymic epithelial cells under the control of Foxn1 regulatory elements (Foxn1-Cre) has been previously reported[89]. Floxed *Ak2* mouse line with 2 floxed *Ak2* alleles ($Ak2^{fl/fl}$) was generously provided by Klaus Schwarz. These two lines were crossed to generate mice lacking AK2 expression in TEC ($Ak2^{fl/fl}$::Foxn1-Cre; designated TEC^{AK2KO}). Littermates negative for the Cre transgene were used as control ($Ak2^{fl/fl}$, designated TEC^{AK2WT}). All animals were kept under specific pathogen-free conditions and experiments were carried out in accordance with local and national regulations and permissions. Mice were euthanized by CO2 inhalation and decapitation.

3.1.2 *Genotyping*

Toes from ±10 days old mice were clipped and digested at 56°C for several hours or overnight in *lysis buffer* prior dilution in distilled water (ratio 1:1). 1 µL of lysate was added to *PCR reaction mix* prior PCR amplification in Mastercycler pro (Eppendorf). PCR programs used in this project are the following ones:

Cre PCR

94°C	4 mins	1X
94°C	30 sec	34X
58°C	30 sec	
72°C	1 min	
72°C	10 mins	1X

Ak2 flox/flox PCR

95°C	3 mins	1X
95°C	15 sec	35X
60°C	15 sec	
72°C	10 sec	
72°C	2 mins	1X

10 µL of PCR products were mixed with 2 µL of Gel Loading Buffer + GelRed Nucleic Acid Gel Stain (Biotium), loaded in a 1.5% agarose TAE gel and electrophoresed for 25 mins at 80V. Separated DNA bands were visualized on UV with GelDoc XR (Biorad).

3.1.3 *Timed mating*

At least 2 days before planned timed mating, one male and two females were put in the same cage for accommodation but separated by a grid to avoid uncontrolled mating. Grid was removed in late afternoon at timed mating day and the presence of vaginal plug was checked the morning after. Plug positive females were considered at gestational age 0.5 (embryonic day 0.5 for the embryo).

3.2 Microscopy

3.2.1 *Cryosectioning*

Organs were surgically removed and were put in a cryo-mold with OCT (Cell Path). The mold was placed superficially on 2-methylbutane (Sigma-Aldrich) cooled with dry ice to solidify the OCT. The frozen organs were sectioned (8 µm sections) on a Leica cryostat and dried overnight at room temperature (RT) or for 2 hours if immediate usage.

3.2.2 *Hematoxylin-Erythrosin staining*

Organs tissue sections were fixed in Delanay's Solution (50 seconds); rehydrated in gradient ethanol solutions (100/96/70/50 %) (1 minute each) then in distillate water (1 minute); stained with Mayers Hematoxylin solution (Merck KGaA) (3 minutes) and Erythrosin B 1% (RAL diagnostics) (40 seconds) with a wash (3x1 minute) in warm water after each stain; dehydrated in gradient ethanol solutions (50/70/96/100 %) (1 minute each) dried at room temperature (+- 20 minutes) then a coverslip was mounted on the slide with Entellan Néo (Merck KGaA). Images were acquired using Eclipse E600 (Nikon) or motorized Axio Imager 2 (Zeiss).

3.2.3 *Histopathological examination*

Liver, pancreas, eyes, stomach, thyroid and salivary glands from 32-38-week-old mice were embedded, sectioned and stained accordingly to sections 3.2.1 and 3.2.2. Histopathological examination assessing the presence of lymphocytic infiltration and disruption of tissue integrity was performed with motorized Axio Imager 2 (Zeiss) microscope. The scores of severity for each animal were evaluated using a semi-quantitative scoring similar to that used by Abdelmageed et al[90]. Severity was graded from 0 to 3: 0=healthy tissue; 1=visible but small lymphocytic infiltrates; 2=medium-size lymphocytic infiltrates and/or disruption of histological integrity 3=large infiltrates and/or severe disruption of histological integrity. Evaluation was performed blind to genotype to avoid biases.

3.2.4 *Immunofluorescence*

Thymic tissue sections were fixed/permeabilised in acetone (Sigma-Aldrich) for 10 mins at RT and quickly dried. Samples were circled using Super Pap Pen (Daido Sangyo) prior rehydration in PBS (2x5 mins) at RT. Tissue sections were blocked with 5% goat serum (GS) in PBS 30 mins at RT. Then samples incubated with primary antibodies diluted in 5% GS solution overnight at 4°C in a wet chamber. The day after, samples were incubated with secondary antibodies for 40 mins at RT prior nucleus staining with DAPI solution for 10 mins at RT. Sections were then embedded in Hydromount (National Diagnostics) prior acquisition or storage. Images were acquired with Visitron Spinning Disk Confocal (Nikon) or Leica DMI8 (Leica).

3.2.5 *Autoantibodies screening*

Blood was collected from aged mice (32-38 weeks of age) by cardiac puncture. Serum was separated from blood cells/clots by using Microtainer tubes SST (BD). Liver, eyes, stomach, thyroid, pancreas and salivary gland from Rag2-knockout mice ($Rag2^{-/-}$) were surgically removed and sections were made as per subsection 3.2.1. Sections were dried and encircled with Pap Pen prior blocking with 5% GS for 20 mins at RT in wet chamber. Then aged mice sera diluted in 5% GS solution (1:20 and 1:50), serum from $Rag2^{-/-}$ mice (negative control) or anti-nuclear antibody (positive control) were added to slides and incubated 1H at

RT in wet chamber. Secondary anti-mouse IgG conjugated was then added to each section and incubated for 30 mins at RT in wet chamber. Afterwards, nuclei were stained with DAPI prior embedding with Hydromount and acquisition with motorized Axio Imager 2. The scores of autoantibodies were evaluated using a semi-quantitative scoring based on negative and positive controls (0=signal obtained with serum of Rag2-deficient mice; 3=signal obtain with anti-nuclear antibody). Evaluation was performed blind to genotype.

3.2.6 *Electron Microscopy*

Transmission electron microscopy was performed at BioEM Lab (Biozentrum - Universität Basel). 800,000 TEC were sorted and mixed with an equivalent cell number of red blood cells (RBC) and centrifuged to generate a pellet. RBC were added to TEC to increase pellet's size and facilitate the manipulation. Cells were fixed in EM fixative solution and incubated for 20 mins at RT. Then fixative solution was replaced twice with fresh one with 15 mins of incubation after each replacement. The pellet was dislodged with a tip and flipped to expose the other side to fixative solution. After 30 mins of incubation at 4°C, pellet was washed 3 times (5 mins per wash) with 0.1M PIPES buffer pH 7.0-7.2. At BioEM Lab, sample was embedded in resin and thin sections were photographed with 120 kV Tecnai G2 Spirit transmission electron microscope (FEI).

3.3 Flow cytometry

3.3.1 *Thymic stromal cell isolation*

Thymi were surgically removed, cleaned of fat and connective tissues, punctured with forceps (for the phenotyping of TEC over time in figure **5**) or cut in 2mm cuboids and then transferred into a tube containing 1mL of collagenase D (1 mg/mL; Roche) or Liberase (200 µg/mL; Roche) solutions containing DNAse I (20 µg/mL; Roche). Collagenase was used when liberase-sensitive markers (e.g. CD205, podoplanin...) were used. Papain (0.5 mg/mL) was also added to Liberase for experiments necessitating higher proportions of TEC (e.g. sorting, metabolic analysis by flow-cytometry...). Tissue pieces were subsequently incubated at 37°C for 15 mins and then gently broken up by pipetting, and again incubated for another 15 mins

before a next round of pipetting to disaggregate cells into a single cell suspension. The cells were then transferred to a FACS tube containing 2 mL of IMDM plus Glutamax (Life technologies) + 5 mM EDTA (Invitrogen) solution, on ice, before adding FACS buffer and centrifugation. Afterwards, cells were resuspended in FACS buffer and counted using Z1 Particle Counter (Beckmann Coulter).

3.3.2 *Thymocyte, splenocyte and lymph node cell isolation*

Thymi, spleen or lymph nodes were surgically removed and kept in FACS buffer on ice. Cell suspension was then prepared by physical disruption of the tissue in FACS buffer using sheets of 100 µm Sefar Nitex nylon mesh (Sefar AG). Cell suspension was kept on ice and cellularity was counted using Z1 Particle Counter (Beckmann Coulter).

3.3.3 *Enrichment of TEC by immunomagnetic separation*

Fraction of TEC in thymic digests were enriched using AutoMACS Pro (Miltenyi Biotec). Depending on the experiment, TEC were either enriched via retaining of TEC (positive selection program; POSSEL) or retaining of thymocytes (depletion program; DEPLETE). For POSSEL, digested samples were incubated with biotinylated EpCAM antibody on ice for 10 mins, incubated with anti-biotin microbeads (Miltenyi Biotec) for 15 mins at 4°C and then enriched via POSSEL program. The TEC-enriched fraction (second one) is collected in IMDM+10% FCS. For DEPLETE, digested samples were incubated with CD45 microbeads (Miltenyi Biotec) for 15 mins at 4°C, filtered through 100 µm nylon mesh to retain particles that may clog the machine, DNAse I (100 µg/mL) was added to cell suspension to avoid cell agglomeration and thymocytes were depleted via DEPLETE program. The thymocyte-depleted fraction (first one) is collected in IMDM+10% FCS.

3.3.4 *Staining for flow cytometry*

Cell suspensions were first incubated at 37°C for 15-30 mins with antibodies (e.g. CCR7) or probes (e.g. Mitotracker) requiring this temperature of incubation. Then, samples were incubated on ice for 20 mins with remaining antibodies targeting extracellular proteins, filtered through 100 µm nylon mesh and resuspended in DAPI and acquired on LSRFortessa

(BD).

For experiments necessitating intracellular staining, samples are incubated with Zombie dye in PBS prior fixation/permeabilization using eBioscience FOXP3 / transcription factor staining buffer set (Invitrogen) or Cytofix/CytoPerm (BD) on ice. Then cells were blocked with 5% GS or mouse serum (home-made) prior staining with antibodies on ice or at RT for 1H or overnight at 4°C. After a second round of labelling with secondary antibodies or streptavidin, cells are filtered through 100 µm nylon mesh and acquired on LSRFortessa (BD).

3.3.5 *Cell proliferation analysis by flow cytometry*

Cell proliferation was assessed detection by flow cytometry of bromodeoxyuridine (BrdU) incorporated in newly synthesized DNA of cells entering and progressing through the S phase of cell cycle. For 3-4-week-old mice, 2x1mg BrdU in PBS was injected intraperitoneally (4 hours interval) 18 hours prior to TEC isolation. For embryos, 2 mg of BrdU was injected into pregnant mice and embryos were collected 4 hours later. BrdU incorporation was analyzed by flow cytometry using BrdU Flow Kit according to manufacturer's protocol (BD).

3.3.6 *Cell sorting*

After enrichment and staining, cells were sorted on FACS Aria II (BD) through 70 µM nozzle into 1.5 mL Eppendorf tubes containing PBS, IMDM+Glutamax or lysis buffer (RNeasy Plus Micro Kit; Qiagen). Cell purity was evaluated after sorting for each sample (minimum 85%). If not used immediately, cells were flash-frozen in liquid nitrogen and stored at -80°C.

3.4 Real-time quantitative PCR

RNA was extracting from sorted cells using RNeasy Plus Micro Kit (Qiagen) according to manufacturer protocol.

For the synthesis of cDNA, 14 µL of RNA were mixed with 1 µL of dNTP 10 mM (Sigma-Aldrich), 1 µL of dT20 (Microsynth) and 1 µL of random hexamers 500 ng/µL (Sigma-Aldrich). The mix was incubated at 65°C for 5 mins prior incubation on ice for 1 minute. Then 1 µL of 10 mM DTT (Invitrogen), 1µl of RNase out (Invitrogen), 1µl of Superscript III RT

200U/µL (Invitrogen) and 5 µL of 5X first strand buffer (Invitrogen) were added and the mix incubated in Mastercycler gradient (Eppendorf) for 5 mins at 25°C, 60 mins at 50°C and finally 15 mins at 70°C. Generated cDNA was stored at -20°C until further processed.

Real-time quantitative PCR (RT-qPCR) was performed using SensiMIX SYBR kit (Bioline). 1 µL of cDNA was mixed with 6.25 µL of SensiMIX, 0.8 µL of primers 5µM, 4.5 µL of nuclease-free water (Ambion) and placed in Rotorgene 3000 (Corbett research).

PCR amplification was performed using following conditions:

Temperature	Time	Number of cycles
95°C	600 s	1X
95°C	10 s	40X
60°C	15 s	
72°C	20 s	

3.5 Single cell RNA sequencing

TEC isolated from 1-week-old and 4-week-old mice were labelled with replicate-specific TotalSeq anti-mouse Hashtag antibodies (Biolegend), sorted, the number of viable cells was counted and an equal number of cells from mutant and wild-type mice were pooled in tandem to limit batch effect between genotypes. From each duo of sample, 10,000 cells (5,000 KO and 5,000 WT) were loaded per well onto Chromium Single Cell B Chip (10X Genomics) coupled with the Chromium Single Cell 3' GEM (10X Genomics), Library and Gel Bead Kit v3 and Chromium i7 Multiplex Kit (10X Genomics) for library preparation, according to manufacturer's instructions. Quality of libraries generated was assessed using capillary electrophoresis on a Fragment Analyzer (AATI) and their concentration was quantified by using Qubit dsDNA HS Assay Kit (Thermo Fisher Scientific). Libraries were pooled and sequenced on NovaSeq 6000 (Illumina) using the NovaSeq 6000 S2 Reagent Kit (100 cycles) (Illumina).

Following bioinformatics analysis was performed by Adam E. Handel (University of Oxford) and conducted in Seurat version 3. Quantification of transcriptome and sequencing of hashtag antibody barcodes were done with Cellranger. Prior analysis, single-cell sequencing data were pre-processed: doublets detected with DoubletFinder and low-quality cells with less than 1,000 detectable genes or high proportion of mitochondrial or ribosomal genes were

excluded. Replicates were integrated using canonical correlation analysis (CCA) prior to clustering. Dimensionality reduction was undertaken by Uniform Manifold Approximation and Projection (UMAP). Confidence interval (95%) of TEC subtypes proportion was calculated with metafor R package.

3.6 ATP/ADP ratio

To measure ATP/ADP ratio, 10,000 $TEC^{Ly51low}$ and cTEC isolated from 4-week-old mice were sorted in 95µL of lysis buffer from ATP/ADP ratio kit (Sigma-Aldrich). Wild-type and knockout samples were sorted in alternance to limit difference of treatment. After transfer into white opaque 96-well plate (Bio-Rad), luciferin and luciferase from the kit were added to cells' lysate and incubated for 1 minute at room temperature in the dark. Then, the plate was loaded in Microplate Luminometer Centro LB 960 (Berthold) and luminescence was recorded for 1 second long per well (Relative Light Unit 1; RLU_1). After 10 mins, remaining bioluminescence was recorded prior addition of kinase from kit to convert ADP into ATP (RLU_2). One minute of incubation at room temperature later, luminescence intensity was recorded (RLU_3). To calculate ATP/ADP ratio, luminescence intensity recorded after addition of luciferase (RLU_1) was divided by RLU after kinase addition (RLU_3) minus remaining intensity (RLU_2).

$$ATP/ADP\ ratio = \frac{RLU_1}{(RLU_3 - RLU_2)}$$

3.7 Scenith

Adapted from Argüello et al[91], thymic lobes were isolated from E18.5 embryos or new-borns. After removing fat and connective tissues, lobes were cut longitudinally and split between conditions in a 48-well plate. Immerged in 100 µL of pre-warmed IMDM, lobes were incubated for 5-10 mins at 37°C. Then, 200 mM of 2-deoxyglucose (2-DG) (Sigma-Aldrich), 2 µM of oligomycin A (OLI) (Sigma-Aldrich) or a mix of 200 mM of 2-DG, 2 µM of OLI and 2 µM of carbonyl cyanide 4-(trifluoromethoxy)phenylhydrazone (FCCP) (Abcam) diluted in 100 µL of pre-warmed IMDM were added to lobes except for negative control which received 100 µL of pre-warmed IMDM. After 30 mins of incubation at 37°C, 50µL of puromycin dihydrochloride (Sigma-Aldrich) at 50 µg/mL were added to lobes which incubated for another 30 mins at 37°C. After washing in PBS, lobes were digested as described in subsection *3.3.1*

and the same number of cells were stained extracellularly and intracellularly as described in subsection *3.3.4.*

For the analysis, a reduction of puromycin incorporation consequent to the exposure to distinct inhibitors (alone or in combination) is related to the maximal reduction of that signal upon complete inhibition of ATP synthesis. These values, based on the frequency of cells with high puromycin content, were multiplied by 100 to give a number between 0 and 100 thus indicating how much of the ATP synthesis is dependent on the inhibited pathway(s) (0: ATP synthesis is independent of this pathway; 100: ATP synthesis is totally dependent of this pathway).

CTRL = % of Puromycin^{high} in Control condition
DG = % of Puromycin^{high} in 2-DG condition
OLI = % of Puromycin^{high} in Oligomycin condition
AI = % of Puromycin^{high} in 2-DG + OLI + FCCP condition

$$Glucose\ dependence = \frac{100(CTRL - DG)}{(CTRL - AI)} \qquad Mitochondrial\ dependence = \frac{100(CTRL - OLI)}{(CTRL - AI)}$$

$$Glycolitic\ capacity = 100 - Mito.dep. \qquad FAO/AADO\ capacity = 100 - Gluc.dep.$$

3.8 Foetal thymic organ culture

Pregnant mice were sacrificed by C02 inhalation at gestational day 14.5 and embryos were collected and put in cold FACS buffer. Embryonic thymic lobes were isolated and placed on a 0.45 micro pore sized filter (Millipore) floating on culture medium, in the additional presence of 1 nM of oligomycin A, 5 mM of N-acetylcystein (NAC) (Sigma-Aldrich) and/or 2.5 µg/mL of RANK-ligand (R&D). After 2 days of incubation (D+2) in CO2 incubator at 37°C, NAC and OLI were renewed from the medium. After 4 days of culture (D+4), floating lobes were collected, digested and stained as described in subsections *3.3.1* and *3.3.4.* It should be noted that lobes were grouped per condition on the same floating membrane to limit technical variabilities.

3.9 Reaggregate thymic organ culture

TEC and thymocytes from 2-week-old mice were isolated and sorted as described in subsections *3.3.1, 3.3.2* and *3.3.6.* Then, 50,000 cTEC or $TEC^{Ly51low}$ and 50,000 pre-selected DP thymocytes ($CD4^{pos}$, $CD8^{pos}$, $CD69^{neg}$) sorted in culture medium were mixed in the same 1.5 mL Eppendorf tube and spun down at 2000g for 45 secs to form a reaggregate. After removal of medium to let 500 µL left, tube was placed in CO2 incubator at 37°C with lid open for 48 hours. Then, medium was removed and cells from aggregate were resuspended and stained in FACS buffer according to subsection *3.3.1* prior analysis by flow cytometry.

3.10 List of software

Analysis of flow cytometry data was conducted in FlowJo (V10.1 and ulterior) (BD). Statistical analysis was conducted in Excel (Microsoft) and Prism 9 (GraphPad Software). Graphs were generated in Prism 9.

3.11 List of buffers and solutions

Toes lysis Buffer	0.1 M Tris pH 8.5 (Sigma-Aldrich); 5 mM EDTA (Invitrogen); 0.2% SDS (Sigma-Aldrich); 0.2 M NaCl (Sigma-Aldrich); proteinase K 100 µg/mL (Merck KGaA); miliQ water.
PCR reaction mix	2.5 µL 10X PCR buffer (Sigma-Aldrich); 0.5 µL 10 µM dNTPs (Sigma-Aldrich); 0.5 µL forward primer; 0.5 µL reverse primer; 0.1 µL TAQ polymerase 5U/µL (Sigma-Aldrich); 19.9 µL nuclease-free water (Ambion).
TAE	4.84 g/L Tris-base; 1.142 mL/L glacial acetic acid; 2 mL 0.5M EDTA; miliQ water; pH adjusted to 8.0
Gel Loading Buffer	0.25% bromophenol blue (Bio-Rad); 0.25% xylene cyanol FF (Fluka); 15% Ficoll 400 in water (Fluka).
Delanay's Solution	50% Absolute ethanol (Sigma-Aldrich); 50% Acetone (Sigma-Aldrich); 1M trichloroacetic acid (Sigma-Aldrich).
PBS	Dulbeco's phosphate buffered saline powder (Sigma-Aldrich); MiliQ water
FACS buffer	2% foetal bovine serum (MP Biomedicals); PBS

EM fixative solution	2% paraformaldehyde (PFA); 2.5% (glutaraldehyde); 0.1M PIPES pH 7.0-7.2
Culture medium	IMDM plus Glutamax (Life technologies); 10% FBS (MP Biomedicals); 50 µM 2-Mercaptoethanol (Life technologies); 100 µg/mL kanamycin sulfate (Life technologies)

3.12 List of primers

	Forward	Reverse
Cre (genotyping)	TCTGATGAAGTCAGGAAGAACC	GAGATGTCCTTCACTCTGATTC
Ak2 lox F-R1 (genotyping)	TGCAGAAGACAAGGTAGAGC	TGAAGCCTATGTGTGGAAGG
Ak2 lox F-R2 (genotyping)	TGCAGAAGACAAGGTAGAGC	TCTCACCCATGCTTTCGTC
Ak2 exons 1-2 (qPCR)	GGCTTCCGAACCGGAGATTC	CAGACACAAAAGTTTTCAGCCAG
Ak2 exons 3-4 (qPCR)	TGGAGACTCCTTCGTGCAAAA	CAATGACTGAATCGAGCTTCTCT
ND1 (mito. DNA) (qPCR)	CTAGCAGAAACAAACCGGGC	CCGGCTGCGTATTCTACGTT
HK2 (genomic DNA) (qPCR)	GCCAGCCTCTCCTGATTTTAGTGT	GGGAACACAAAAGACCTCTTCTGG
Cathepsin L (qPCR)	ATCAAACCTTTAGTGCAGAGTGG	CTGTATTCCCCGTTGTGTAGC
Cathepsin S (qPCR)	CCATTGGGATCTCTGGAAGAAAA	TCATGCCCACTTGGTAGGTAT
Beta-actin (qPCR)	CAATAGTGATGACCTGGCCGT	AGAGGGAAATCGTGCGTGAC

3.13 List of antibodies and fluorescent reagents

3.13.1 List of antibodies

Antigen	Conjugation	Reference	Fixative	Dilution
Cytokeratin 8	/	Progene 61038	Acetone	200
Cytokeratin 14	/	BioLegend 905301	Acetone	1000
ERTR7	/	Bio-Rad MCA2402	Acetone	100
Mouse IgG	Alexa Fluor 488	Invitrogen A21121	/	800
Rat IgG	Alexa Fluor 555	Invitrogen A21434	/	800
Rabbit IgG	Alexa Fluor 647	ThermoFisher A21244	/	800

Rabbit IgG	Alexa Fluor 647	ThermoFisher A21244	/	800
CD4	PE-Texas Red	Abcam 51467	/	1000
CD8	Alexa Fluor 700	BioLegend 100730	/	500
TCRγδ	Biotin	BioLegend 118103	/	1000
FR4/80	Biotin	BioLegend 123106	/	2000
CD11c	Biotin	BioLegend 117304	/	2000
CD11b	Biotin	BioLegend 101204	/	1000
TER119	Biotin	Selfmade (TER119)	/	200
MHCII	Biotin	BioLegend 116404	/	2000
CD19	Biotin	BioLegend 260220	/	500
GR1	Biotin	BioLegend 108404	/	500
NK1.1	BV650	BioLegend 108736	/	400
CD69	PE	BioLegend 104508	/	200
TCRß	FITC	BioLegend 109206	/	400
CD44	APC-Cy7	BioLegend 103028	/	1000
c-kit	APC	BioLegend 135108	/	200
CD25	BV605	BioLegend 102036	/	1000
CD71	PE-Cy7	BioLegend 113812	/	200
CCR7	BV421	BioLegend 120120	/	200
CD44	BV785	BioLegend 103059	/	500
CD24	PerCP-Cy5.5	Biolegend 101824	/	1000
CD69	PE-Cy7	Biolegend 104512	/	500
FOXP3	PE	Invitrogen 145773-82	eBioscience	50
TCRß	APC-Cy7	BioLegend 109220	/	200
CD19	PE-Texas Red	Invitrogen RM7717	/	500
CD4	BV421	BioLegend 100438	/	500
ICOS	PE-Cy7	Biolegend 313520	/	200
FOXP3	APC	Invitrogen 17-5773-82	eBioscience	50
CD44	BV785	BioLegend 103059	/	500
CD62L	PerCP-Cy5.5	BioLegend 104432	/	1000

CD73	PE	BioLegend 127206	/	200
EpCAM	BV421	BioLegend 118225	/	500
CD45	PE-Texas red	Invitrogen MCD4517	/	500
MHCII	APC-Cy7	BioLegend 107628	/	2000
Ly51	PE-Cy7	BioLegend 108306	/	1000
Sca-1	BV785	BioLegend 108139	/	1000
AIRE	APC	eBioscience 50-5934-82	BD Cytofix	1000
BrdU	APC	BD 51-23619L	BD Cytofix*	100
Active caspase 3	V450	BD 560627	BD Cytofix	500
Total caspase 3	Alexa Fluor 700	NovusBio NB100-56708AF700	BD Cytofix	500
CD40	Cy5	Selfmade (FGK45.5)	/	200
CD205	PE	BioLegend 138214	/	500
FOXN1	PE	Kindly provided by H-R Rodewald	/	
Ly51	Biotin	BioLegend 108304	/	500
E-cadherin	eFluor 660	eBioscience 50-3249	BD Cytofix	100
CD200	APC	BioLegend 123810	/	1000
ß5t	/	MBL PD021	/	200
CD31	FITC	BioLegend 102406	/	1000
CD45	A700	BioLegend 103128	/	500
Podoplanin	PE	BioLegend 127408	/	1000
EpCAM	BV605	BioLegend 118227	/	2000
CD26	APC	BioLegend. 137807	/	500
CD146	PerCP-Cy5.5	BioLegend 134710	/	500
Sirt1	/	Millipore 07-131	/	500
MHCII	PerCP-Cy5.5	BioLegend 107626	/	500
Phosphorylated AMPK α1+2	/	Abcam 23875	BD Cytofix	25
AMPK α1	/	NocusBio	BD Cytofix	400
Puromycin	Alexa Fluor 647	Millipore MABE343-AF647	BD Cytofix	800

HK1	/	Abcam 150423	BD Cytofix	200
ASS1	/	Abcam 170952	BD Cytofix	400
CPT1A	/	Abcam 128568	BD Cytofix	200
IDH2	/	Abcam 131263	BD Cytofix	200
Mouse IgG	/	Molecular probe A21236	/	800
Ly51	PE	BioLegend 108308	/	1000
CCL21	Biotin	LSBio LS-C104633	Cytofix	100
CCL25	Biotin	R&D BAF481	eBioscience	200
CD8	PerCP-Cy5.5	BioLegend 100733	/	400
CD69	FITC	BioLegend 104506	/	500
Helios	APC	eBioscience 17-9883-42	eBioscience	50
PD-1	BV785	BioLegend 135225	/	200
CD5	APC-eFluor 780	eBioscience 47-0051-82	/	400

Fixatives: Ebioscience = eBioscience FOXP3 / transcription factor staining buffer set

BD Cytofix = BD Cytofix/CytoPerm

BD Cytofix* = BD Cytofix/CytoPerm + BD Permeabilization buffer plus

3.13.2 *List of viability dyes*

Viability dye	Reference	Dilution
Zombie Red	BioLegend	2000
DAPI	Sigma-Aldrich	0.5µg/mL

3.13.3 *List of fluorescent reagents*

Fluorescent reagents	Conjugation	Reference	Dilution
Lactadherin	FITC	ThermoFisher BLAC-FITC	50
Streptavidin	BV510	BioLegend 405234	500
Mitotracker Deep Red	/	ThermoFisher	200000
MitoSOX Red	/	ThermoFisher	2000

JC-1	/	ThermoFisher	2000
UEA-1	FITC	Reactolab FL-1061	1000
Streptavidin	APC	BioLegend 405207	800

4. Results

4.1 AK2 deletion in thymic epithelial cells

To determine specifically the role of AK2 in TEC, we crossed transgenic mice expressing the Cre recombinase under the control of TEC-specific *Foxn1* locus (*Foxn1-Cre*)[89] with mice with conditional *Ak2* alleles ($Ak2^{flox/flox}$). AK2-deficient TEC mice homozygous for the "floxed" *Ak2* alleles and heterozygous for the expression of the Cre recombinase (designated TEC^{AK2KO}) have a deletion of exons 3 and 4 of the conditional *Ak2* locus. This deletion results in a truncated AK2 protein that lacks the LID domain (Figure **1A**) which initiates the transfer of the phosphate group. $Ak2^{flox/flox}$ mice missing *Cre* transgene were used as controls and are referred to as TEC^{AK2WT}. The presence of the *Foxn1-Cre* allele and recombination of the *Ak2* loci were confirmed by PCR using genomic DNA extracted from toe clips of 1-2-week-old mice (Figure **1B**).

Full *Ak2* transcripts could not be detected by RT-qPCR in TEC^{AK2KO} mice using primers specific for exons 3-4 (Figure **1C**). Shorten version of *Ak2* could be detected but at lower level using primers specific for exons 1-2. Efforts to detect the protein either by flow cytometry or immunohistochemistry were repetitively unsuccessful. AK2 antibody did not give specific signal distinct from background nor isotype control.

4.2 AK2 deficiency in TEC decreases thymic cellularity and disrupts medullary architecture

TEC^{AK2KO} mice are viable and could live as long as wild-type mice. In addition to thymic epithelial cells, FOXN1 is also expressed in skin epithelium[89]. However, skin and fur of mutant mice didn't show obvious differences. Adult TEC^{AK2KO} mice have a smaller thymus which occasionally has also macroscopically visible cysts at the surface (Figure **2A**). The reduced organ size correlates with lower total thymus cellularity (Figure **2B**). Differences in cellularity between control and mutant mice were observed as early as E16.5 and continued to be observed as late as week 38 of life. A histological analysis revealed that the thymus tissue of TEC^{AK2KO} mice displayed a regular segregation into an outer cell dense cortex and a centrally positioned medulla (Figure **2C**) while TEC^{AK2WT} thymi showed multiple medullary

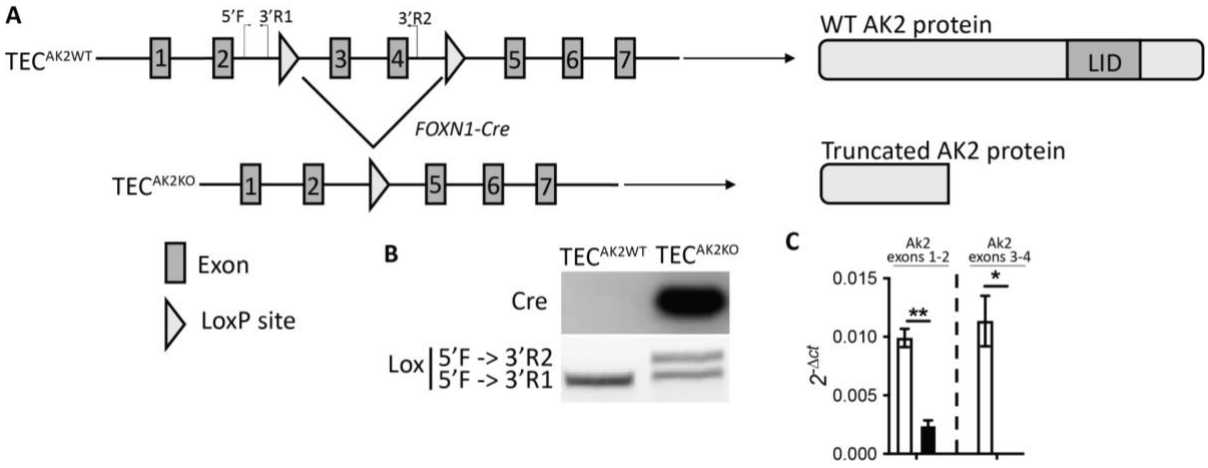

Figure 1: ***Genetic construct of AK2-deficient TECs mouse model.***

(**A**) Schematic illustration of Ak2 knock-out construct. (**B**) Agarose gel electrophoresis results of PCR genotyping for the presence of the *FOXN1-Cre* transgene and the loxP sites using genomic DNA isolated from TEC^{AK2WT} and TEC^{AK2KO} respectively. (**C**) Detection of transcript encoding exons 1-2 and exons 3-4 of *Ak2* normalised to *Beta-actin* transcripts expressed in TEC. *p<0.05, **p<0.01 (Student's t test, **c**). Representative data from at least 2 independent experiments.

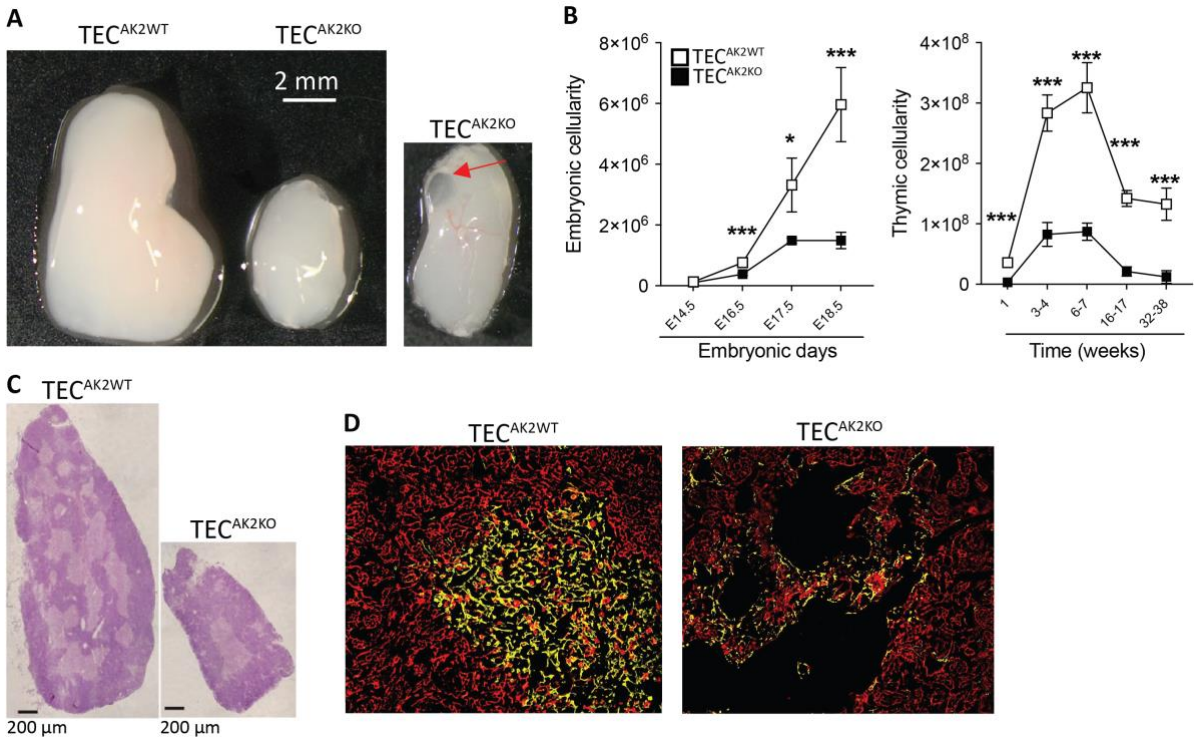

Figure 2: ***Loss of AK2 expression in TEC causes thymic hypoplasia and impacts thymic architecture.***

(**A**) Left: Photomicrograph of single thymus lobes isolated from 4-week-old TEC^{AK2WT} and TEC^{AK2KO} mice. Right: cyst in a thymic lobe of a TEC^{AK2KO} mouse (red arrow). (**B**) Thymic cellularity in TEC^{AK2WT} and TEC^{AK2KO} mice at the indicated ages. (**C**) Hematoxylin and Erythrosine B stain of thymus tissue sections of 4-week-old TEC^{AK2WT} and TEC^{AK2KO} mice. (**D**) Representative immunohistology of thymus tissue sections for the detection of cytokeratin 8 (CK8; red), a marker for cTEC, and cytokeratin 14 (CK14, yellow), a marker for mTEC. *p<0.05, **p<0.01, ***p<0.001 (Student's t test, **B**). Representative data from at least 2 independent experiments.

islands. TEC^{AK2KO} thymi also displayed few tiny medullary islands which are not connected to each other in contrast to medullary islands in TEC^{AK2WT}mice. Keratin-free zones were also observed in the medulla as indicated by the absence of cytokeratin stains (Figure **2D**).

These data demonstrate that AK2-deficiency impairs thymic growth and the organization of the medulla. Impairment starts already during embryogenesis.

4.3 Impaired thymopoïesis of TEC^{AK2KO} mice.

4.3.1 *Recruitment of T cell progenitors and their development is negatively affected by the absence of AK2 expression in TEC.*

To determine whether a thymic microenvironment composed of AK2-deficient TEC is competent to support normal thymocyte development (a.k.a. thymopoïesis), intrathymic differentiation of thymocytes was investigated in 3-4-week-old mice employing phenotypic markers that identify distinct developmental stages.

Among the phenotypically most immature thymocyte stages (defined as $lineage^{neg}$, thymocytes, i.e. $CD4^{neg}$, $NK1.1^{neg}$, $TCR_{\gamma\delta}{}^{neg}$, $TCR_{ß}{}^{neg}$, $CD69^{neg}$) cells with a double negative (DN) 1 ($CD44^{pos}$, $c\text{-}kit^{pos}$ and $CD25^{neg}$) and DN2 ($CD44^{pos}$, $c\text{-}kit^{pos}$ and $CD25^{pos}$) phenotype were significantly reduced in TEC^{AK2KO} mice when compared to age matched controls (Figure **3A**). The lower frequency of DN1 subset that contain the early thymic progenitors (ETP)[92] suggests a lower attraction of these progenitors from the periphery.

The mutant mice also displayed an increased frequency of the DN3a subpopulation ($CD44^{neg}$, $CD71^{neg}$ and $CD25^{pos}$) of thymocytes (Figure **3A**). This finding suggests that thymocytes are partially blocked at DN3a stage at ß-selection checkpoint. Hence, positive pre-TCR signal needed for the development at thymocytes from DN3a stage to DN3b is impaired by the absence of AK2 in TEC. The molecular cause of this decreased signalling remains to be elucidated.

The developmental stages following the differentiation of DN thymocytes are marked by the concurrent expression of the cell surface markers CD4 and CD8, a phenotype referred to as double positive (DP). TEC^{AK2KO} mice had a significantly increased frequency of DP thymocytes while their subsequent maturational stages which are marked by single positivity for either CD4 (designated SP4) or CD8 (SP8) were both reduced (Figure **3B**). This finding

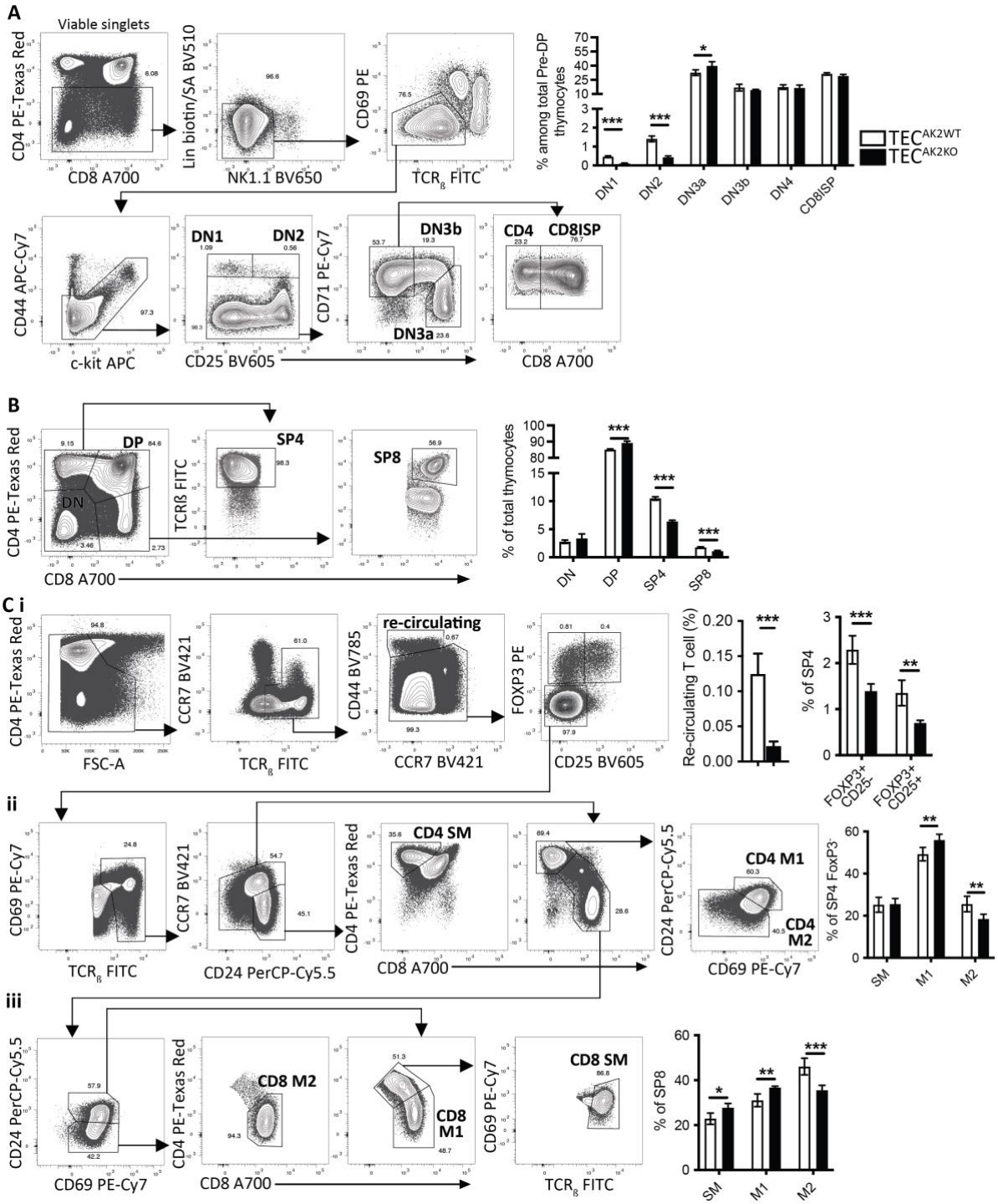

Figure 3: ***AK2-deficiency in TEC impairs early and later stages of thymocyte maturation.***

(**A**) Maturational progression of thymocytes from DN1 to CD8ISP stage within the pre-DP population. Left: Gating strategy to define pre-DP subpopulations; right: relative frequency of pre-DP thymocyte subpopulations isolated from TEC^{AK2WT} and TEC^{AK2KO} mice. Viable singlets thymocytes were defined by FSC and SSC, exclusion of DAPI staining and F4/80, TCRγδ, CD11c, CD11b, TER119, MHCII, GR1 and CD19 expression (Lin). (**B**) Relative frequency of thymocyte subpopulations defined by CD4, CD8 and $TCR_ß$ expression. Left: Contour plot and gating analysis; right: relative frequency of DN, DP, SP4 and SP8 thymocytes. (**C**) Maturational progression within $TCR_ß^{pos}$ thymocytes. (**Ci**) Left: Gating strategy to define re-circulating T cells and Treg subpopulations; right: Proportion of recirculating T cells among all thymocytes and Treg subpopulations among total SP4

thymocytes. (**Cii-iii**) Left: gating strategy to define (**ii**) SP4 and (**iii**) SP8 developmental stages; right: Proportion of subpopulations within (**ii**) CD4 lineage and (**iii**) CD8 lineage. *p<0.05, **p<0.01, ***p<0.001 (Student's t test, A-C). Numbers shown in individual contour plots represent the frequency of the indicated cell population. Data in graphs represent the mean and standard deviations (SD) and are representative of at least 2 independent experiments with 4 to 6 replicates each from TEC^{AK2WT} or TEC^{AK2KO} mice at 3-4 weeks of age.

suggests a partial block during lineaging maturation. Within the SP4 population, the frequency of developing Tregs (SP4 $FOXP3^{pos}$) was decreased for both immature[93] $CD25^{neg}$ and mature $CD25^{pos}$ populations (Figure **3C**).

Analysis of SP4 maturational stages revealed increased frequency of SP4 mature 1 (SP4 M1; $CD24^{pos}$ $CD69^{pos}$) and decreased frequency of SP4 mature 2 (SP4 M2; $CD24^{neg}$ $CD69^{neg}$) (Figure **3C**). TEC^{AK2KO} mice showed increased frequency of SP8 SM (SP8 SM; $CD24^{pos}$ $CD4^{int}$ $CD8^{int}$), increased frequency of SP8 mature 1 (SP8 M1; $CD24^{pos}$ $CD69^{pos}$ $CD4^{neg}$ $CD8^{pos}$) and decreased frequency of SP8 mature 2 (SP8 M2; $CD24^{neg}$ CD4neg $CD8^{pos}$) (Figure **3C**). These data indicate a partial block of maturation between the stages M1 and M2, populations which differ by their CD24 expression. Since this step of maturation occurs in the medulla, we can conclude that the support of mTEC to developing thymocytes is decreased in absence of AK2 expression.

The number of re-circulating cells ($CD44^{pos}$ $CCR7^{neg}$)[94] was also decreased in mutant mice (Figure **3C**). The mechanisms behind the re-circulation remain largely unknown[95–97]. However, the persistence of re-circulating T cells in the medulla[95] suggest that medullary epithelium has a substantial role in their retention or attraction. Hence, the disruption of medullary epithelium in absence of AK2 (see Figure **2D**) may be responsible of the lower proportion of re-circulatory cells.

Taken together, these data demonstrate that the absence of AK2 in TEC impairs the cell's capacity to support normal thymocyte development in both cortex and medulla.

4.3.2 *Decreased thymopoiesis in TEC^{AK2KO} mice leads to T cell lymphopenia.*

To probe whether decreased thymocyte development impacts the peripheral T cell compartment, lymph nodes were analysed for the presence of different T cells subsets. TEC^{AK2KO} mice revealed a severe T cell lymphopenia (60-70% less T cells) as demonstrated by a lower frequency of T cells in these tissues when compared to B cells (Figure **4A**). This difference affected both SP4 and SP8 T cells (Figure **4A**) albeit the observed reduction was more pronounced for SP4 T cells (-73%) when compared to SP8 T cells (-64%).

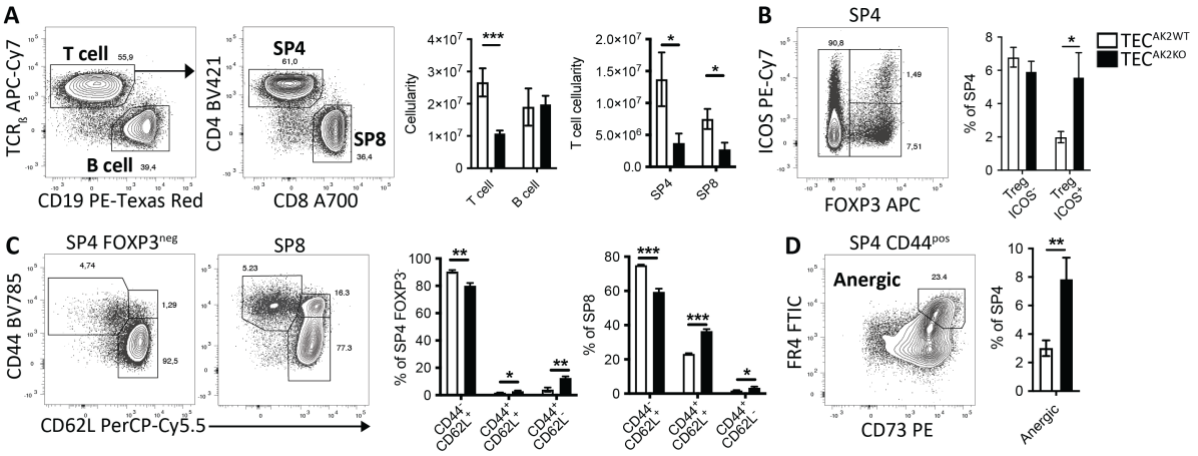

Figure 4: ***TEC^{AK2KO} mice developed T cell lymphopenia.***

(**A-D**) Flow cytometric analysis of lymph nodes isolated from 3-7-week old TEC^{AK2KO} and TEC^{AK2WT} mice. Gating strategy for defined subpopulation is shown in the left panels, respective quantification in graphs. (**A**) Absolute numbers of T and B cells (middle) and CD4 T cells (SP4) and CD8 T cells (SP8) (right). (**B**) Frequencies of ICOS^{pos} and ICOS^{neg} Treg within SP4. (**C**) Frequencies of naive (CD44^{neg}CD62L^{pos}), central memory (CD44^{pos}CD62L^{pos}) and effector memory (CD44^{pos}CD62L^{neg}) populations in FOXP3^{neg} SP4 and SP8 populations. (**D**) Frequencies of anergic T cells within SP4 population. Numbers shown in individual gates within contour plots represent the frequency of the indicated cell population. Data in graphs represent the mean and standard deviations (SD) and are representative of 3 independent experiments with 3 to 6 replicates each from TEC^{AK2WT} or TEC^{AK2KO} mice at 3-7 weeks of age (**A-C**) or 32-38 weeks of age (**D**). *p<0.05, **p<0.01, ***p<0.001 (Student's t test, **A-D**).

The proportion of activated regulatory T cells (SP4 FOXP3^{pos} ICOS^{pos}) was increased in the mutant mice (Figure **4B**). Distinguishing naïve from T cells with previous antigen experience, TEC^{AK2KO} mice displayed a reduced frequency of naïve T cells (CD44^{neg} CD62L^{pos}) at the cost of an expansion of central (CD44^{pos} CD62L^{pos}) and effector memory T cells (CD44^{pos} CD62L^{neg}) for both SP4 and SP8 T cells (Figure **4C**). Higher proportions of effector/central memory T cells, as well as an increased frequency of activated Tregs, can be attributed to T cell lymphopenia since lymphopenic environment induces rapid homeostatic proliferation and acquisition of characteristics of effector cells[98].

Since thymopoïesis is altered in AK2-deficient mice (see Figure **3A-C**), these mice may be more prone to autoimmunity. Then, anergic T cells were investigated since anergy induction is one of the peripheral tolerance mechanisms to prevent the development of autoimmune disease[99]. Anergic T cells were investigated in older mice (32-38 weeks of age) because the risk to develop autoimmunity as well as the frequency of anergic T cells increase with age[99,100]. In elder mutant mice, a higher proportion of anergic SP4 T cells (CD44^{pos} FR4^{pos} CD73^{pos}) was

detected (Figure **4D**). Together with the increased frequency of $ICOS^{pos}$ Treg, these data show that TEC^{AK2KO} mice induce mechanisms to promote central tolerance.

Hence, these data show that the decreased thymocyte development in TEC^{AK2KO} mice leads to a reduction of T cells at the periphery. However, compensatory mechanisms that limit the risk of autoimmunity remain.

4.4 Altered TEC development of AK2-deficient mice.

4.4.1 *TEC^{AK2KO} mice display a TEC population with low Ly51 expression and demonstrate an alteration of TEC subsets over time.*

Experiments (see section 4.2. and 4.3.) have demonstrated that TEC^{AK2KO} mice display abnormalities in the number of earliest thymic progenitors and development of thymocytes and demonstrate a histologically abnormal medullary region with keratin-free areas. Since all these observations originate from the absence of functional AK2 expression in TEC, changes of TEC subpopulations were investigated by flow cytometry.

The absence of AK2 expression by TECs correlated with a higher frequency of these cells in the thymus of mutant mice at both 1 week and 16-17 weeks of age (Figure **5A**). Mutant mice also showed a decreased absolute TEC cellularity (Figure **5A**). However, this finding will need to be appreciated with caution as the efficiency of recovering TEC might be a function of the organ's size (unpublished data).

TEC are classically phenotypically divided in two: cortical (cTEC) and medullary (mTEC) thymic epithelium. cTEC are typically defined by their expression of Ly51 and their absence of reactivity to *Ulex Europeanus Agglutinin-1* lectin (UEA-1) ($Ly51^{pos}$ $UEA\text{-}1^{neg}$) while mTEC show no expression of Ly51 but react to UEA-1 ($Ly51^{neg}$ $UEA\text{-}1^{pos}$). In addition to the phenotypically defined cTEC and mTEC, the mutant mice also displayed an abundant subpopulation of TEC with low Ly51 expression and missing reactivity UEA-1 (Figure **5B**), a feature normally observed in cTEC from old mice (data not shown). This subpopulation is referred throughout the work described here as $TEC^{Ly51low}$. The frequency and absolute cellularity of $TEC^{Ly51low}$ were increased in mutant mice at all time points investigated with the

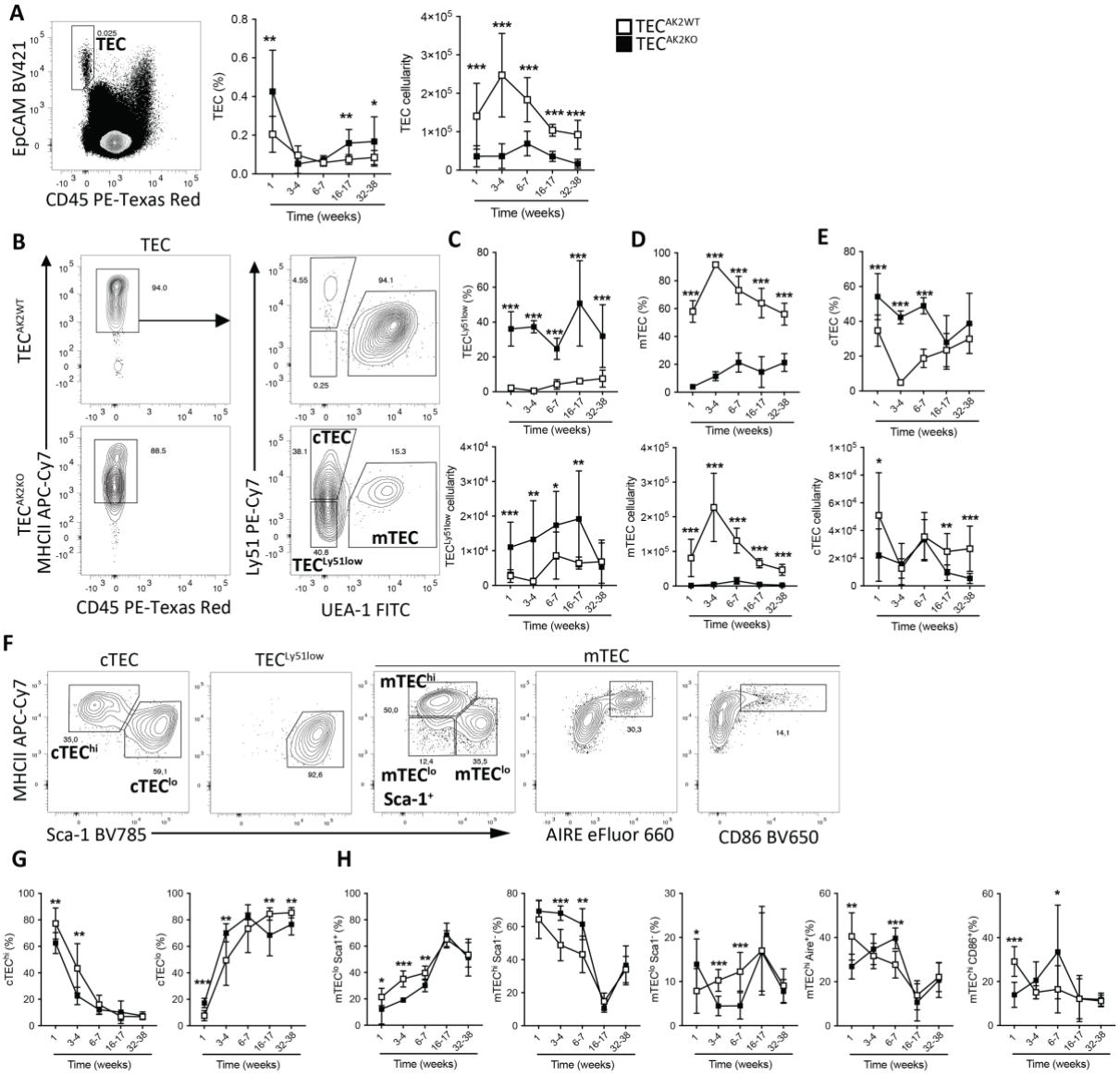

Figure 5: ***Loss of AK2 in TEC leads to partial block in mTEC development.***

(**A**-**E**) Flow cytometric analysis of TEC subpopulations isolated from TEC^{AK2KO} and TEC^{AK2WT} mice at indicated ages. (**A**) Relative (middle) and absolute (right) numbers of TEC (EpCAM^{pos} CD45^{neg}) within viable cells. (**B**) Gating strategy for detection of cTEC (Ly51^{pos} UEA-1^{neg}), TEC^{Ly51low} (Ly51^{neg} UEA-1^{neg}) and mTEC (Ly51^{neg} UEA-1^{pos}) based on Ly51 expression and UEA-1 reactivity. (**C**-**E**) Absolute (lower graphs) and relative (upper graphs) numbers of (**C**) TEC^{Ly51low} (**D**) mTEC and (**E**) cTEC within TEC. (**F**) Flow cytometric analysis of cTEC and mTEC for MHCII, Sca-1, CD86 and AIRE expression in 3-4-week-old mice. (**G**) Relative numbers of cTEC^{lo} (MHCII^{low} Sca-1^{pos}) and cTEC^{hi} (MHCII^{high} Sca-1^{neg}) within cTEC isolated TEC^{AK2KO} and TEC^{AK2WT} mice at indicated ages. (**H**) Relative numbers of mTEC^{lo} (MHCII^{low} Sca-1^{pos}), mTEC^{hi} (MHCII^{high} Sca-1^{neg}), mTEC^{lo}Sca-1^{-} (MHCII^{low} Sca-1^{neg}), mTEC^{hi}AIRE^{+} (MHCII^{high} AIRE^{pos}) and mTEC^{hi}CD86^{+} (MHCII^{high} CD86^{pos}) within mTEC isolated from TEC^{AK2KO} and TEC^{AK2WT} mice at indicated ages. Data in graphs represent the mean and standard deviations (SD) and are pooled from 2 (dataset from 3-4 and 6-7-week-old mice) or 3 (dataset from 1, 16-17 and 32-38-week-old mice) independent experiments with 3 to 5 biological replicates each. *p<0.05, **p<0.01, ***p<0.001 (Student's t test, **A**-**H**).

exception of weeks 32-38 for the absolute cell numbers recovered from mutant mice (Figure **5C**).

The frequency and absolute cellularity of mTEC was severely decreased (8-to-45-fold reduction in cellularity) at each post-natal time point tested (Figure **5D**). The lower number of mTEC can explain the lack of keratin^{pos} cells in the medulla as well as the absence of several medullary islands normally developed in wild-type thymi (see Figure **2C-D**). The frequency of cTEC was significantly increased in TEC^{AK2KO} mice of 1, 3-4 and 6-7 weeks of age (Figure **5E**)**.** When compared to controls, the absolute cTEC cellularity was decreased at distinct time points including 1 week of age and after week 16 of life (Figure **5E**).

TEC diversity as defined by the differential expression of distinct phenotypic intracellular and extracellular markers is required for a stepwise provision of signals necessary for thymocyte development[101]. These distinguishing markers are developmentally regulated and are therefore suitable features to probe TEC differentiation by flow cytometry. Using this approach, cTEC can be subdivided based on their expression of MHCII and Sca1 into seemingly mature cells (MHCII^{high} Sca-1^{neg}; referred to as cTEC^{hi}) (Figure **5F**) and cTEC with a MHCII^{low} Sca1^{pos} phenotype (designated cTEC^{low}) considered as their progenitors but may also give rise in adult mice to mTEC[102,103]. The frequency of cTEC^{hi} was increased whereas that of cTEC^{lo} was reduced in the first 3-4 weeks of life but not thereafter (Figure **5G**). In older mutant mice (>16 weeks of age) the frequency of these seemingly immature cTEC was again increased when compared to control animals.

mTEC are typically phenotypically divided into different subpopulations based on the expression of several markers including MHCII, Sca-1, CD86 and the autoimmune regulator (AIRE). The sequential acquisition and loss of these markers, respectively, allows to place these cellular phenotypes along a developmental trajectory: mTEC differentiate from an immature phenotype (MHCII^{low} Sca-1^{pos} designated mTEC^{lo}) to cells with more mature features (MHCII^{hi} Sca-1^{neg}, referred to as mature mTEC^{hi}) which includes a completely mature subset (MHCII^{hi} AIRE^{pos} CD86^{pos}) and finally to a so called post-mature stage (MHCII^{low} Sca-1^{neg}, marked as mTEC^{lo}Sca-1^{neg}). The frequency of mTEC^{lo} within mTEC was decreased in mutant mice at 1 to 7 weeks of age (Figure **5H**). The frequency of mTEC^{hi} (MHCII^{hi} Sca-1^{neg}) was significantly increased from 3 to 7 weeks of age and decreased at 16-17 weeks of age. The frequency of mTEC^{hi} expressing CD86 or AIRE was reduced at 1 week of age but increased at 6-7 weeks of age. The frequency of mTEC^{lo} Sca-1^{neg} (MHCII^{hi} Sca-1^{neg}) within mTEC was significantly increased at 1 week of age and decreased from 3 to 7 weeks of age.

The population of $TEC^{Ly51low}$ featured a low MHC expression but were positive for the marker Sca-1 (i.e. $MHCII^{low}$ $Sca\text{-}1^{pos}$) (Figure **5F**). $cTEC^{lo}$ with low Ly51 expression is normally a phenotype observed on older mice and suggest that the absence of AK2 induces an early ageing of cTEC. Another possibility is that AK2-deficiency forces the development of TEC into a progenitor state since TEC^{lo} are potential progenitors[103,104]. More detailed analysis of $TEC^{Ly51low}$ phenotyping and TEC development in embryos will clarify the situation.

Taken together, the phenotyping of TEC revealed that the composition of the epithelial scaffold was clearly affected by a loss of AK2 expression in TEC. The changes in the frequencies of distinct TEC subpopulations when compared to control thymus tissue demonstrated an impairment of TEC development in absence of functional AK2. mTEC development is particularly affected. These findings are indicative of a change in proliferation and/or apoptosis or would argue for block in TEC differentiation. Changes in cTEC subpopulations as well as the emergence of $TEC^{Ly51low}$ would explain the partial block of thymocyte development occurring in the cortex (see Figures **3A-B**). The loss of mTEC can be associated with the impaired thymocyte development taking place in the medulla (see Figure **3C**). However, differences diminish with age and suggest that the role of AK2 is less important when thymus start to involute.

4.4.2 *Deficiency of AK2 in TEC in adult mice impacts their proliferation but not survival.*

The observed changes in relative contributions of individual TEC subpopulations to the epithelial scaffolds can be accounted for being either changes in proliferation, alterations in the survival of specific TEC subpopulations or their differentiation from an immature (possibly precursor) stage to alter differentiation state within a given TEC lineage. The mechanism underlying these explanations differ significantly and imply different roles for AK2 in TEC biology.

Changes in cell proliferation could account for the differences in frequencies of individual TEC subpopulations – at least in part. For this purpose, 3-4-week-old control and mutant mice were exposed *in vivo* to Bromodeoxyuridine (BrdU), a nucleoside analogue that is incorporated in newly synthetised DNA strands. The frequency of $BrdU^{pos}$ cells provides an estimate for the frequency of dividing TEC in a time between BrdU injection and the isolation of the cells.

In 3-4-week-old mice, AK2-deficient cTEC^{hi} showed a lower BrdU incorporation when compared to the corresponding controls (KO:7,3±0,6% vs WT:12,4±3,3%) (Figure **6A**). This result correlates with a relative lower frequency of cTEC^{hi} at this age (see Figure **5G**) and may indicate that the regular maintenance of this population of cTEC is dependent on cell proliferation which is reduced in their absence of AK2. In contrast, the absence of AK2 expression in mTEC^{lo} correlated with a higher frequency of BrdU incorporation and was not aligned with the cells reduced in relative and absolute frequency within the mTEC compartment of TEC^{AK2KO} mice (Figure **5H** and **6A**). These results indicate that a change in proliferation is not the mechanism behind lower frequency of these cells within mTEC compartment. These results also indicate that the influence of AK2 on cell proliferation is context dependent (i.e. relates to the specific subpopulation of TEC in which the protein is operative) and may therefore act only as an indirect driver of cell proliferation.

The size of a specific cell population is also determined by the frequency of cells with that particular phenotype to undergo programmed cell death or, alternatively to differentiate to a different phenotype with little or no cell proliferation. To probe the former possibility determining the size of the individual TEC subpopulations, I next determined the spontaneous rate of apoptosis among the different TEC subpopulations. For this purpose, I used two independent measures, namely the recognition of active caspase 3 (identifying early events in programmed cell death) and the surface detection of lactadherin (late marker of apoptosis). Experiments quantifying either of these two markers failed to reveal in a reproducible fashion significant differences between mutant and wild-type TEC (Figure **5B-C**). This result would argue for similar rate of spontaneous cell death despite the absence of AK2 at this age (i.e. 3-4 weeks of age). One possible explanation for this finding could be that lack of AK2 prevents TEC^{AK2KO} to differentiate normally but does not induce more cell death. Since differentiation requires a higher levels of energy[105], TEC^{AK2KO} may not meet the level of energy resources needed to differentiate but is sufficient enough for their survival. Energy metabolism had been investigated to verify this hypothesis.

Taken together, differences in TEC proliferation or cell death in adult mice do not align with the observed severe loss of mTEC (±50-fold reduction in 3-4-week-old mice) or the abundance of TEC^{Ly51low} in mutant mice. These data rather support the hypothesis of an impaired TEC development: differentiation into mTEC would be blocked and TEC^{Ly51low} would be favoured. Another, but not mutually exclusive, hypothesis would be that at 3-4 weeks of age the thymus had reached a steady-state and biological processes responsible of mTEC decrease and TEC^{Ly51low} abundance take place earlier in the development.

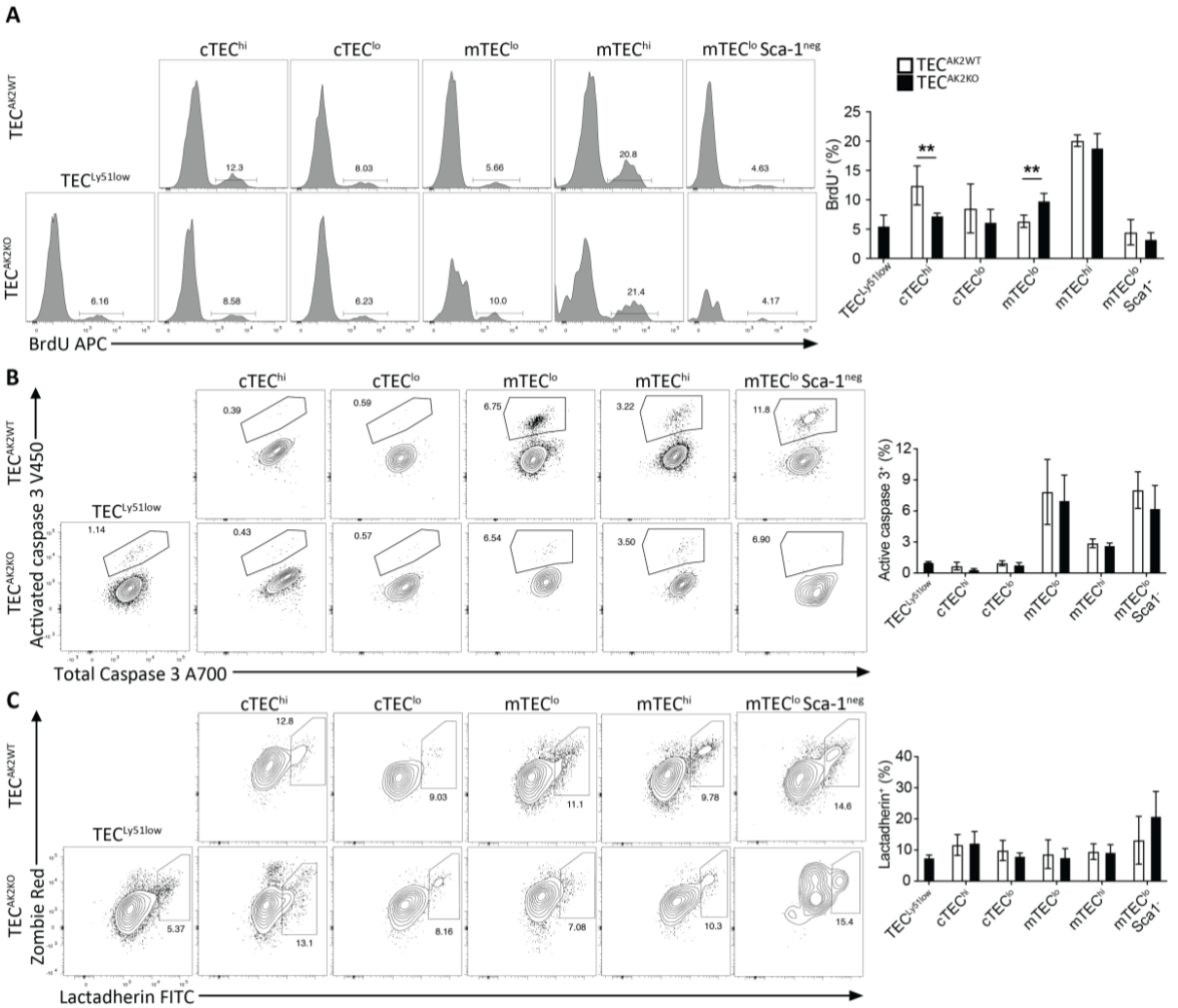

Figure 6: ***Altered proliferation but normal cell survival of TEC subpopulations from 3-4-week-old TEC^{AK2KO} mice.***

Flow cytometric analysis of TEC subpopulations isolated from 3-4-week-old TEC^{AK2KO} and TEC^{AK2WT} mice for proliferation as assessed by BrdU incorporation and for cell survival as assessed by active caspase 3 and Lactadherin. Gating strategy (Left) and quantitative analysis (Right) of (**A**) BrdU^{pos}, (**B**) active caspase 3^{pos} and (**C**) Lactadherin^{pos} within TEC subpopulations. Exclusion of Zombie^{pos} cells was not applied to quantify the proportion of lactadherin^{pos} TEC since a substantial number of Zombie^{pos} cells are also largely positive for lactadherin. Data in graphs represent the mean and standard deviations (SD) and data are representative of 4 (proliferation) or 5 (apoptosis) independent experiments with 3 to 6 biological replicates each. *p<0.05, **p<0.01, ***p<0.001 (unpaired Student's t test, **A-C).**

4.4.3 *Thymic development of mutant mice is severely compromised as early as embryonic day 16.5.*

Previous sections have demonstrated that the absence of AK2 expression in TEC results in severe thymus defects in adult mice, particularly affecting the mTEC compartment. However, TEC proliferation and cell death in adult mice could not provide an explanation for the observed cellular differences when comparing TEC^{AK2KO} with TEC^{AK2WT} mice. To probe whether changes to proliferation and programmed cell death occur during thymus formation in mutant embryos but not thereafter and to establish thus that the observed post-natal differences reflect the consequences of an abnormal prenatal differentiation and growth, thymocytes and TEC were comparatively investigated in wild type and mutant animals between embryonic day 14.5 (E14.5) to 18.5 (E18.5).

Both total thymic cellularity (See Figure **2B**) and the absolute number of DN thymocytes at distinct developmental stages (Figure **7A**) remained unchanged in mutant mice at E14.5 when compared to age-matched wild type animals. Changes in cellularity as a consequence of AK2 expression in TECs became however apparent at E16.5 and onwards as thymocytes at DN3a, DN3b and DN4 stages were decreased in TEC^{AK2KO} (Figure **7A**). This result suggested either an inefficient expansion or an increased frequency of apoptosis among thymocytes at the DN3a stage. Since differences in thymocyte cellularity became apparent from E16.5 onwards, proliferation and apoptosis were investigated. While differences in cell proliferation (as measured by in vivo BrdU uptake) were not observed (Figure **7B**), there was a significant increase in the frequency of DN3a cells undergoing apoptosis (WT:0.16±0.01% vs KO:0.44±0.09%; $p<0.001$)

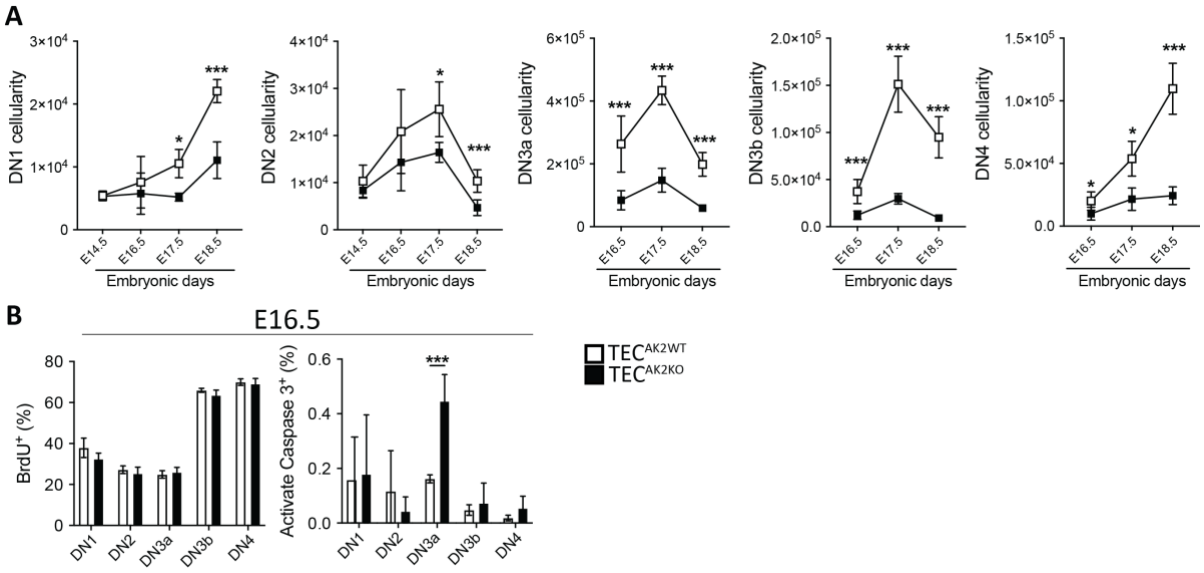

Figure 7: ***Thymopoïesis in TEC^{AK2KO} mice is altered starting from embryonic day 16.5.***

(**A**) Cellularity of DN thymocytes isolated from TEC^{AK2WT} and TEC^{AK2KO} embryos between day 14.5 (E14.5) to 18.5 (E18.5) isolated from. (**B**) Frequencies of DN thymocyte subsets isolated from embryos at E16.5 that have incorporated BrdU or display activated caspase 3 protein. Data in graphs represent the mean value and standard deviations (SD). Data are representative of (**A**) 3 or (**B**) 2 independent experiments with 3 to 9 biological replicates each. *p<0.05, **p<0.01, ***p<0.001 (unpaired Student's t test, **A**-**B**).

cTEC, but not mTEC, isolated from E18.5 TEC^{AK2KO} embryos showed a reduced expression of the transcription factor FOXN1 which is essential for normal TEC development[106](Figure **8B**). Low FOXN1 protein expression in a subset of AK2-deficient cTEC coincided with low Ly51 protein expression (Figure **8C)**, possibly indicating a direct relationship between the two markers. This atypical TEC phenotype (designated TEC^{Ly51low}) mice emerged at E17.5 (Figure **8D**) and was also observed in postnatal mutant mice. A comparable phenotype has been observed in aged wild type mice[107] which may indicate that AK2-deficient TEC undergo premature senescence. However, any link between AK2-deficiency in TEC and a reduced expression of FOXN1 remains to be resolved.

From E14.5 onwards, TEC^{AK2KO} mice showed an increased frequency of Sca1^{pos} cells among the total population of TEC (Figure **8E**). This observation may be an additional indication that AK2-deficient TEC undergo premature senescence since the frequency of TEC^{hi} Sca1^{neg} decreases and that of TEC^{lo}Sca-1^{pos} increases over time in postnatal thymi (Figure **5G**)

In light of the observed differences in TEC cellularity between wild type and mutant embryos, both TEC proliferation and apoptosis were investigated and demonstrated for cTEC and mTEC from TEC^{AK2KO} embryos a higher rate of apoptosis and a frequency of proliferation when compared to age-matched controls (Figure **8F**).

In aggregate, the data shows that thymic growth is impaired in mice secondary to a loss of AK2 expression targeted to TEC and this defect becomes already apparent as early as E16.5. Reduced TEC proliferation and increased cell death in embryos likely account for but certainly correlate with lower TEC cellularity in adult TEC^{AK2KO} mice. Moreover, AK2-deficient cTEC display downregulation of Ly51 and FOXN1 as well as an upregulation of Sca-1 expression, features that we also observe in cTEC from old mice (see Figure **5G**). This particular phenotype could result from an impaired mitochondrial function consequent to the loss of AK2 expression since early aging has been associated with a reduction or dysfunction of energy metabolism[108–110]. This hypothesis will be investigated and discussed later in the thesis.

Embryonic TEC subpopulations are commonly defined by their expression of CD40 and CD205[27] (also known as DEC205). Three distinct subsets of TEC can be identified using these two markers: $CD205^{pos}$ $CD40^{neg}$ and $CD205^{pos}$ $CD40^{pos}$ (considered as embryonic cTEC) and $CD205^{neg}$ $CD40^{pos}$ (considered as embryonic mTEC). The absolute cellularity of each of these subpopulations (i.e. $CD205^{pos}$ $CD40^{neg}$; $CD205^{pos}$ $CD40^{pos}$; $CD205^{neg}$ $CD40^{pos}$) was reduced in E16.5 and older embryos with AK2 deficient TEC (Figure **8A**). A comparable set of findings was observed in adult mutant mice when TEC subpopulations were defined by their Ly51 expression and UEA-1 reactivity (data not shown).

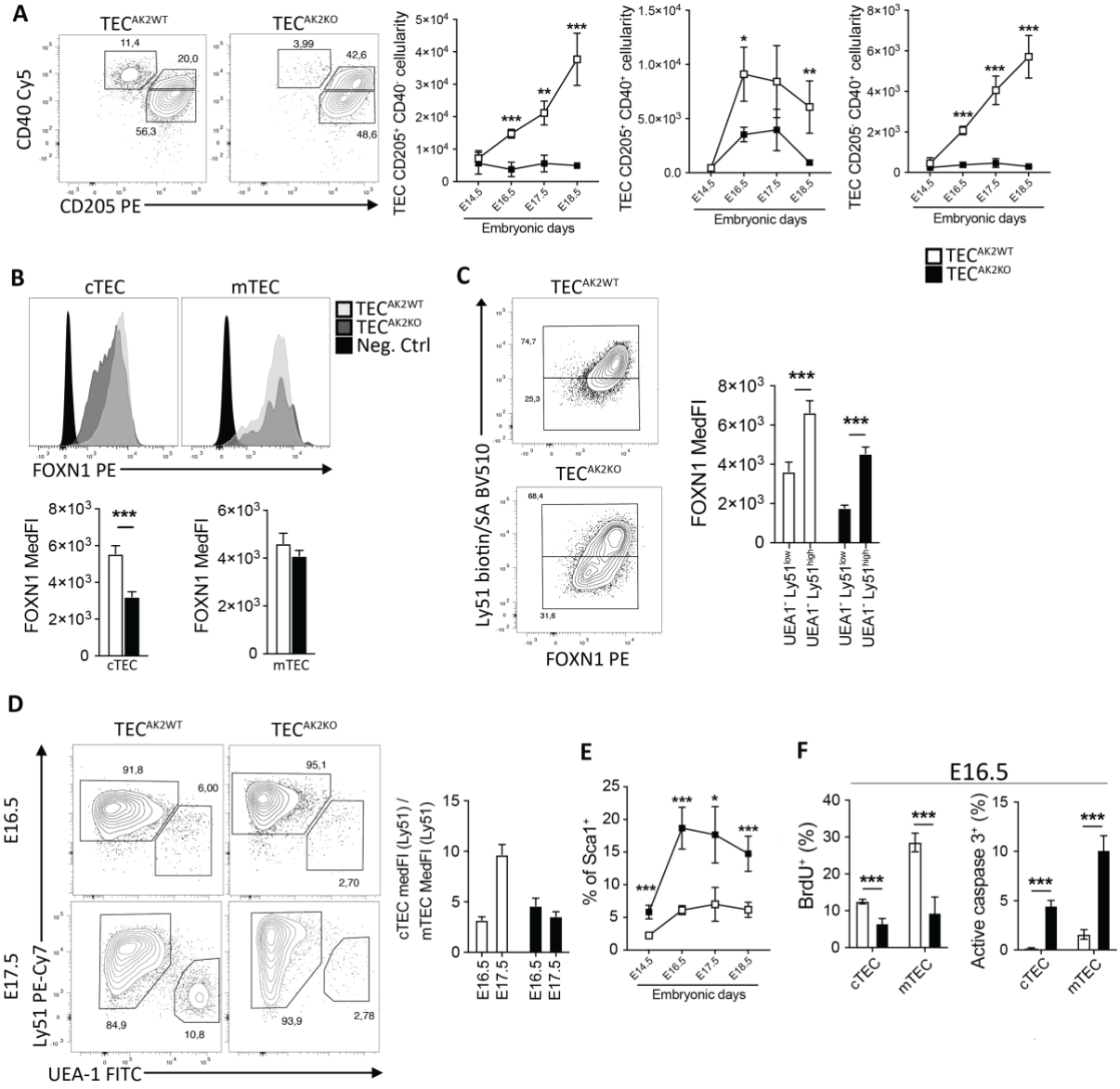

Figure 8: ***TEC development in TEC^{AK2KO} mice is altered from embryonic day 14.5 onwards.***

(**A**) Cellularity of embryonic TEC subpopulations defined by CD40 and CD205 expression (CD205^{pos} CD40^{neg} and CD205^{pos} CD40^{pos} are embryonic cTEC; CD205^{neg} CD40^{pos} are embryonic mTEC). Left: contour plots and gating strategy at E17.5; right: cellularity of embryonic TEC subpopulations at indicated ages. White symbols: TEC^{AK2WT}, black symbols: TEC^{AK2KO}(**B**) Representative histograms and quantification of median fluorescence intensity for FOXN1 expression in cTEC (UEA-1^{neg}) and mTEC (UEA-1^{pos}) isolated from E18.5TEC^{AK2WT} (light grey) and TEC^{AK2KO} (dark grey) mice, respectively. Panel B: Negative control (black histogram) shows the fluorescence signal in the absence of a FOXN1-specific antibody. (**C**) Flow cytometric analysis of Ly51 and FOXN1 expression in cTEC at E18.5. Left: contour plots and gating strategy; right: MedFI of FOXN1 in cTEC Ly51^{hi} and Ly51^{low} isolated from TEC^{AK2WT} (white bars) and TEC^{AK2KO} (black bars) (**D**) Flow cytometric analysis of Ly51 expression and UEA-1 reactivity in TEC at E16.5 and E17.5. Left: contour plots and gating strategy; right: relative cTEC to mTEC Ly51 staining in TEC isolated from TEC^{AK2WT} (white bars) and TEC^{AK2KO} (black bars) at E16.5 (left bar) and E17.5 (right bar). (**E**) Frequency of Sca1 expressing TEC from TEC^{AK2WT} and TEC^{AK2KO} mice at indicated ages. (**F**) Frequencies of cTEC and mTEC isolated from embryonic mice at E16.5,

respectively that have incorporated BrdU to quantify cell proliferation and express activated caspase 3 to identify cells undergoing programmed cell death. Data in graphs represent the mean and standard deviations (SD). Data are representative of 5 (E14.5 TEC), 4 (E16.5-E17.5 TEC), 3 (E18.5 TEC) or 2 (FOXN1 expression; apoptosis-proliferation) independent experiments with 3 to 9 biological replicates each. *p<0.05, **p<0.01, ***p<0.001 (unpaired Student's t test, **A-F**).

4.4.4 *TEC^{Ly51low} display features of cTEC lineage.*

TEC deep-phenotyping and the establishment of lineage development are severely curtailed by the difficulty to harvest sufficient number of TECs from at early embryonic ages and the present dearth of informative cell surface markers unequivocally recognized by specific antibodies. This limitation has recently been overcome by the development and use of single cell transcriptomics[32]. A comparison of the frequencies of individual TEC subtypes using 10x single cell transcriptomics demonstrated that the majority of TEC in TEC^{AK2KO} mice corresponded to the mature cTEC subtype (Figure **9B**). The second most abundant TEC subtype observed in these mice were intertypical TEC, a TEC cluster with a transcriptional profile that contains gene expression features characteristic of either cortical and medullary TEC and likely represent a precursor to mature mTEC. Flow cytometric phenotype of intertypical TEC largely but not exclusively relate to mTEC with low MHC class cell surface expression (i.e. mTEC^{lo})[33]. The proportion of intertypical TEC increased with age, to a similar extent observed in wild-type and mutant animals (+90,4% in TEC^{AK2WT} vs +80,7% in TEC^{AK2KO}). This finding could indicate that TEC development continues to occur in the postnatal thymus of TEC^{AK2KO} mice despite an absence of AK2. The reduction of differences in the frequency of TEC subpopulations, observed from 6-7 weeks of age onwards, supports this hypothesis (see Figure **5G-H**).

AK2-deficient intertypical TEC had elevated gene expressions within different pathways including those regulating mitochondrial component structure (e.g *Chchd1*), electron transport chain (e.g *Atp5g1*, *Cox5a*) and glycolysis (e.g *Aldoc*) (Figure **9D**). These data are compatible with a mechanism to compensate an impaired energy metabolism resulting from the absence of AK2 expression.

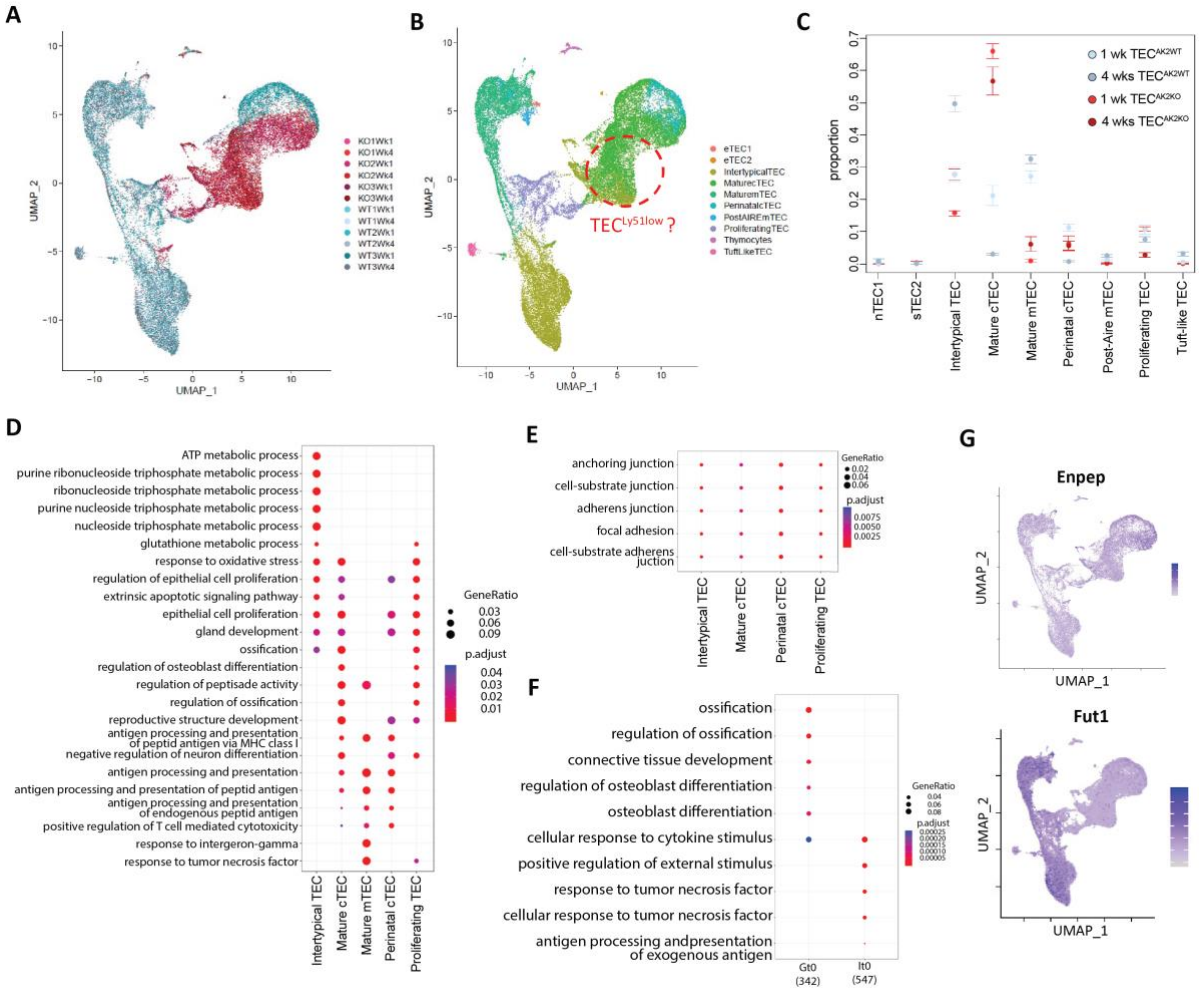

Figure 9*: Single-cell RNA-seq identifies decreases in the relative frequency of intertypical TEC and mature mTEC in favour of mature cTEC as a result of a loss of AK2 expression.*

Uniform Manifold Approximation and Projection (UMAP) graphs representing individual subtypes as defined by RNAseq among AK2-proficient (blue) and –deficient (red) TEC isolated from 3 TEC^{AK2WT} and 3 TEC^{AK2KO} mice at 1 week and 4 weeks of age. UMAP clustering of 36,615 single-cell transcriptomes (1 week: TEC^{AK2KO} 7,962 cells ; TEC^{AK2WT} : 9,390 cells ; 4 weeks: TEC^{AK2KO} : 7,627 cells; TEC^{AK2WT} : 11,636 cells). Data displayed by (**A**) genotype and (**B**) TEC subtypes. Putative localization of $TEC^{Ly51low}$ estimated by low *Enpep* (Ly51 gene) and *Fut1* (fucosyltransferase 1, a coarse proxy to predict UEA-1 binding as UEA-1 lectin binds to fucosyl residues) levels is annotated with a dashed red circle (**C**) Proportion of TEC subtypes as a function of age and genotype. Error bars shows 95% confidence intervals calculated with metafor R package. (**D**) Differences in biological processes as per Gene ontology (GO) analysis for intertypical TEC, mature cTEC and mature mTEC, perinatal TEC and proliferating TEC isolated from TEC^{AK2WT} and TEC^{AK2KO}. The size of the dot represents the proportion of differentially expressed genes (DGEs) in the given GO term and the colour of the dot represents the p-value adjusted for multiple tests. (**E**) Downregulated biological GO-defined processes in AK2-deficient intertypical TEC, mature cTEC, perinatal TEC and proliferating TEC subtypes in comparison to their wild-type counterpart. (**F**) Biological GO-defined processes in putative $TEC^{Ly51low}$ cluster compared to other TEC. Processes shown in

the Gt0 column are defined by higher gene expression whereas processes in the It0 column identify biological processes with lower gene expression in $TEC^{Ly51low}$ when compared to other TEC. (**G**) Projection of *Enpep* and *Fut1* expression onto the combined UMAP graph of wild type and mutant TEC. Darker tones denote maximal expression while lighter tones denote low expression.

Gene Ontology (GO) analysis showed in several AK2-deficient TEC subtypes (intertypical TEC, mature cTEC, perinatal cTEC and proliferating TEC) a decreased expression of processes involved in cell-cell contact or cell-matrix adhesion (Figure **9E**). This finding may relate to changes in the capacity for epithelial-mesenchymal transition (EMT) since these processes are highly regulated during EMT[111]. This hypothesis will be investigated and discussed later in the thesis.

I next sought to identify UEA1-negative TEC that expressed low levels of Ly51 by identifying cells with a low expression of *Enpep* coding for Ly51 and an absence of *Fut1* transcripts coding for fucosyltransferase 1 involved in the fucosylation of proteins, thus creating binding sites for UEA-1 (Figure **9G**). The latter was used as a coarse proxy to predict UEA-1 reactivity in TEC. Employing this approach, UEA-1 negative $TEC^{Ly51low}$ cells were projected to be represented within the Uniform Manifold Approximation and Projection (UMAP) graphs in a location characteristically occupied by mature cTEC containing a low proportion of intertypical TEC (Figure **9B**). The gene ontology analysis of the differentially expressed loci in $TEC^{Ly51low}$ identified several biological processes that appear to be differently engaged when compared to other TEC subtypes in either TEC^{AK2KO} or TEC^{AK2WT} mice. For example, the analysis identified several molecular processes involved in ossification and osteoblast differentiation (Figure **9F**). While there were no obvious calcifications or other changes related to osteoblast differentiation, the gene expression profiling identified increased transcripts of *Bmp4*[112], *Notch1*[39], *Tgfbr3*[113], *Sox9*[114] and *Cyr61*[115] which are found in these processes as well as in thymus morphogenesis.

GO processes associated to cell-cell interaction or cell-matrix contact in AK2-deficient intertypical TEC, mature cTEC, perinatal cTEC and proliferating TEC were downregulated as assessed by scRNAseq. As EMT is characterised by a loss of cell junction complexes and proteins involved in interactions with extracellular matrix[116], the decrease of these GO pathways possibly indicate a reduced epithelial-mesenchymal transition for AK2-deficient TEC.

Among hallmark genes differentially regulated during EMT, epithelial markers *Cdh1* (E-cadherin) and *Dsp* (desmoplakin) were decreased in mutant intertypical TEC. Mesenchymal markers such as *Vim* (vimentin), *Zeb1* (Zinc finger E-box-binding homeobox), *Mmp9* and *Mmp14* (matrix metallopeptidase 9 and 14), normally downregulated during EMT[116], were decreased in intertypical TEC. Typical mesenchymal marker *Cdh2* (N-cadherin) remained unchanged at transcript level in any subtype while transcripts of collagen mediating EMT were either upregulated (*Col4a1* and *Col4a2*)[117] or downregulated (*Col9a3*)[118] in intertypical TEC. The heterogeneity in changes of epithelial and mesenchymal markers at transcripts level does not support the hypothesis of an enhanced EMT in any AK2-deficient subtype.

In addition to changes in transcript expression revealed with scRNAseq, hallmark markers differentially regulated during EMT were investigated at protein level. To expand on this endotype, protein expression of E-cadherin, a cell adhesion molecule downregulated in EMT[116], and CD200, a membrane glycoprotein that when overexpressed in tumour cell lines favours the expression of genes involved in EMT and enhances invasiveness[119], were investigated by flow-cytometry. Efforts to detect additional markers such as N-cadherin, beta-catenin or vimentin were repetitively unsuccessful due to the absence of specific signal distinct from background nor isotype control (data not shown).

The frequency cells expressing E-cadherin was increased AK2-deficient $mTEC^{low}$ but not in other TEC subpopulations (Figure **10A**). The frequency of $CD200^{pos}$ cells was significantly decreased among mutant $cTEC^{lo}$ ($p<0,001$) but significantly increased in AK2-deficient $mTEC^{lo}$ and $mTEC^{hi}$ (Figure **10B**) ($p=0,016$ and $p=0.025$ respectively).

Hence, data from transcript and protein level do not support the hypothesis of an enhanced EMT in mutant mice. The downregulation of proteins involved in cell-cell junctions and in the adhesion to extra-cellular matrix (ECM) seems to not be related to EMT. Hence, the cause of the downregulation of these GO-defined processes and its consequence on TEC biology and function remain to be elucidated. It is noteworthy that the frequency of E-$cadherin^{high}$ and $CD200^{pos}$ cells in $TEC^{Ly51low}$ are more similar to those observed in cTEC from both mutant and wild-type mice than to those noticed in mTEC, supporting the cortical lineage of $TEC^{Ly51low}$. Transcriptomic data also indicated that the phenotypically defined $TEC^{Ly51low}$ belong mainly to the subtype of mature cTEC and or possibly some of the cells could also relate to the transcriptionally defined intertypical TEC (Figure **9B**). To date, the relation of TEC

subtypes which are defined by their transcriptional programmes and cytometrically defined TEC subpopulations is challenging due to the lack of appropriate cell markers and fails to identify several of these subtypes by flow cytometry[33].

To link $TEC^{Ly51low}$ to one of the better defined TEC lineage markers, these cells were next probed for their expression of ß5t, a cTEC-specific subunit of the proteasome, and cathepsin S as well as L, two proteases preferentially expressed in mTEC and cTEC respectively[27]. ß5t expression could not be detected in $TEC^{Ly51low}$ (Figure **10C**) whereas L-cathepsin (but not S-cathepsin) was readily detected in $TEC^{Ly51low}$ (Figure **10D**). Given the MHCII and Sca1 expression profile of these cells mentioned earlier (see Figure **5F**), $TEC^{Ly51low}$ are likely a variant of $cTEC^{lo}$ although their Ly51 and ß5t expressions are reduced or even absent with the latter correlating with a reduced FOXN1 expression. Thus, AK2 deficient TEC preferentially differentiate into Sca1-positive TEC^{lo} which appear after the first weeks of postnatal life whereas the differentiation into the mTEC is ostensibly limited.

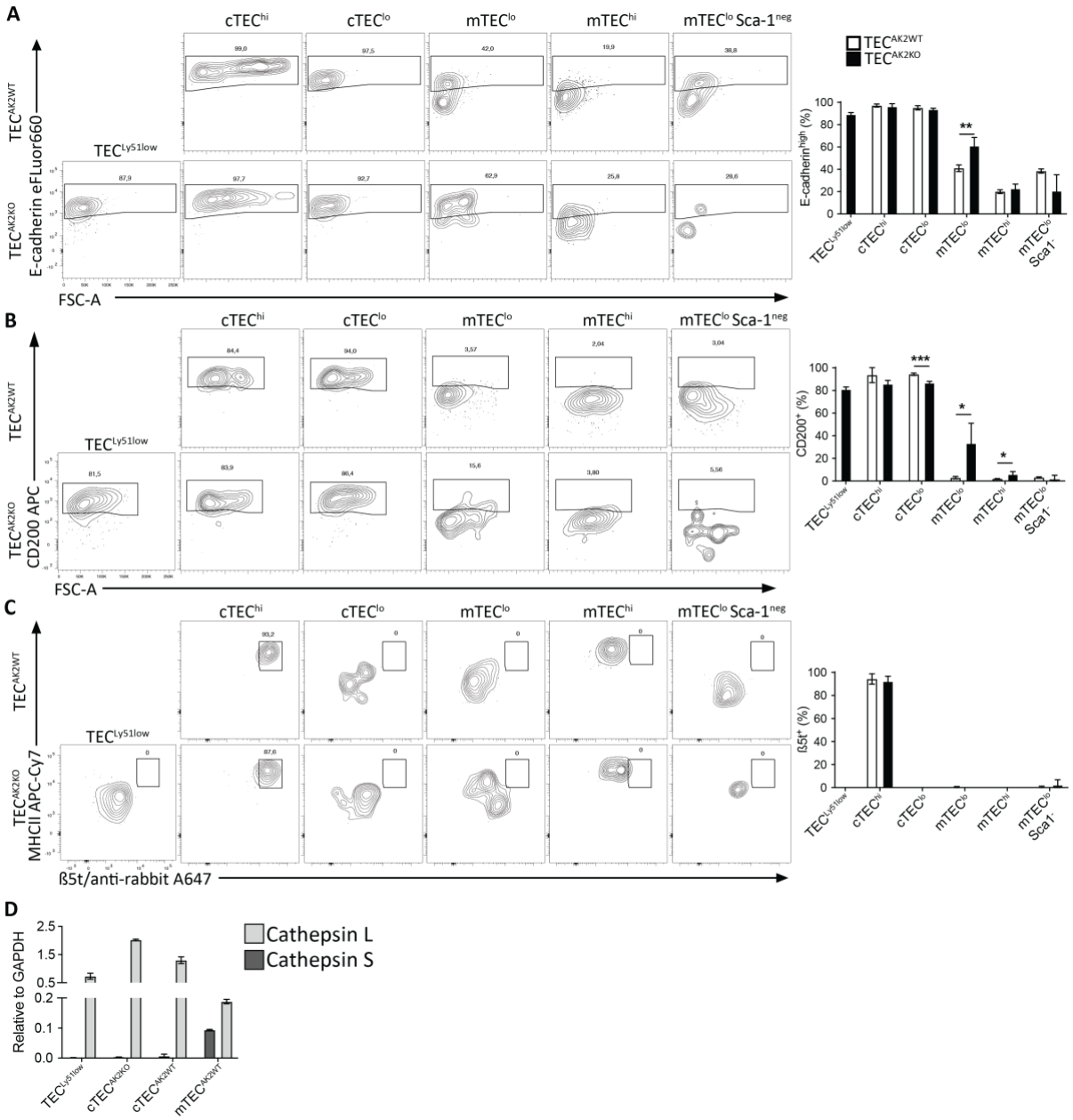

Figure 10: ***TEC^{Ly51low} express cTEC markers except ß5t that is restrained to cTEC^{hi} subpopulation.***

(**A-C**) Flow cytometric analysis of TEC subpopulations isolated from 4-week-old TEC^{AK2KO} and TEC^{AK2WT} mice to probe phenotypic hall marks of epithelial-mesenchymal transition as assessed by E-cadherin and CD200 expression. cTEC lineage are identified by their expression of the proteasome component ß5t. Gating strategy (Left) and quantitative analysis (Right) of (**A**) E-cadherin, (**B**) CD200 and (**C**) ß5t^{pos} within the indicated TEC subpopulations. (**D**) RT-qPCR analysis of TEC^{Ly51low} sorted from mutant and wild-type cortical subpopulations of the indicated phenotpyes and from medullary TEC for transcripts encoding cathepsin L and cathepsin S. qPCR results are normalised to *Gapdh* expression. Graphs represent the mean and standard deviations (SD) and are representative of 2 independent experiments with 3 to 4 biological replicates each (**A-C**) or 2 independent experiments with 2-3 technical replicates (**D**). *p<0.05, **p<0.01, ***p<0.001 (unpaired Student's t test, **A-C)**

4.5 AK2-deficiency in TEC affects other thymic stromal cells.

Non-TEC stroma of AK2-deficient mice was next investigated using flow-cytometry as mesenchymal cells are a prominent non-epithelial stromal component of the thymus microenvironment and contribute to central immune tolerance[120] as well as TEC development[121].

Pericytes represent a diverse population of stromal cells positioned in intervals along the walls of capillaries that regulate blood stream flow[122] and the egress of mature thymocytes to the periphery[123]. The frequency but not the absolute cellularity of pericytes was significantly increased in TEC^{AK2KO} mice (Figure **11D, E**). Capsular (cFbs) and medullary fibroblasts (mFbs), mesenchymal populations supporting thymic structure and function[121], were both increased in frequency in mutant mice (Figure **11D**). Whereas the total number of capsular fibroblasts was comparable for mutant and wild-type mice (Figure **11E**) medullary fibroblasts were increased in absolute cellularity in TEC^{AK2KO} animals. The keratin-free areas identified earlier in the medulla of mutant mice (see Figure **2D**) were filled with fibroblasts displaying a reticular pattern commonly found in fibroblasts of lymph nodes[12] and known to promote the motion of lymphocytes and antigen presenting cells[124,125](Figure **11F**). Then, the mFbs in the medulla of TEC^{AK2KO} mice likely improve thymocyte development through a facilitated access to antigen presenting cells in absence of medullary epithelial network. The frequency of endothelial cells was significantly higher in AK2-deficient mice (Figure **11D**). These cells form the inner-most layer of blood vessels[126] and participate in recruiting blood-borne haematopoietic progenitors to the thymic microenvironement[123]. However, the absolute cellularity of endothelial cells was decreased (Figure **11E**), which correlated with smaller size of the medulla and the absence of medullary islands in the thymus of mutant mice (See Figure **2C**).

Hence, the TEC-targeted absence of AK2 expression affected also other cells of the thymus stromal compartment thus unravelling a non-cell autonomous mechanism of interference. The medulla was particularly affected by TEC-unrelated changes to its stroma where in TEC^{AK2KO} mice an increased frequency of fibroblasts may fill the space left void by fewer mTEC. Whether this increase in fibroblasts also compensates for some of the lost mTEC functions is rather unlikely or at least at present speculative but could be formally tested.

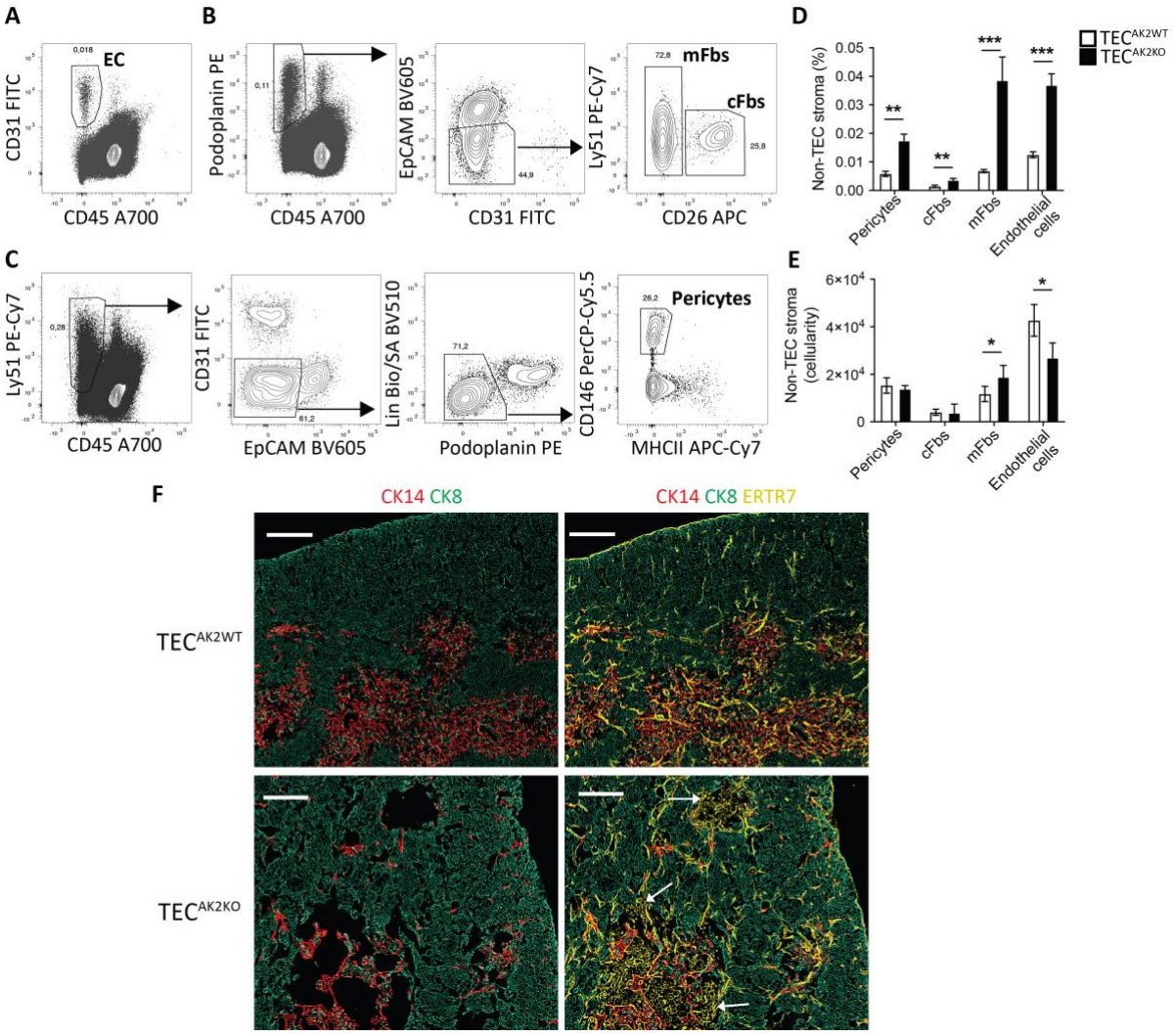

Figure 11: ***Frequency of non-TEC stroma subsets is increased in AK2-deficient mice.***

Gating strategy (**A**-**C**) and quantitative analysis (**D**-**E**) of pericytes, capsular fibroblasts (cFbs), medullary fibroblasts (mFbs) and endothelial cells (EC) isolated from 4-week-old mice. (**F**) Representative immunohistology of thymus tissue sections from wild-type (upper panels) and mutant mice (lower panels). Tissue sections were stained for cytokeratin 8 (CK8; green), cytokeratin 14 (CK14, red), and ERTR7 (yellow), a marker for fibroblasts and endothelial cells. White arrows highlight keratin-free regions with fibroblasts with reticular pattern in mutant mice. Scale bar represents 250 µm. Data in panels D and E represent the mean value and standard deviations (SD) and its data is representative of 2 independent experiments with 3 to 5 biological replicates each. *p<0.05, **p<0.01, ***p<0.001 (unpaired Student's t test, **D-E).**

4.6 Altered energy metabolism of AK2-deficient TEC.

4.6.1 *Number of mitochondria and mitochondrial superoxide production are increased in AK2-deficient cTEC and mTEC^{lo}.*

Mitochondria provide the majority of ATP necessary for highly complex and energetically demanding cellular processes. AK2 is a critical factor that regulates the homeostasis of mitochondrial adenine nucleotides (ATP, ADP and AMP) by catalysing the reaction ATP + AMP ↔ 2ADP in the intermembrane of the mitochondria. Its deficiency in human fibroblasts or HL60 (human promyoblast cell line) impairs mitochondrial functions including routine respiration, oxidative respiration and mitochondrial polarization[77,86]. A loss of the regular ATP::ADP::AMP balance may therefore affect TEC differentiation and function, as previously shown for hematopoiesis[77].

Several parameters were investigated by flow cytometry to understand how a lack of AK2 expression affects the function of mitochondria. The mass of metabolically active mitochondria was assessed using the cell permeable fluorescent probe (Mitotracker Deep Red)[127] whereas mitochondrial superoxide production was measured with another cell permeable probe (MitoSOX Red) that acquires fluorescent properties following a reaction with superoxide. In accordance to Cossarizza's guidelines for flow cytometry[128] to limit staining artefacts, median fluorescence intersity (MedFI) was chosen over mean fluorescence intensity (MFI) and the MedFI was normalized to FSC-W^3 as estimation of cell volume since the AK2-deficient TEC displayed higher FSC-W values (data not shown). The mitochondrial probe 5,5′,6,6′-tetrachloro-1,1′,3,3′-tetraethylbenzimidazolylcarbocyanine iodide (JC-1) was used to detect changes in mitochondrial polarization since the synthesis of ATP is driven by mitochondrial membrane polarization. JC-1 aggregates in hyperpolarized mitochondria are spectrally distinguishable from monomers which permits to identify cell with hyperpolarized mitochondria by flow cytometry[129]. cTEC and mTEC^{lo} isolated from TEC^{AK2KO} mice showed an increased mass of active mitochondria (Figure **12A**), enhanced mitochondrial superoxide production (Figure **12B**) and a higher degree of mitochondrial membrane polarization (Figure **12C**). The two latter findings are likely interconnected as increased superoxide production can be attributed to the hyperpolarization of mitochondria[130] which could be the consequence of a decreased ADP renewal secondary to an absence of AK2 in mitochondria. In the absence of sufficient ADP, ATP synthase cannot generate sufficient ATP in exchange of a reduction of mitochondrial polarization which is why the latter remains high[131]. An increased superoxide

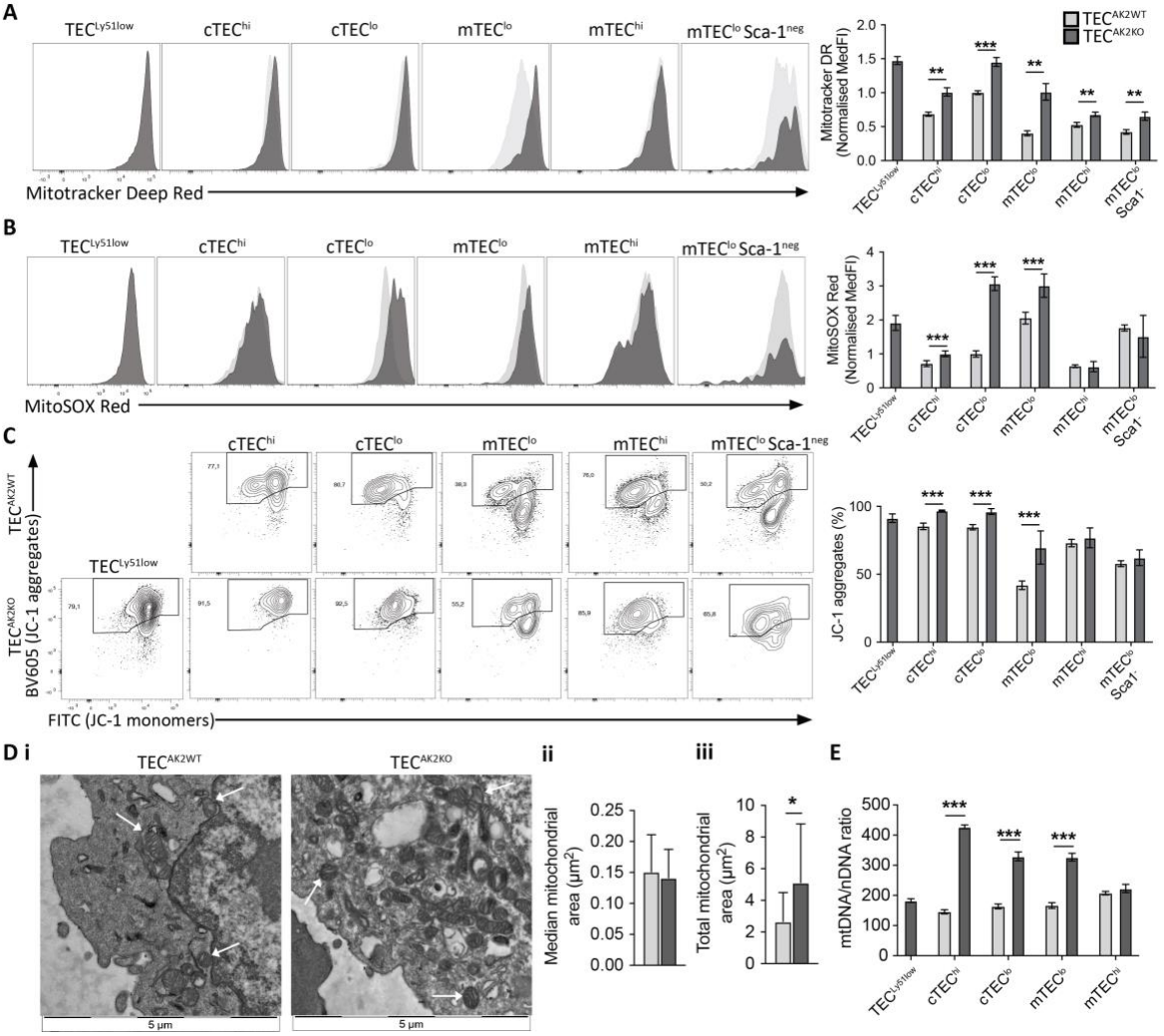

Figure 12: ***Mitochondrial mass, mitochondrial polarization and mitochondrial superoxide production is increased in AK2-deficient cTEC and mTEC^{lo}.***

(**A-C**) Flow cytometric analysis of mass of active mitochondria (Mitotracker DR), mitochondrial superoxide production (MitoSOX Red) and mitochondrial membrane polarization (JC-1) in the indicated TEC subpopulations isolated from 4-week-old TEC^{AK2WT} and TEC^{AK2KO} mice, respectively. (**A-B**) Left: Representative histograms of (**A**) Mitotracker DR and (**B**) MitoSOX Red signals; right: normalized median fluorescent intensity. To correct for cell size[128], the median fluorescence intensity (MedFI) was divided by the median FSC-W^3 value as a proxy to estimate cell size. To adjust for inter-sample variability during the experiment, MedFI values from thymocytes or B cells added to every sample were analysed in parallel as internal standard. Resulting values were normalized to the mean value obtained for wild type cTEC^{lo} set to an arbitrary value of "1". (**C**) Left: Representative contour plots and gating strategy of indicated TEC subpopulations to assess JC-1 signals; right: relative frequency of JC-1 aggregates (BV605^{pos}) in the indicated TEC subpopulations. (**D**) (**i**) Transmission electron micrograph of cytometrically sorted TEC from 4-week-old TEC^{AK2WT} and TEC^{AK2KO} mice; (**ii**) median area per mitochondrion in TEC; (**iii**) total mitochondrial area per cell. White arrows highlight some individual mitochondria. (**E**) qPCR analysis of the mitochondrial DNA (mtDNA) copy number in the indicated TEC subsets presented as ratio of mitochondrial genome to nuclear genome (nDNA). Amplicons of the *Hexokinase 2* (*Hk2*) *locus* was used as a reference for the nuclear genome copy number and *NADH Dehydrogenase 1* locus (*Nd1*) for that of the

mitochondrial genome. Data in graphs represent the mean and standard deviations (SD). Data are representative of 3 (**A-B**) and 4 (**C**) independent experiments with 3 to 6 biological replicates each (**A-C**); 20 cells per genotype were analysed in panel (**D**) or 3 independent experiments were assessed with 3 technical replicates each for data shown in panel (**E**). *p<0.05, **p<0.01, ***p<0.001 (unpaired Student's t test, **A-E).**

production has been shown to be deleterious for some cells and could thus explain, at least in part, the reduction in mTEC devoid of AK2 expression. In the developmental trajectory context where mTEC develop from an intertypical TEC, a TEC subtype mainly composed of $cTEC^{lo}$ and $TEC^{Ly51low}$ in TEC^{AK2KO} mice, an enhanced amount of ROS in these two subpopulations may limit the differentiation into mTEC as the level of ROS can play an essential role in fate decision[132]. This aside, the increased quantity of ROS at this age does not trigger more apoptosis since cell death remained similar between mutant and wild-type TEC subsets at this age (Figure **6B-C**). However, an involvement of ROS in the increased apoptosis observed in embryonic TEC (Figure **8F**) cannot be excluded nor confirmed as it has not been investigated in this work. AK2-deficient $mTEC^{hi}$ and $mTEC^{lo}Sca1^{neg}$ showed an increased mass of active mitochondria (Figure **12A**) but no differences of superoxide production nor mitochondrial membrane polarization (Figure **12B-C**). Unlike other subsets, AK2-deficient $mTEC^{hi}$ did not display an augmentation of mtDNA (Figure **12E**) that parallels an increased mitochondrial mass. The relatively low increase of Mitotracker signal (±25% of increase for $mTEC^{hi}$ vs ±74% for $cTEC^{hi}$; ±77% for $cTEC^{lo}$; ±180% for $mTEC^{lo}$; ±90% for $mTEC^{lo}Sca1^{neg}$) and the similar mitochondrial genome copy number suggest that the number of mitochondria remain very comparable between mutant and wild-type $mTEC^{hi}$. Taken together, the similarity of mitochondrial characteristics with his wild-type counterpart, whether at the level of mass, polarization or level of superoxide, suggests that the absence of AK2 does not drastically impair the cellular physiology of $mTEC^{hi}$.

Cytometrically sorted total TEC ($CD45^{neg}$ $EpCAM^{pos}$ $MHCII^{pos}$) were next analysed by transmission electron microscopy to determine whether the increased mass of active mitochondria was reflective of an overall increase in these organelles themselves whilst keeping a normal frequency of the fraction of activated mitochondria or, alternatively, whether each of these mitochondria increased their individual volumes without the extending number as a consequence of an absence of AK2. This analysis revealed that an AK2-deficiency in TEC increased the cells' total cross-sectional area occupied by mitochondria (Figure **12D iii**). However, individual mitochondrion in mutant TEC displayed an estimated mean volume, as measured by the organelle's median cross-sectional area, that was comparable to that of wild

type TEC (Figure **12D ii**). Hence, the absence of AK2 expression in TEC resulted in an increase of regularly sized mitochondria. To confirm this finding with an orthogonal method, I determined the mitochondrial genome copy number employing a qPCR-mediated amplification of *Hexokinase 2* (*Hk2*) genomic sequences which are part of the mitochondrial DNA and compared this result that the amplicons of *NADH dehydrogenase 1* (*Nd1*), a sequence with two copies encoded in the nuclear DNA[133]. This analysis demonstrated a significant increase in the mitochondrial genome copy number in AK2-deficient cTEC and $mTEC^{lo}$ (Figure **12E**). Of note, among TEC subpopulations that can be defined based on their Sca-1 and MHCII expression, the number of mitochondrial DNA copies could not be quantified in AK2-deficient $mTEC^{lo}Sca1^{neg}$ due to the low abundancy of this subpopulation and then could not be compared to the increased Mitotracker signal observed in this subset (Figure **12A**).

These observations collectively demonstrated that mitochondria in TEC are significantly affected in their numbers and function secondary to the lack of AK2. In particular, cTEC and $mTEC^{lo}$ demonstrated an increased number of mitochondria, mitochondrial superoxide production and mitochondrial membrane hyperpolarization. Unlike other AK2-deficient TEC subsets, $mTEC^{hi}$ do not display increases of mitochondrial superoxide production as well as mitochondrial membrane polarization, and the number of mitochondria in this TEC subpopulation is likely unchanged or softly increased. It remains undetermined why mitochondrial characteristics are substantially affected by the loss of AK2 in others TEC but not in $mTEC^{hi}$. Mitochondrial biogenesis was increased as a likely compensatory mechanism to maximise the mitochondrial ATP production despite the absence of AK2 to renew the ADP within the mitochondrion for the ATP synthase.

4.6.2 *Increased mitochondrial biogenesis is likely driven by AMPK activation.*

Silent mating-type information regulation 2 homolog 1 (SIRT1) and AMP-activated protein kinase (AMPK) act centrally as regulators of energy homeostasis and together coordinate metabolic pathways balancing nutrient supply with a cell's demand for energy[134]. To identify the molecular mechanism(s) that underly the enhanced mitochondrial biogenesis observed in AK2-deficient TEC, the expression of these two main metabolic cell sensors was next investigated. In parallel, the expression of Transcriptional Factor A Mitochondrial (TFAM), a nuclear encoded transcription factor that regulates mitochondrial encoded gene expression and mitochondrial genome replication[135], was quantified as the absence of AK2

expression in TEC correlates in some TEC subsets (cTEC^{lo}, cTEC^{hi} and mTEC^{lo}) with an increase in mitochondrial genome copy number (Figure **12E**). However, it must be noted that changes in mitochondrial mass or mitochondrial DNA content do not necessarily correlate with changes in TFAM expression[135].

SIRT1 protein expression was detected only in the mTEC^{hi} subpopulation (Figure **13A**), an observation already reported by Chupron and his team[36]. Moreover, the frequency of Sirt1^{pos} cells was comparable between mTEC^{hi} isolated from either TEC^{AK2KO} or TEC^{AK2WT} mice. These findings showed that Sirt1 is not involved to the enhanced mitochondrial biogenesis observed in AK2-deficient cTEC and mTEC^{lo} (Figure **12A & 12E**) and its expression in mTEC^{hi} is not affected by the loss of AK2 expression.

Next, the protein expression of both active and total AMPK was investigated using flow cytometry. AMPK is activated by phosphorylation as a result of decreased ATP/AMP or ATP/ADP ratio[136]. Alternatively, AMPK can also be activated by reactive oxygen species[136]. TEC showed a similar expression level of total AMPK irrespective of AK2 expression with the notable exception of mTEC^{lo}Sca1^{neg} in TEC^{AK2KO} mice where a reduced expression of AMPK was observed (Figure **13B**). Active AMPK expression was increased in AK2-deficient cTEC^{hi}, mTEC^{lo} and mTEC^{hi} (Figure **13C**). AK2-deficient cTEC showed a decreased ATP/ADP ratio (Figure **13D**). Due to the paucity of mTEC in TEC^{AK2KO} mice, analysis of ATP/ADP ratio in this subpopulation could not be achieved with the kit used in this work due to the lack of sensitivity (data not shown). Since the activation of AMPK can be triggered by a diminution of ATP/ADP ratio, it can be hypothesized that the reduction of ATP/ADP ratio observed in cTEC (Figure **13D**) may be responsible, at least partially, of the increased activation of AMPK in cTEC^{hi} subpopulation (Figure **13B**). The absence of data regarding the ATP/ADP levels in mTEC prevents us from adopting similar reasoning regarding the increased levels of active AMPK in AK2-deficient mTEC^{lo} and mTEC^{hi}. Despite the increased mitochondrial mass (Figure **12A**), cTEC^{lo} do not display significant augmentation of active AMPK (Figure **13C**). The increased number of mitochondria observed in AK2-deficient cTEC^{lo} could come from when these cells were cTEC^{hi} and that they would have kept once differentiated in cTEC^{lo}. However, this speculative proposition is not supported by the higher Mitotracker signal observed in cTEC^{lo} in comparison to their cTEC^{hi} counterpart (Figure **12A**). An alternative hypothesis is that the increased mitochondrial mass in cTEC^{lo} from TEC^{AK2KO} mice is driven by an AMPK-independent pathway but this has not have been proven so far.

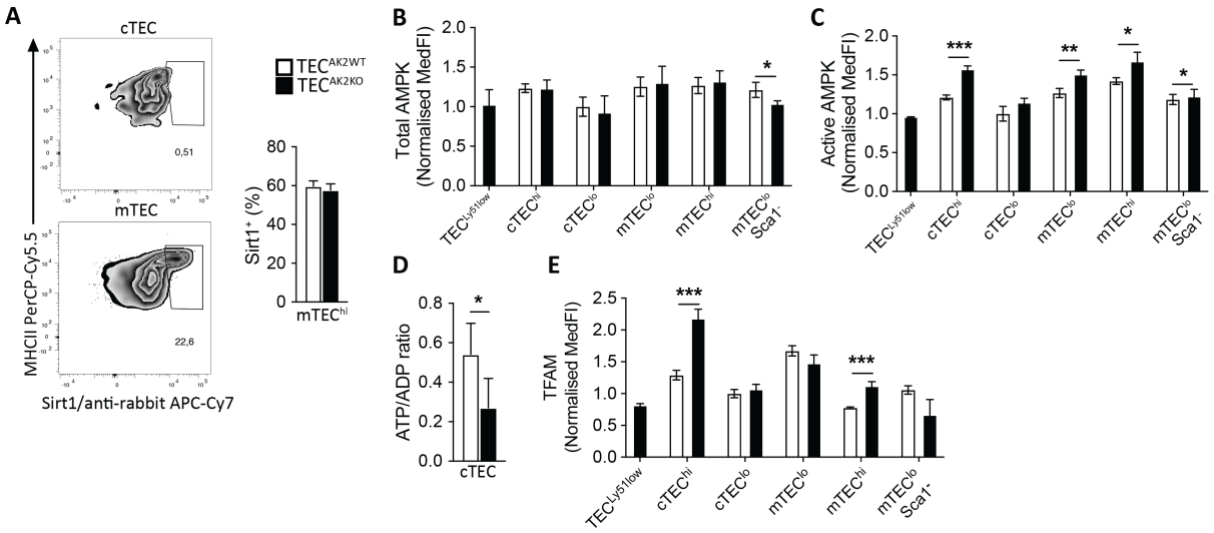

Figure 13: ***AK2-deficient TECs display an increased expression of factors involved in mitochondrial biogenesis.***

(**A**) Left: Representative zebra plots of MHCII and Sirt1 expression in unseparated cTEC and mTEC, respectively, which had been isolated from 4-week-old mice of either genetic background. Right: Frequency of $Sirt1^{pos}$ cells within $mTEC^{hi}$ isolated from 4-week-old TEC^{AK2WT} and TEC^{AK2KO} mice as these cells are the only TEC subpopulation expressing SIRT1. (**B, C, E**) Flow cytometric analysis of (**B**) total and (**C**) active AMP-activated protein kinase (AMPK). (**D**) ATP/ADP ratio in unseparated cTEC isolated from 4-week-old TEC^{AK2WT} and TEC^{AK2KO} mice as not enough mTECs could be isolated and sorted from TEC^{AK2KO} mice for this assay. (**E**) Transcription Factor A mitochondrial (TFAM) in TEC subpopulations. Normalisation method is described in Figure **12A-C.** Data in graphs represent the mean and standard deviations (SD) and data are representative of 2 (**B**), 3 (**A**, **C, E**), or 4 (**D**) independent experiments with 3 to 5 biological replicates each. *p<0.05, **p<0.01, ***p<0.001 (unpaired Student's t test, **A-E).**

TFAM expression was significantly increased in $cTEC^{hi}$ and $mTEC^{hi}$ (Figure **13E**) but not in $cTEC^{lo}$ and $mTEC^{lo}$ from TEC^{AK2KO} mice despite the increased copy number of mtDNA (Figure **12E**) and increased mitochondrial mass (Figure **12A**). The discrepancy between TFAM expression and mitochondrial biogenesis has been reported in the literature[135]. According to authors, the relationship between TFAM and mitochondrial biogenesis or the replication of mitochondrial genome is more complex than often appreciated and TFAM cannot be assumed to be the only factor involved in the mitochondrial biogenesis although no alternative nor additional factor was mentioned by the authors.

Hence, these data, reported in a summary table for readers' convenience (Table **1**), show that the increased mitochondrial biogenesis in AK2-deficient $cTEC^{hi}$ and $mTEC^{lo}$ is likely mediated by an increased activation of AMPK because the increased number of mitochondria and the increased amount of active AMPK were correlated. The increased activation of AMPK

	Mass of active mitochondria	Mitochondrial superoxide	Mitochondrial memb. polar.	Active AMPK	mtDNA	TFAM
$cTEC^{hi}$	+	+	+	+	+	+
$cTEC^{lo}$	+	+	+	=	+	=
$mTEC^{lo}$	+	+	+	+	+	=
$mTEC^{hi}$	+	=	=	=	=	+
$mTEC^{lo}\ Sca1^{neg}$	+	=	=	+	n.d.	=

Table 1: ***Summary table of mitochondrial characteristics and factors involved in mitochondrial biogenesis significantly changed in AK2-deficient TEC subpopulations.***

Parameters significantly increased in AK2-deficient subpopulation in comparison to their wild-type counterpart are represented with a plus sign (+). Parameters not significantly changed are represented with an equal sign (=). The copy number of mitochondrial genome was not determined (n.d.) in $mTEC^{lo}\ Sca1^{neg}$ due to the scarcity of this subpopulation in TEC^{AK2KO} mice. The parameters reported in the table are the following: the mass of active mitochondria (Mitotracker DR), the amount of mitochondrial superoxide (MitoSOX Red), the mitochondrial membrane polarization (JC-1 aggregates), the amount of active AMPK (pAMPK), the copy number of mitochondrial genome (mtDNA) and the amount of TFAM.

may result from an impaired balance of ATP and ADP, a finding reported for AK2-deficient cTEC but not confirmed in AK2-deficient mTEC due to the scarcity of these cells. The absence of AK2 to mediate adenine nucleotide homeostasis can explain the impairment of ATP/ADP balance. Since ROS can also induce the activation of AMPK, the enhanced mitochondrial superoxide production, resulting from a hyperpolarization of mitochondrial membrane, may also play a role the activation of AMPK in AK2-deficient $cTEC^{hi}$ and $mTEC^{lo}$. The molecular mechanism underlying greater number of mitochondria in mutant $cTEC^{lo}$ remains unclear since neither AMPK nor TFAM are enhanced in this subpopulation. The involvement of additional mitochondrial biogenesis pathways as well as a retention of a greater number of mitochondria generated in a previous $cTEC^{hi}$ developmental stage may explain the findings but these propositions remain purely speculative and would need to be confirmed experimentally.

4.6.3 *Contribution of glycolysis to total ATP production is increased in cTEC from TEC^{AK2KO} mice.*

Experiments (detailed in sections 4.6.1 and 4.6.2) demonstrated that TEC from TEC^{AK2KO} mice display an increased mitochondrial mass and mitochondrial hyperpolarization in likely response to an unbalanced adenine nucleotide homeostasis. Since the overall energy metabolic profile in TEC is likely altered by the absence of AK2 involving a switch from OXPHOS to glycolysis, which doesn't require AK2, additional compensatory mechanisms may also be in play. I therefore analysed other aspects of the energy metabolism employing the Scenith method[91].

Approximatively half of the total energy that is production in mammalian cells by degrading glucose, amino acids and/or lipids is immediately consumed by the protein synthesis (PS) machinery[91]. Contribution of each of these individual pathways to the generation of ATP can be probed separately employing specific inhibitors of critical steps within each of the separate pathways. Because ATP production is correlated with protein synthesis, the incorporation of the tyrosyl-tRNA analogue, puromycin, into nascent polypeptide chains[137] is used as a quantifiable readout for protein synthesis. Thus, ATP production can be indirectly measured by puromycin incorporation using flow cytometry. ATP production via OXPHOS can be blocked using oligomycin (OLI), an inhibitor of complex V of the electron transport chain (ETC), whereas ATP production via glycolysis can be inhibited by glucose analogue 2-Deoxyglucose (2-DG). ATP production via a combination of OXPHOS and glycolysis is repressed using a combination of 2-DG, OLI and Carbonyl cyanide 4-(trifluoromethoxy)phenylhydrazone (FCCP), an "uncoupler" of OXPHOS that disrupts the mitochondrial membrane potential.

In a first step, the Scenith assay was adapted for the analysis of embryonic and newborn TEC as these cells provided the most robust and reliable data sets. To this end, thymic lobes were cultured in medium complemented with puromycin and in the absence or presence of specific pathway inhibitors as detailed in material and methods section. After incubation, TECs were isolated from the lobes and analysed by flow cytometry. The addition of oligomycin substantially decreased puromycin incorporation (PI) in cTEC (relative puromycin incorporation in comparison to control condition: 0,44±0,07) and $TEC^{Ly51low}$ (0,27±0,08), respectively, isolated from TEC^{AK2KO} mice and cTEC isolated from TEC^{AK2WT} (0,16±0,12). The reduction of PI as a result of blocking glycolysis was less pronounced with 2-DG (0,82±0,12; 0,94±0,03; 0,97±0,01 for cTEC from TEC^{AK2WT}, cTEC and $TEC^{Ly51low}$ from

TEC^{AK2KO} mice respectively) (Figure **14C**). Thus, cTEC and $TEC^{Ly51low}$ are highly dependent on mitochondria and amino and fatty acid oxidation and less dependent on glucose and glycolysis (Figure **14C**). AK2-deficient cTEC displayed a lower dependency on mitochondria but a higher reliance on glycolysis for the generation of ATP used for protein synthesis when compared to wild type cTEC (Figure **14C**). The comparably analysis of AK-2 proficient mTEC revealed high dependence on glucose and glycolysis (Figure **14D**). This result could not be compared to the corresponding TEC subpopulation isolated from age-matched TEC^{AK2KO} mice as the cells' absolute and relative frequency precluded the isolation of a sufficient cells for testing.

Taken together these data show that in wild type (TEC^{AK2WT}) mice cTEC use preferentially the oxidative phosphorylation whereas mTEC rather use glycolysis for their ATP production. In the absence of AK2, both cTEC and $TEC^{Ly51low}$ remain mainly dependent on oxidative phosphorylation to generate their ATP but with cTEC adapting their metabolism to be less mitochondria-dependent for the generation of this resource.

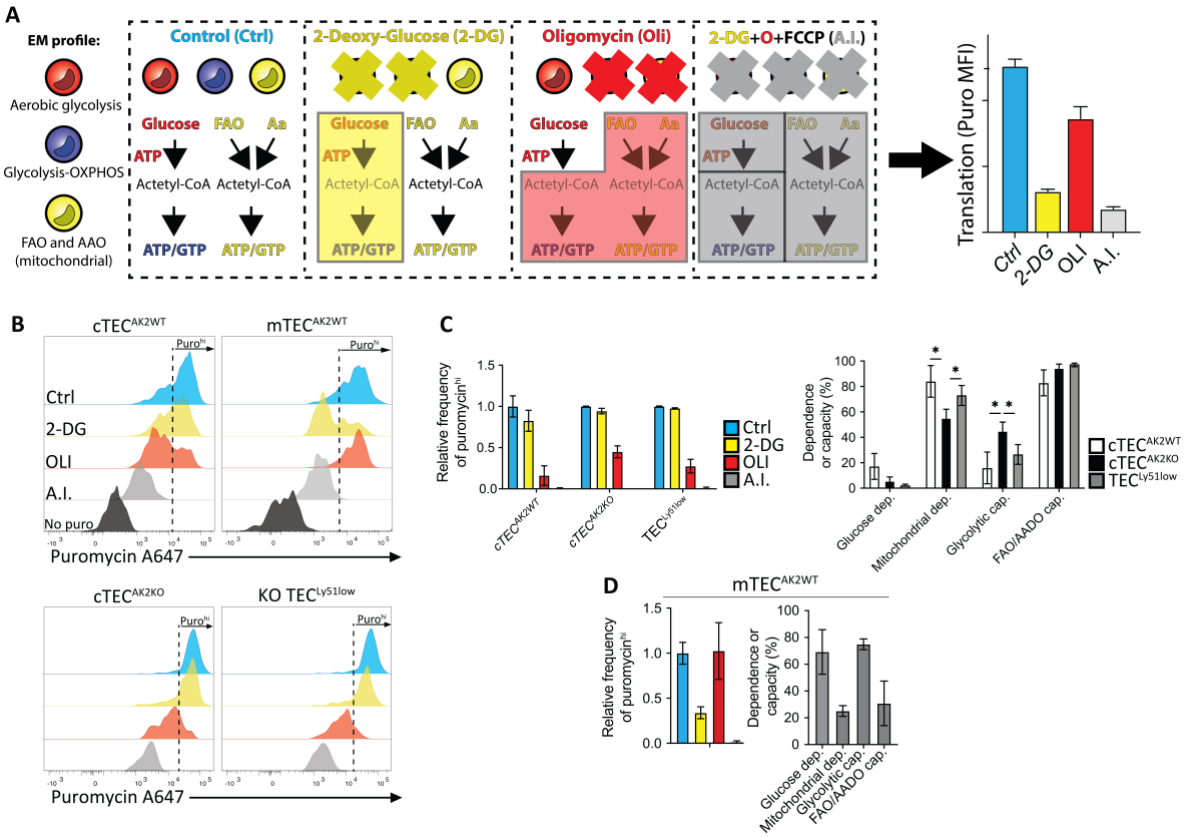

Figure 14: ***Contribution of glycolysis the production of ATP is increased in AK2-deficient cTEC.***

(**A**) Schematic representation of a sample containing three cell types with different metabolism profiles (aerobic glycolysis, glycolysis-OXPHOS, fatty acid oxidation and amino acid oxidation OXPHOS) and the inhibition of their energy metabolism pathways in Scenith assay. Schema is adapted from Argüello et al[91]. (**B**) Flow cytometric analysis of cTEC, TEC^{Ly51low} and mTEC isolated from TEC^{AK2WT} or TEC^{AK2KO} mice that were exposed to puromycin incorporation without addition of any inhibitor (Ctrl; blue), combined with either 2-deoxyglucose (2-DG; yellow), oligomycin (OLI; red), or three inhibitors, namely oligomycin, 2-DG, and Carbonyl cyanide 4-(trifluoromethoxy)phenylhydrazone (FCCP) (A.I.; grey). An additional condition in which lobes from wild-type E18.5 embryos were not exposed to puromycin (no puro; black) serves as negative control to demonstrate the incorporation of puromycin in TEC. Thymic tissue was harvested at E18.5 or 1 day after birth and cultured under the above conditions. Dashed line indicates the separation between the puromycin antibody signal peak of TEC with high puromycin content (puro^{hi}) and that of TEC with lower puromycin content. (**C-D**) (Left panels) Relative frequency of puromycin^{high} among defined TEC subpopulations cultured under the indicated conditions; (**C**, right panel) energy metabolic profiles of cTEC^{AK2WT}, cTEC^{AK2KO}, TEC^{Ly51low} and (**D,** right panel) energy metabolic profiles of mTEC^{AK2WT} calculated[91] based on the relative frequency of puromycin^{high} cells. Due to scarcity of mTECs in TEC^{AK2KO} mice at this age, a comparable analysis could not be performed in mutant mice. Data in graphs represent the mean and standard deviations (SD) and data are representative of 5 independent experiments with 3 to 5 biological replicates each. *p<0.05, **p<0.01, ***p<0.001 (unpaired Student's t test)

4.6.4 *Enzymes involved in energy metabolism are increased in TEC subpopulations of TEC^{AK2KO} mice.*

The relative dependence of separate TEC subpopulations on different metabolic pathways was established using the Scenith method. However, this approach does not quantify the key and rate-limiting enzymes involved in these pathways[138]. Individual TEC subpopulations isolated from TEC^{AK2WT} and TEC^{AK2KO} mice were therefore investigated for the expression of pathway relevant enzymes using flow cytometry. The following experiments in this section were conducted using 3–4-week-old mice in order to get a sufficient number of AK2-deficient mTEC for the analysis although it limits to some extent the comparison with data obtained with Scenith assay.

The expression of the Hexokinase 1 (HK1) was quantified as the first rate-limiting enzyme that catalyses the first step in glycolysis, namely, the conversion of glucose into glucose-6-phosphate. The analysis demonstrated an increase of HK1 in all AK-2 deficient cTEC and mTEC subpopulations (Figure **15A**). This finding correlated with the Scenith analysis which demonstrated in AK2-deficient cTEC an increased contribution of glycolysis to total ATP production (Figure **14C**). An increase in rate-limiting HK1 enzyme enables a higher ATP production through glycolysis and so renders the cell less dependent on OXPHOS, likely impaired by the absence of AK2, for their energy production.

Argininosuccinate synthase 1 (ASS1) is a rate-limiting enzyme of urea cycle that catalyses the production arginino-succinate which is then metabolised by the Argininosuccinate Lysase into arginine and fumarate, an intermediate of tricarboxylic acid (TCA) cycle[139] also known as Krebs cycle. Analysis of ASS1 by flow revealed an increased expression in $mTEC^{lo}$ and $mTEC^{hi}$ from TEC^{AK2KO} mice (Figure **15B**). Upregulation of ASS1 may provide supplementary fumarate to TCA cycle to improve OXPHOS. However, the similar ASS1 expression observed in AK2-deficient cTEC and $mTEC^{lo}$ Sca-1^{neg} suggests that this mechanism of compensation, if confirmed, is restricted to $mTEC^{lo}$ and $mTEC^{hi}$ rather than being a global mechanism. Moreover, we cannot exclude that the upregulation of ASS1 could be due to its role in urea cycle.

Carnitine palmitoyl-transferase 1A (CPT1A) is a key enzyme for the transport of fatty acids through the mitochondria prior fatty acid oxidation. The analysis revealed an increase in all cTEC and mTEC subpopulations from TEC^{AK2KO} mice with the exception of $mTEC^{lo}$ Sca-1^{neg} (Figure **15C**). As embryonic (Figure **8E**) and post-natal cTEC (not shown) are almost exclusively composed of $cTEC^{hi}$, the highest expression of CPT1A observed in $cTEC^{hi}$ is in

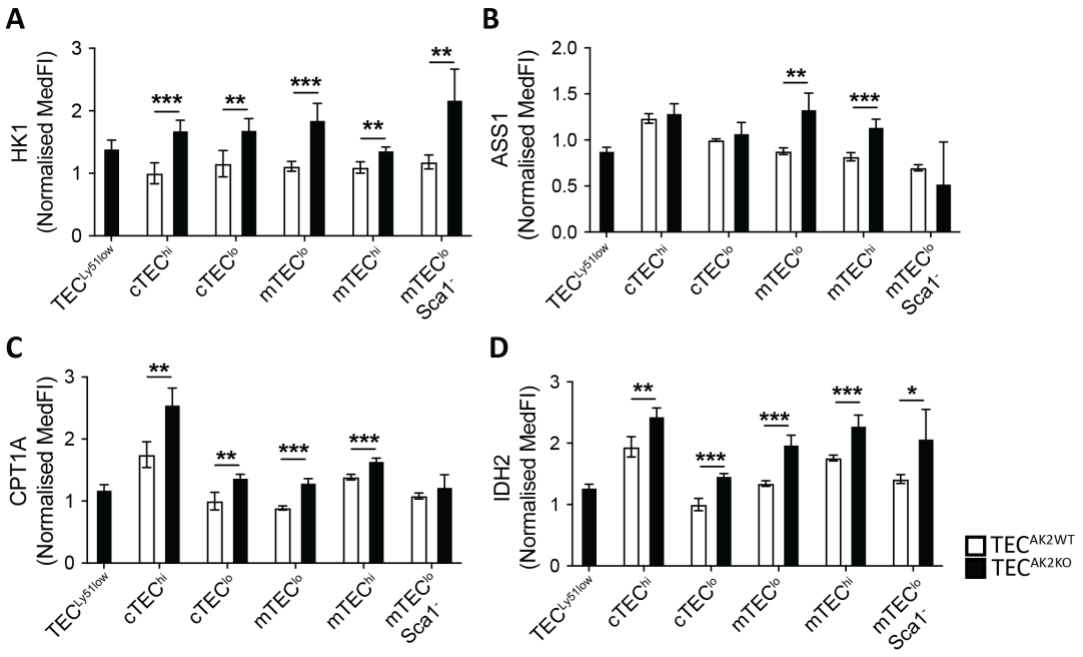

Figure 15: ***AK2-deficiency increased metabolic enzymes in a TEC subpopulation-restricted fashion.***

(**A**-**D**) Flow cytometric analysis of (**A**) Hexokinase 1 (HK1), (**B**) Argininosuccinate synthase 1 (ASS1), (**C**) Carnitine palmitoyl-transferase 1A (CPT1A) and (**D**) Isocitrate dehydrogenase (NADP(+)) 2 (IDH2) in TEC subpopulations isolated from 3-4-week-old TEC^{AK2KO} and TEC^{AK2WT} mice. The method to normalise the data is described in Figure **12**. Data in graphs represent the mean and standard deviations (SD) and data are representative of 4 (**A, B**, **D**) or 3 (**C**) independent experiments with 3 to 5 biological replicates each. *p<0.05, **p<0.01, ***p<0.001 (unpaired Student's t test, **A**-**E).**

accordance with the high dependence on fatty acid oxidation observed in cTEC (Figure **14C**). However, a caution must be applied as the metabolism of $cTEC^{hi}$ from embryos/new borns and at 3-4 weeks of age may differ, either by a global change of metabolism or by a change of subtypes composing this subpopulation[33]. Although less dependent than cTEC, mTEC are also partially dependent on FAO and AAO (Figure **14D**) and an upregulation of CPT1A may also be beneficial for their ATP production via the supplemental generation of Acetyl-Coa, NADH and $FADH^2$ during ß-oxidation[134]. Then, the upregulation of CPT1A could be compensatory mechanism adopted by AK2-deficient TEC in response to a deficient OXPHOS.

Isocitrate dehydrogenase (NADP(+)) 2 (IDH2) is a key enzyme catalysing the decarboxylation of isocitrate in TCA cycle. IDH2 expression was increased in each TEC subpopulation isolated of from TEC^{AK2KO} mice (Figure **15D**). Increase in TCA cycle activity could be a compensatory mechanism to improve energy production through an enhanced NADH, FADH2 and GTP generation[139]. Another possibility is that the increase of IDH2 could be an antioxidant response to the increased superoxide production (see Figure **12B**) since it regenerates reduced glutathione (GSH), an antioxidant molecule, via NADPH[140].

In aggregate, the loss of AK-2 expression targeted to TECs resulted in subpopulation-specific changes in metabolism and alterations in expression of key enzymes of several metabolic pathways (glycolysis, OXPHOS, fatty acid oxidation). The latter likely occurred as a compensatory mechanism to improve the antioxidant response and the generation of ATP.

4.6.5 *Increased ROS production is partially responsible for mTEC reduction in TEC^{AK2KO} mice.*

Two possible explanations were formulated to account for the reduction of mTEC in TEC^{AK2KO} mice: (i) The increased ROS production resulting from the hyperpolarization of mitochondria (see Figure **12B**) could be "toxic" and impair the differentiation of TEC progenitors to mTEC; or, alternatively, (ii) insufficient cellular energy is available secondary to impaired OXPHOS which in turn hinders normal TEC development. The latter explanation would match with several mechanisms in place to generate energy in AK2-deficient cTEC via a compensatory mechanism: we observed in these cells an increased number of mitochondria, a higher reliance on glycolysis for the production of ATP, and yet decreased ATP/ADP ratio (see Figure **13D**).

To test these hypotheses, foetal thymic organ cultures (FTOC) were exposed either to 5mM of N-Acetyl-L-Cysteine (NAC), an antioxidant molecule expected to improve differentiation of AK2 deficient mTEC, or to 1 nM of oligomycin, an inhibitor of OXPHOS anticipated to further impair mTEC differentiation in cultured thymus lobes isolated from TEC^{AK2KO} embryos. mTEC differentiation was assessed by the relative frequency of semi-mature mTEC (SM mTEC; UEA-1^{int}) and mature mTEC (UEA-1^{hi}; Figure **16A**).

The addition of NAC to FTOC cultures increased the number of AK2-deficient semi-mature and mature AK2-deficient mTEC by 74% and 55%, (Figure **16B**) relative to untreated cultures. However, the cellularity remained low in comparison to wild-type lobes (±3,866 semi-mature mTEC and 519 mature mTEC for AK2-deficient treated lobes VS ±17,518 semi-mature mTEC and 2,398 mature mTEC for wild-type untreated lobes). In contrast, a reduction of wild type mature mTEC was observed using identical culture conditions is likely due to the inhibition of αß T cell development by NAC[141] and the resulting decreased cell-cell interactions necessary for the development of mTEC[142]. The same effect likely occurs with mutant lobes but the improvement provided by reduction of ROS surpassed the impairment of

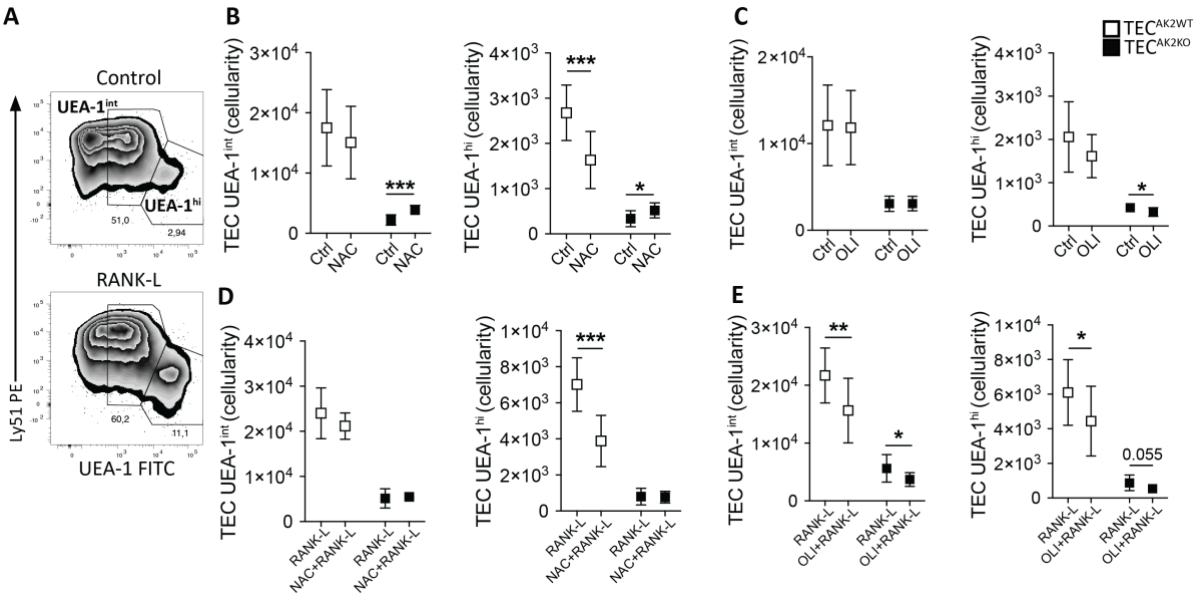

Figure 16: ***Antioxidant treatment improved development of AK2-deficient mTEC in FTOC and oligomycin treatment impaired RANK-induced mTEC differentiation.***

(**A**) Gating strategy to define semi-mature UEA-1^{int} TEC and mature UEA-1^{hi} TEC. Representative zebra plots of Ly51 expression and UEA-1 reactivity. Upper row: TEC under control condition (control); Lower row: TEC in presence of RANK-ligand (RANK-L). RANK-L added to cell culture medium fosters mTEC. (**B-E**) Thymic lobes were isolated from TEC^{AK2KO} and TEC^{AK2WT} E14.5 embryos and incubated in Fetal Thymus Organ Culture (FTOC) for 4 days. Number of UEA-1^{int} TEC (left) and UEA-1^{hi} TEC (right) collected from individual thymus lobes cultured either (**B-C**) under control conditions (ctrl); (**B**) in the presence of in presence of 5 mM of N-Acetyl-L-Cysteine (NAC); (**C**) 1 nM of oligomycin (OLI); (**D-E**) RANK-L treatment; (**D**) RANK-L and 5 mM of NAC; (**E**) RANK-L and 1 nM of oligomycin. NAC and oligomycin were renewed at day 2. Data in graphs represent the mean and standard deviations (SD) and are pooled of 3 independent experiments with 2 to 6 biological replicates each. *p<0.05, *¨p<0.01, ***p<0.001 (Student's t test, **B-E**).

thymocyte development and the following decreased cell-cell interactions. These data demonstrate that a reduction in ROS availability increased the number of mTEC in TEC^{AK2KO} mice but is not the only factor involved in mTEC reduction since treatment with NAC reversed the loss of mTEC only partially.

Culturing TEC^{AK2KO} thymic lobes in the presence of oligomycin significantly (p-value<0,029) decreased the number mature mTEC (23,3%) (Figure **16C**). Number of mature wild type mTEC cultured in the presence of oligomycin was reduced (22,7%) but not significantly (p-value ≈ 0,1) due to the high variance. These observations indicate that the inhibition of OXPHOS reduces the number of mature mTEC, either by a block of maturation, induction of apoptosis or a reduction of proliferation. An indirect effect of oligomycin treatment via thymocytes cannot be excluded.

Embryonic mTEC development is critically dependent on the cells' receptor activator of NF-kB (RANK) binding to its cognate ligand (RANK-L) which is provided by different hematopoietic cells[24,25]. Indeed, previous experiments had demonstrated that the addition of RANK-L to appropriate FTOC culture conditions increases differentiation into mTECs. Hence, RANK-L was added to FTOCs either alone or in combination with NAC or OLI. Thymic lobes from E14.5 TEC^{AK2WT} and TEC^{AK2KO} embryos were treated with RANK-L with or without inhibitors for 4 days with addition of new drug after 48 hours.

Exposure to RANK-L increased the number of AK2-deficient semi-mature and mature mTEC by 86-131% and 106-139%, respectively (Figure **16D-E**). However, this treatment did not catch up the gap with untreated wild-type lobes. Semi-mature and mature mTECs remained 2- to 3-fold times less abundant in mutant lobes incubated with RANK-L than in wild-type lobes without any treatment. The addition of NAC to RANK-L supplemented cultures did not increase mutant mTEC cellularity (Figure **16D**). This observation suggests that the reduction in ROS amount in mutant TEC does not bring additional improvement when mTEC differentiation is stimulated by RANK-L. In contrast, the number of mature wild type mTEC was decreased under identical conditions. Hence, the indirect impairment of NAC on mTEC differentiation via thymocytes development remained despite the induction of mTEC differentiation by RANK-L.

The combination of RANK-L and oligomycin in the culture decreased the number of semi-mature mTEC in control and mutant lobes significantly (p-value≈0,007 for WT and ≈0,042 for KO) and substantially (-28% for WT and -34% for KO) (Figure **16E**). The cellularity of mature mTEC was significantly decreased in control lobes (-27,2%, p-value≈0,045) while mutant lobes displayed a reduction (-38,9%) that did not reach statistical significance (p-value ≈ 0,055). These data indicated that OXPHOS was crucial for mTEC development when triggered by RANK signalling. Moreover, the bigger decrease of semi-mature (-28% for WT vs -34,2% for KO) and mature mTECs (-27,2% for WT vs -38,2% for KO) in TEC^{AK2KO} lobes grown in the combined presence of RANK-L and oligomycin suggested the impairment of OXPHOS had a bigger impact on RANK-induced development of AK2-deficient mTEC when compared to the corresponding controls. A possible explanation is a more severe impairment of OXPHOS by the combination of oligomycin and AK2-deficiency. Hence, the oxidative phosphorylation is even less able to respond to the greater energy demand following RANK-induced mTEC differentiation.

Taken together, these data showed that the generation of ROS and the impairment of OXPHOS were likely crucial factors responsible for a reduction in mTEC cellularity in TEC^{AK2KO} mice.

4.7 Impaired recruitment of lymphoid progenitors to the thymus of TEC^{AK2KO} mice and compromised thymopoïetic function in the presence of AK2-deficient TEC.

4.7.1 *The expression of chemokines required for the recruitment of lymphoid progenitors to the thymus is reduced in TEC^{AK2KO} mice.*

The decreased frequency of the earliest T cell precursors in TEC^{AK2KO} mice (see Figure **3A**) could be explained by two different yet not mutually exclusive mechanisms, namely an impaired recruitment of these cells from the blood to the thymic microenvironment and, alternatively, a compromised survival of these precursors once recruited to the thymus. The mechanism for homing of blood-borne precursor to the thymus microenvironment is controlled by different chemokines expressed in separate TEC subsets[143], including the cc-chemokine ligands 21 (CCL21) and 25 (CCL25)[47].

In the thymus, CCL21 is mainly expressed by mTEC^{lo} and mTEC^{lo}Sca1^{neg} (Figure **17A**). The frequency of CCL21-positive cells was greatly decreased in both mTEC^{lo} (reduction of 40-76% in comparison to wild-type cells) and mTEC^{lo}Sca1^{neg} (reduction of 40-68% in comparison to wild-type cells) lacking AK2 expression (Figure **17A**). Though detected also in other TEC subpopulations, CCL21 expression was limited in expression and comparable between wild type and mutant TEC. CCL25 expression was decreased in AK2-deficient cTEC in both subpopulations (cTEC^{hi} and cTEC^{lo}) in comparison to the corresponding controls (Figure **17B**).

In aggregate, these data correlated the limited attraction of T cell progenitors to the thymus of TEC^{AK2KO} mice to a decrease in CCL21 and CCL25 suggesting a mechanistic link between the two results. However, this point has not been formally tested.

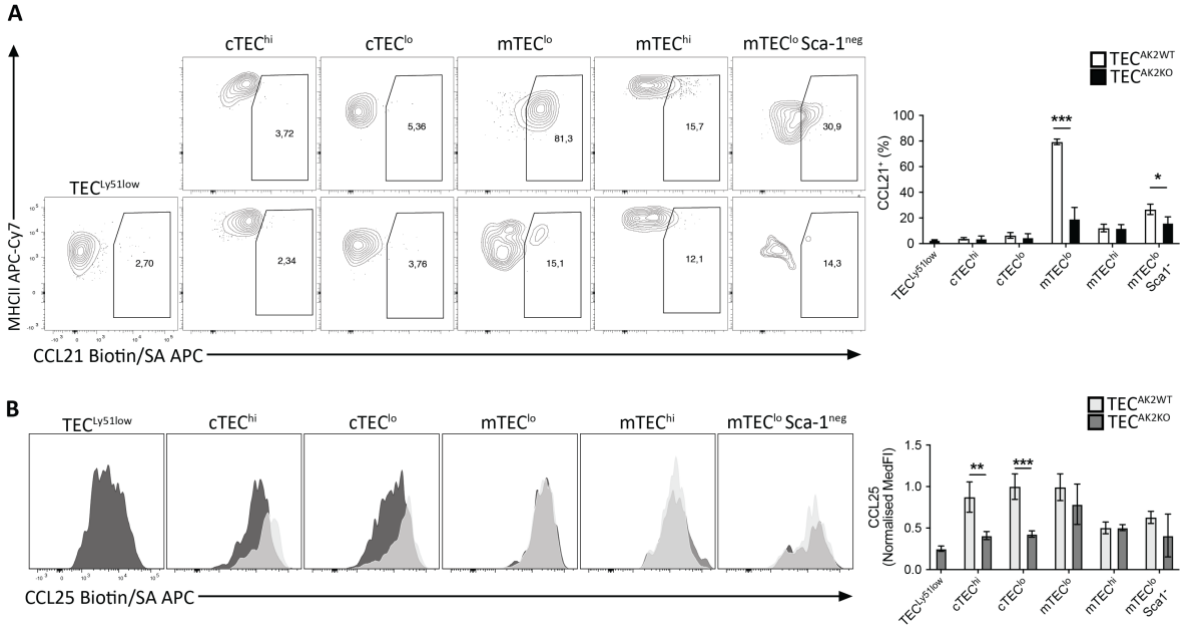

Figure 17: ***CCL21-expressing TEC and CCL25 expression are decreased in TEC^{AK2KO} mice.***

(**A-B**) Flow cytometric analysis of CCL21 and CCL25 expression in distinct TEC subpopulations isolated from 3-4-week-old TEC^{AK2WT} and TEC^{AK2KO} mice, respectively. (**A**) CCL21 expression Left: Gating strategy; right: quantitative analysis of CCL21 expression in indicated TEC subpopulations isolated from TEC^{AK2WT} (upper row) and TEC^{AK2KO} mice (lower row). (**B**) Left: Representative histograms of CCL25 expression in TEC isolated from TEC^{AK2WT} (grey) and TEC^{AK2KO} mice (black), respectively right: normalized median fluorescent intensity. To correct for cell size, the median fluorescence intensity (MedFI) was divided by the median FSC-W^3 value as a surrogate to estimate cell size. Resulting values were normalized to mean value of cTEC^{lo} from TEC^{AK2WT} mice for comparison purpose. Data in graphs represent the mean and standard deviations (SD). Data are representative of 3 (**A**) or 2 (**B**) independent experiments with 3 to 5 biological replicates each. *p<0.05, **p<0.01, ***p<0.001 (unpaired Student's t test, **A-E).**

4.7.2 *Positive and negative selection are decreased in TEC^{AK2KO} mice.*

An essential role of the TEC scaffold during thymocyte differentiation is to enforce positive and negative selection of their TCR specificities[29]. Because the loss of AK2 targeted to TEC resulted in substantial changes in their cellularity and differentiation, the efficiency of thymocyte selection was assessed in TEC^{AK2KO} mice.

Positive thymocyte selection is exclusively effected by cTEC. To probe the efficiency of the different cTEC subpopulations in implementing positive thymocyte selection, different cTEC populations were purified from wild type and mutant mice and their capacity were compared in reaggregate thymic organ culture (RTOC). Unseparated cTEC from TEC^{AK2WT}

mice and $TEC^{Ly51low}$ and cTEC from TEC^{AK2KO} mice were sorted by FACS, reaggregated with purified pre-positive selection DP thymocytes ($CD69^{neg}$ $CD4^{pos}$ $CD8^{pos}$) and analysed two days later by flow cytometry (Figure **18A-D**). Under these conditions, thymocytes that had successfully undergone positive selection were scored by their upregulation of the activation marker CD69 and a mild reduction in CD8 expression (Figure **18E** and ref. [57]). In comparison to wild type cTEC, both types of cortical epithelia isolated from TEC^{AK2KO} mice displayed a lower capacity to induce positive selection (Figure **18E**) demonstrating that AK2 was required to effect this selection step efficiently.

The negative thymocyte selection, which follow positive thymocyte selection, occur in two separate consecutive waves, first in the cortex (wave 1) and then in the medulla (wave 2). Each of these waves are further differentiated into two separate events, designated "a" and "b" depending on the specific stage of thymocyte maturation when they occur. Thymocytes that are subject to these selection events are marked by the cell surface expression of PD1 and/or Helios[37]. Wave 1a negative selection (phenotypically marked by the expression of Helios and PD-1 on $TCR_{ß}^{pos}$ $FOXP3^{neg}$ $CCR7^{neg}$ $SP4^{excl}$ $SP8^{excl}$ thymocytes) was decreased in TEC^{AK2KO} mice (Figure **18F**). As this specific event occurs in the cortex[37], these data indicate that AK2-deficient cTEC and $TEC^{Ly51low}$ have a reduced capacity to negatively selection. Wave 1b negative selection (phenotypically marked by the expression of Helios and PD-1 on SM CD4 thymocytes) remained unchanged in TEC^{AK2KO} mice. Wave 2a of negative selection (marked by the expression of Helios on CD4 M1 thymocytes) is mediated by mTEC and dendritic cells[39] and was also decreased in TEC^{AK2KO} mice when compared to control animals. Wave 2b of negative selection (marked by the expression of Helios on CD4 M2 thymocytes) is also mediated by mTEC and dendritic cells and was unchanged between mutant and control mice.

In summary, positive and negative selection were both reduced in thymi composed of TEC lacking AK2 expression. This defect was most likely a composite consequence of the cells' functional impairment, alterations in their lineage differentiation and changes in their relative and absolute representation within cortex and medulla.

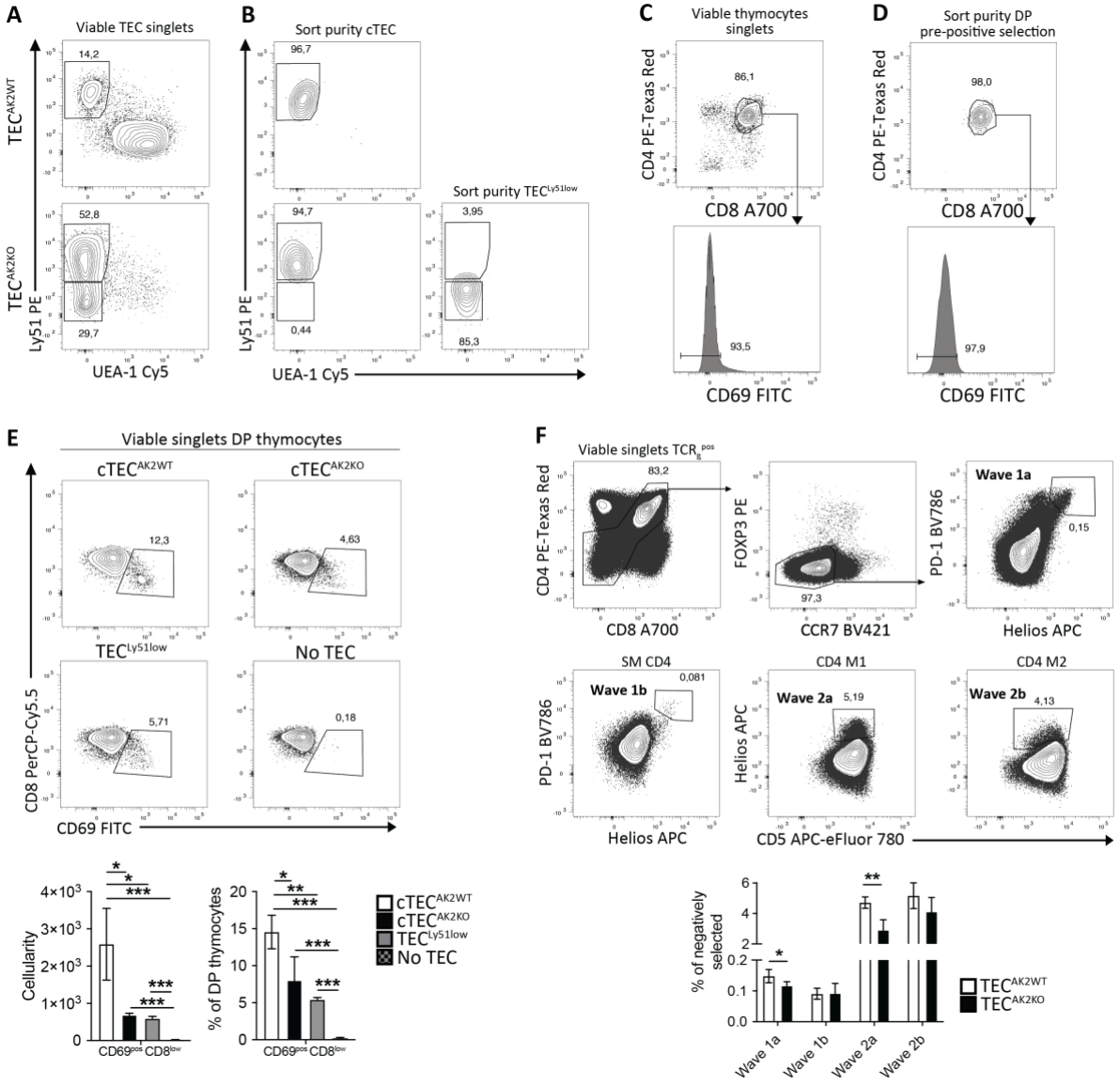

Figure 18: ***AK2-deficiency in TEC results in decreased positive and negative selection.***

(**A**-**E**) *In vitro* analysis of positive thymocyte selection using reaggregate thymic organ cultures (RTOC). (**A**, **C**) Flow cytometric sorting and gating strategies as indicated. (**B**) sort purity of cTEC from TEC^{AK2WT}, and cTEC and $TEC^{Ly51low}$ from TEC^{AK2KO} mice, isolated at the animals' age of 2 weeks. (**D**) Sort purity of $CD69^{neg}$ DP thymocytes (pre-positive selection). (**E**) Upper panel: flow cytometric analysis of positively selected thymocytes ($CD69^{pos}$ $CD8^{low}$) within DP thymocytes; Lower panels: relative and absolute cellularity of positively selected thymocytes after co-culture for 2 days with the indicated populations of thymic epithelia.. (**F**) Analysis of negative selection. Upper panels: flow cytometric analysis with display of electronic gates to identify negatively selected thymocytes; lower panels: frequencies of negatively selected cells at individual developmental stages (i.e. waves). Data shown in panels A-E were from 2-week-old TEC^{AK2WT} and TEC^{AK2KO} mice, whereas data displayed in panel F are derived from 3-4-week-old TEC^{AK2WT} and TEC^{AK2KO} mice. Data in graphs represent the mean and standard deviations (SD) and are representative of (**E**) 2 independent experiments with 3 biological replicates each or (**F**) 3 independent experiments with 4-5 biological replicates each (F). *p<0.05, **p<0.01, ***p<0.001 (Student's t test, **E**-**F**).

4.7.3 *TEC^{AK2KO} mice do not display signs of autoimmunity.*

TEC^{AK2KO} mice displayed a number of features suggesting that the resultant repertoire of selected TCR specificities may be inappropriate and could thus give rise to enhanced autoreactivity and possible autoimmunity. To test whether TEC^{AK2KO} mice harbour autoreactive T cells, typical target tissues of autoimmunity were investigated in older mice (32-38 weeks of age) for the presence and extent of mononuclear infiltrations using histology [113]. For this purpose, tissue sections of pancreas, liver, salivary gland, eye, kidney, stomach and thyroid gland were prepared and stained with Haematoxylin-Erythrosine B. The analysis and the scoring of the degree of infiltration occurred in a blinded fashion. The direct comparison of several tissue sections for each of the separate organs isolated from both mutant and control mice demonstrated that the absence of AK2 expression in TEC did not result in a higher likelihood to develop autoimmunity as read out by target organ infiltration (Figure **19A**).

To assess whether TEC^{AK2KO} mice harbour auto-reactive antibodies, as another sign of a loss of normal thymic self-tolerance induction, the serum was screened by indirect immunofluorescence for reactivity to an array of tissues isolated from Rag2-deficient mice (which lack B cells and thus antibodies altogether). To score the presence of antibody binding, anti-nuclear antibodies and sera from Rag2-deficient mice were used as positive and negative controls, respectively. The analysis of sera from TEC^{AK2WT} and TEC^{AK2KO} mice revealed comparable staining patterns on all tissue sections investigated (Figure **19B**). Hence, the absence of AK2 expression engineered to TECs did not result in a loss of humoral self-tolerance.

Taken together, these data demonstrate that TEC^{AK2KO} mice are not more prone to autoimmunity despite a number of functional and structural features that could impact on the efficiency of the thymus to effectively establish self- tolerance. The lack of overt autoreactivity may be the consequence of compensatory mechanisms such as an increased frequency of active Treg and anergic T cells, and an increased presence of medullary fibroblasts which may serve as an additional source of self-antigens[120] , all features observed in TEC^{AK2KO} mice.

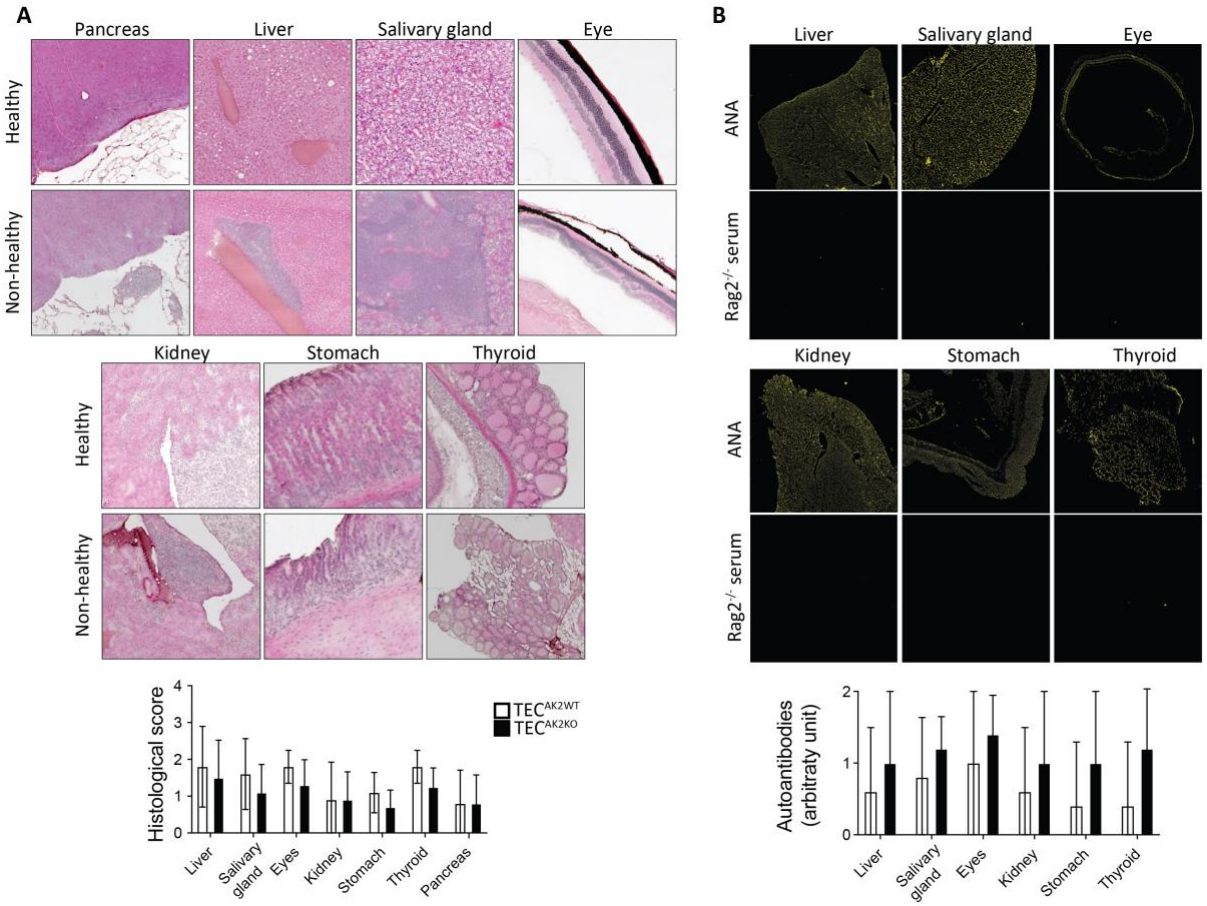

Figure 19: ***TEC^{AK2KO} mice do not reveal signs of autoimmunity.***

(**A**) Top and middle panels: haematoxylin and erythrosine B staining of histological sections from pancreas, liver, salivary gland, eye, kidney, stomach and thyroid gland tissue isolated from 32-38-week-old TEC^{AK2KO} and TEC^{AK2WT} mice, respectively. Bottom panel: Statistical analysis of histological scores based on severity (0=healthy tissue; 1=visible but small lymphocytic infiltrates; 2=medium-size lymphocytic infiltrates and/or disruption of histological integrity 3=large infiltrates and/or severe disruption of histological integrity). (**B**) Top and middle panels: Immunohistology of the indicated tissues isolated from Rag2-deficient mice and incubated with serum obtained from Rag2$^{-/-}$ mice or anti-nuclear antibodies (ANA). Anti-nuclear antibodies and sera from Rag2-deficient mice were used as positive and negative controls respectively. An arbitrary score of 3 was given for a staining intensity alike that of ANA whereas as score of 0 was computed for a staining intensity identical to that obtained with serum from Rag2-deficient mice. Bottom panel: Bar graph displaying the staining scores for each of the indicated tissues comparing sera of 32-38-week-old TEC^{AK2KO} and TEC^{AK2WT} mice Data in bar graphs are from 5 biological replicates per group. *p<0.05, **p<0.01, ***p<0.001 (non-parametric Mann-Whitney test, **A-B**).

5. Summary of findings

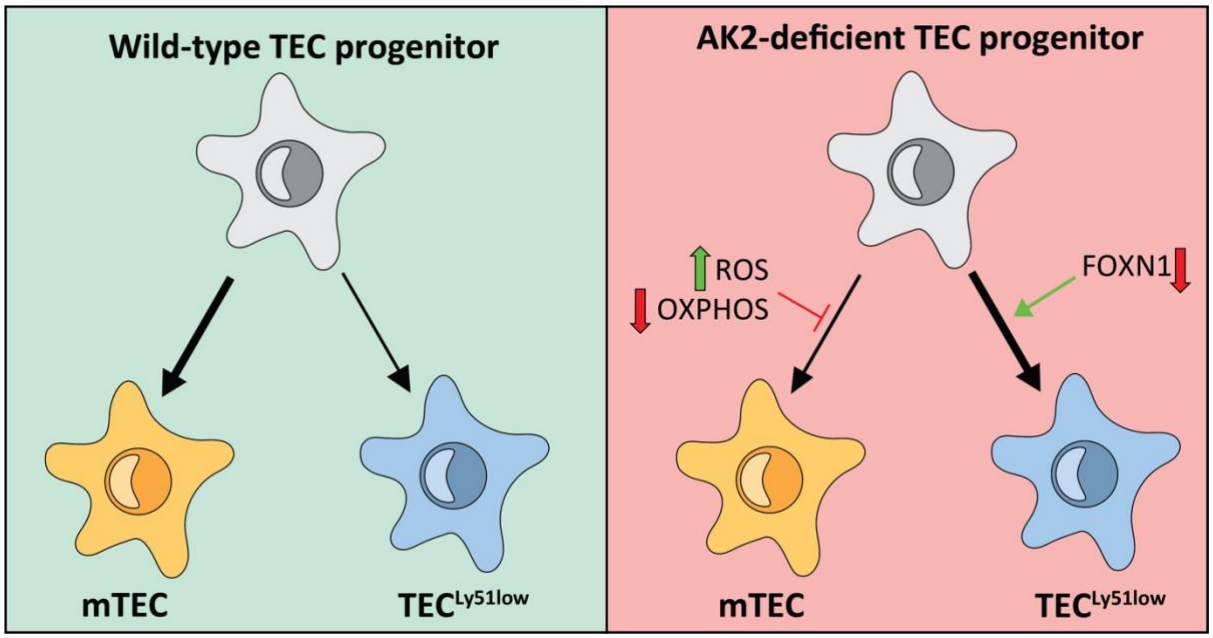

Figure 1: TEC development is biased toward $TEC^{Ly51low}$ in TEC^{AK2KO} mice.

In the absence of AK2 targeted to TEC, the cellularity of medullary epithelia is reduced and the frequency of a rare TEC phenotype, designated $TEC^{Ly51low}$, is increased. The emergence of $TEC^{Ly51low}$ correlates with a decreased expression of the transcription factor FOXN1. Increased ROS and impaired OXPHOS partially block the development of mTEC.

AK2-deficiency targeted exclusively to mouse thymic epithelial cells (TEC) is compatible with life, yet thymic size and cellularity are reduced as early as embryonic day (E) 16.5. These features become more prominent during the postnatal parts of the life course and are observed as late as 38 weeks of age. The absence of AK2 in TEC also impacts on the architectural organisation of the thymic medulla as its reduced size generates islands that are largely confined to a single, central position area within the tissue in lieu of a branched structure resulting in separate medullary islands on tissue cross sections. Furthermore, the medullary compartments formed in AK2 mutant mice also contain areas where epithelia are replaced by fibroblasts.

The make-up of the thymic microenvironment is significantly altered consequent to a loss of AK2 expression with a reduction mTEC cellularity by as much as 10- to 75-fold. In embryos, AK-2-deficient TEC show a reduced proliferation and increased apoptosis whereas in young adult mice, $mTEC^{lo}$ display a higher rate of cell growth whilst cTEC proliferation is

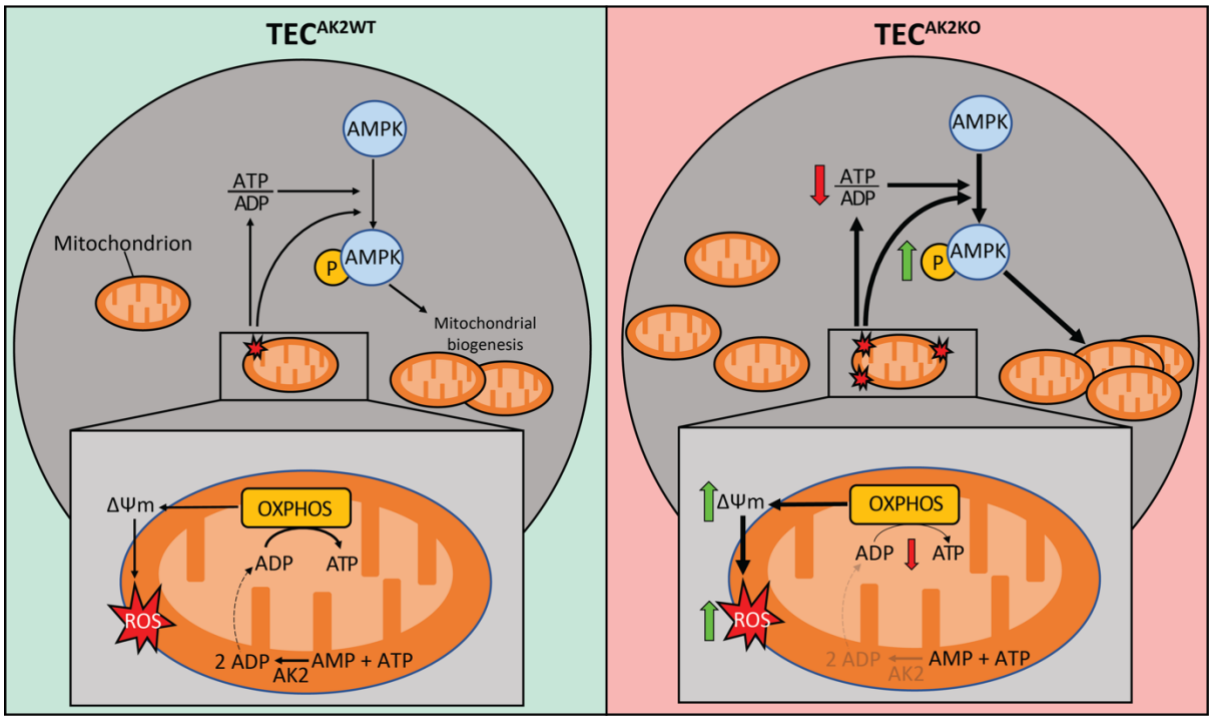

Figure 2: AK2-deficiency in TEC impairs the energy metabolism and enhances mitochondrial biogenesis.
In the absence of AK2, the renewal of ADP via oxidative phosphorylation is compromised resulting in a reduction in ATP generation. Mitochondria accumulate H^+ protons in the intermembrane space and increase their membrane potential (Ψm) as a result of a loss of AK2 availability. The consequent hyperpolarization results in the heightened generation of reactive oxygen species (ROS). Increased ROS concentrations combined with a decreased ATP/ADP ratio activate in parallel the cell biosensor AMPK which increases mitochondrial biogenesis.

maintained. A TEC population lacking classical cortical (Ly51) and medullary markers (UEA-1) is progressively identified as early as E17.5. Designated TECLy51^{low} and marked by low FOXN1 expression, these cells display many molecular features known to define immature cortical TEC including gene transcripts specific for *BMP4*[102] and *Notch1*[144] and others related to thymus morphogenesis.

The energy metabolism of AK2-deficient TEC is changed and hinders the renewal of mitochondrial ADP. The consequent reduction leads to a hyperpolarization of mitochondrial membranes and therefore the generation of higher superoxide concentrations. Because high concentrations of free radicals are toxic[145], the accumulation of reactive oxygen species are likely responsible for the low frequency of mTEC in mutant mice. In addition, the enzyme AMPK is activated in mitochondria of mutant TEC as a likely result of either a decreased ATP/ADP ratio or as a direct consequence of an exposure to reactive oxygen species[136].

Moreover, OXPHOS is reduced in AK2-deficent TEC which in turn triggers a compensatory mechanism that increases key enzymes related to the cell's energy metabolism (HK1, CPT1A, ASS1 and IDH2). Indeed, mutant cTEC adapt their metabolism to be less dependent on oxidative phosphorylation to maintain the production of ATP.

The engineered loss of AK2 expression in TEC impairs the cells' capacity to attract blood-borne haematopoietic T cell precursors and to support their development and selection along the T cell lineage. The absolute number of the most immature intrathymic T cell progenitors is reduced in TEC^{AK2KO} mice as early as E17.5 and continues after birth to remain low due to the diminished availability of CCL25 and an almost complete absence of CCL21. Moreover, partial blocks are observed in the maturational progression of thymocytes along distinct developmental stages secondary to alterations in the composition and function of thymic epithelia. These changes include the progression across beta-selection, positive thymocyte selection, CD4/CD8 lineage commitment, Treg differentiation, negative selection at multiple checkpoints and post-selection maturation of mature thymocytes. Collectively, functional aberrations in AK2-deficient TEC account for substantial T lymphopenia with peripheral T cells preferentially adopting effector and anergic phenotypes, respectively, and favouring a differentiation into effector Treg. Some of these changes deem to explain why TEC^{AK2KO} mice lack signs of autoimmunity

Taken together, the loss of AK2 expression targeted to TEC results in multiple developmental and functional changes within this haematopoietically essential stromal compartment that collectively impact on the cells' capacity to attract, select and mature thymocytes.

6. Discussion

Patients suffering from Reticular Dysgenesis have a hypoplastic thymus[86]. This clinical feature may be the result of a compromised survival and development of AK2-deficient lymphoid progenitors[146] because the cellular bulk of thymus largely (>98%) composed of developing T cells. In addition and quantitatively less prominent, defects in early thymocyte development impair TEC differentiation and growth, phenomenon defined as cross-talk and well established in experimental model systems[13] as well as in patients with primary immunodeficiencies[147]. In addition and because AK2 is also physiologically expressed in TEC, a deficiency of this enzyme due to an inborn error may also affect the cellularity and function of distinct TEC subpopulations (and other thymic stromal cells) that collectively compromise thymopoiesis. It has been reported by Hoenig et al.[68] and Bertand et al.[148] that patients that achieve successful hematopoietic stem cell transplantation show normal T cell counts. However, even though *de novo* generation of immune cells from donors' bone marrow seems to durably prevent patients to develop serious or life-threatening infections, the quality of their immune response mounted after exposition to pathogen or after vaccination has not been investigated in details.

The focus of this thesis was therefore to interrogate whether a targeted loss of AK2 expression in TEC would impact thymic stromal biology. We therefore created mice with a TEC targeted AK2 deficiency by crossing mice expressing Cre recombinase under the control of *Foxn1* promoter with mice homozygous for LoxP flanked *Ak2* exon 3 and 4. This breeding resulted in mice lacking functional AK2 in TEC.

Analysing these mice in detail unequivocally demonstrated that thymi isolated from TEC^{AK2KO} mice are smaller in size and occasionally display cysts which are visible on the organ's surface, a feature typically observed in defects of the TEC compartment consequent to the loss of gene functions. On histological analysis, the thymic tissue of TEC^{AK2KO} mice reveals a regular segregation into an outer, cell dense cortex and a centrally positioned medulla. However, the latter displays epithelial- (i.e. keratin-) free areas in which fibroblasts with a medullary phenotype (designated medullary fibroblasts, mFbs)[120] are abundantly present. Medullary fibroblasts accumulate in clusters in the centre of the medulla in the form of small islands. These morphological findings correlate with an absolute reduction in mTEC cellularity

as confirmed by flow cytometry of single thymus stromal cell suspension of mutant mice when compared to control animals. The mFbs detected in the medulla of TEC^{AK2KO} mice are seemingly increased in number and organised in an obvious reticular pattern which is reminiscent of and commonly found in lymph nodes[12]. Two possible explanations can account for the finding that medullary fibroblasts were prominently detected in the medulla, namely either the expansion of a different organization of medullary fibroblasts network predominates to medullary epithelium growth or, alternatively, a compensatory expansion of this type of fibroblasts as a consequence of the loss of mTEC. To determine the cause for this morphological observation of increase medullary fibroblasts, total and relative cellularity of medullary fibroblasts was measured in TEC^{AK2KO} mice. In comparison to wild type controls, the computed ratio of medullary fibroblasts to total thymus cellularity was higher in the mutant mice. Moreover, the total number of these cells was increased in TEC^{AK2KO} mice, suggesting that the reduction of mTEC favours the expansion of mFbs in the TEC-free space of the medulla.

The question that could be raised from these findings is whether the increased presence of medullary fibroblasts is a compensatory mechanism to compensate the reduction of mTECs. The entire mTEC population expresses thousands of tissue-restricted antigens (TRAs) that translates into faithful presentation of self, ensuring an efficient central tolerance[29,149]. Medullary fibroblasts also express TRAs but to a lower extent than mTECs[120]. Mice lacking lymphotoxin-β receptor (LTβR) specifically in fibroblasts exhibit a decreased expression of TRAs, resulting in a breakdown of immune tolerance against those TRAs with marked T cell infiltration and autoantibody production[120]. Since fibroblasts do not express MHCII to shape CD4 TCR repertory, Nitta et al.[120] suggest that, similarly to mTEC-derived TRAs that are transferred to and presented by thymic DCs[150], mFb-specific MHC-II-associated antigens might be indirectly presented by DCs to enforce CD4 T cell tolerance, which consequently establishes B cell tolerance. This combination of findings provides some support for the explanatory proposal that mFbs are expanding in medullary areas lacking medullary epithelium to maintain central tolerance. The effectiveness of mFbs to prevent the emergence of autoimmunity in TEC^{AK2KO} mice will be discussed later in the thesis with additional mechanisms of prevention observed in mutant mice.

The thymic epithelial scaffold of TEC^{AK2KO} mice displays, in addition to the aforementioned reduction of mTEC an abundant subpopulation of cells with low Ly51 expression, which I have designated $TEC^{Ly51low}$. These cells have a high phenotypic similarity

with AK2-deficient cTEC^{lo} that express low levels of cell surface MHCII and intracellular thymeoproteasome subunit-ß5t, high levels of Sca-1, CD200 and E-cadherin. To further characterise the nature of these cells, an extensive RNAseq analysis was undertaken which demonstrated an upregulation of genes previously associated with ossification and osteoblast differentiation pathways, like *Bmp4* whose implication in bone morphogenesis[151] has been established prior to that in thymus morphogenesis[152,153]. In addition to *Bmp4*, further analysis of these ossification-related pathways revealed an upregulation of *Sox9*, a transcription factor controlling TEC proliferation and differentiation[114], *Cyr61*, an ECM cell adhesive protein inducing cTEC and mTEC proliferation[115], and *Fgf9* and *Id2*, two molecules whose downregulation in ß-catenin-deficient TEC coincides with a reduced frequency of mTEC[154]. Moreover, the gene expression profile of TEC^{Ly51low} also revealed a high copy number of transcripts belonging to the Notch signalling pathway. In addition to *Notch1* itself, downstream targets such as *Hes1*[155] and *Pax1*[144] were also upregulated. This finding is of relevance as engagement of the Notch signalling pathway occurs early in TEC development but is subsequently repressed in mTEC differentiation[144]. It is therefore conceivable that TEC^{Ly51low} represent a population of cells which accumulates due to a partial block in mTEC differentiation and which would otherwise represent a transient and infrequent phenotype in wild type controls.

The differentiation along the mTEC lineage pathway is only incompletely deciphered. Findings obtained from reporter mouse strains revealed that adult cortical and medullary thymic epithelia are derived from embryonic cTEC[40–42]. Present understanding drawn from pseudo-time analyses of single cell transcriptomic data[33] however suggests that post-natal mTEC originate from intertypical TEC, a TEC subtype present in both cortical and medullary subpopulations, and expressing gene markers associated with a progenitor-like TEC^{lo} phenotype. The level of expression of proteins associated with a progenitor-like TEC^{lo} in TEC^{Ly51low} such as low levels of MHCII and high levels of Sca-1, in addition to reduction of mTEC, suggested that TEC^{Ly51low} could be blocked in intertypical TEC subtype. To probe the block at intertypical TEC stage serving as precursors to mature cortical and medullary TEC, respectively, thymic epithelia from 1 and 4-week-old wild type and mutant mice were isolated and subjected to single cell RNAseq. This approach allowed the identification and quantification of the different TEC subtypes which, in addition, could be related to distinct developmental stages.

This analysis reveals a reduction of both intertypical TEC and mature mTEC subtypes at both 1 week of 4 weeks of age. Intertypical TEC from mutant mice showed a downregulation of *Krt5*, *CCL21a* and *Ctss*, markers of mTEC fate, while markers of cTEC fate such as *Psmb11* and *Prss16* remained unchanged. Moreover, knockout intertypical TEC showed an upregulation of *Bmp4,* a gene marker associated with intertypical sub-cluster 4. This last would be, according to authors, the intertypical TEC progenitor sub-cluster from which arise cTEC and mTEC. These findings indicate that AK2-deficiency in intertypical TEC blocks the development into medullary lineage which remains in a progenitor-like state. Other subtypes in mTEC lineage, namely post-Aire and tuft-like TEC, were also decreased in TEC^{AK2KO} mice and then account for less than 0,3% of total TEC pool. All together, these findings corroborate results obtained by flow cytometry, confirming that differentiation in the mTEC lineage, regardless of the subtype, is impended by AK2-deficiency. In contrast, the relative representation of epithelia with a mature cortical transcriptional profile is increased, confirming once again results obtained by flow cytometry. This partial block to mTEC lineage can be explained by the higher energy demands for cells undergoing differentiation[74,156], likely not supplied by the oxidative phosphorylation of AK2-deficient TEC which remain at their cortical state. A direct relationship between $TEC^{Ly51low}$ representing an intermediate cell population in the trajectory of TEC precursors to differentiated mTEC could be experimentally probed with an experimental design whereby AK2 expression is specifically rescued in $TEC^{Ly51low}$ cells. Under these conditions, the questions could be asked whether $TEC^{Ly51low}$ can give rise to mTEC after that the energy metabolism was restored. However, the realisation of this experiment is technically highly challenging (if at all possible) due the present lack of suitable cell surface markers that unequivocally identifies this transient TEC stage and thus allows a temporally controlled expression of AK2 *in vivo*. An alternative approach would be to separate these cells, restore the expression of AK2 through transfection and graft them under the kidney capsule of a recipient mouse[157]. Once again, the realisation of this experiment is challenging due to the paucity of $TEC^{Ly51low}$ and the difficulty to transfect primary TECs. Such experiments are highly technically specialised and time consuming, and were, therefore, beyond the scope of this study.

In order to highlight changes in pathways potentially involved in mTEC differentiation, Gene Ontology analysis (GO analysis) was performed on the RNAseq data. Cellular location pathways GO analysis revealed a decrease of pathways involved in cell-cell junctions and cell-extracellular matrix adhesion in intertypical TEC, mature cTEC and perinatal cTEC subtypes

of TEC^{AK2KO} mice. Loss of cell-cell junctions and adhesion to extracellular matrix is one of the hallmark of epithelial-mesenchymal transition[111] and so suggests that AK2-deficient TEC may undergo an enhanced EMT. This hypothesis would have explained the reduction of mTEC through a favoured differentiation into medullary fibroblasts, increased in TEC^{AK2KO} mice, rather than a normal development from cTEC to mTEC. However, flow cytometric analysis of E-cadherin, whose downregulation is a hallmark of EMT[111], and CD200, a receptor inducing EMT in head and neck squamous cell carcinoma (HNSCC) cells[119], do not support this hypothesis since they remained similar at protein level in AK2-deficient TEC subpopulations, except for mTEC^{lo} where they are both upregulated. Moreover, the discrepancy of changes in epithelial and mesenchymal markers at transcripts level do not argue for any directional transition.

Therefore, there is no clear evidence that TEC^{AK2KO} mice are more prone to EMT, furthermore that molecular mechanisms involved in EMT processes in TECs remain largely unknown[158]. However, the potential epithelial origin of medullary fibroblasts may still be tested using a lineage tracing model or by investigation on genomic recombination generated by TEC-driven Cre recombinase.

AK2 expression in TEC also influences the capacity of these cells to proliferate and survive. A comparative analysis of AK2 proficient and deficient TEC at embryonic age 16.5 (E16.5) already reveals both a reduced proliferation and increase in the capacity of these cells to undergo spontaneous apoptosis. As a consequence, significant differences in TEC cellularity for both cTEC and mTEC can already be observed during foetal development. Comparable levels of proliferation and apoptosis are then observed in young adult TEC^{AK2KO} mice (3-4 weeks of age) yet AK2-deficient cTEC^{hi} display a lower proliferation rate when compared to the corresponding wild-type cells while AK2-deficient mTEC^{lo} of young adult TEC^{AK2KO} mice proliferate more. These differences may, in part, reflect the separate developmental dynamics in TEC differentiation between embryonic and young adult mice[40,44,102]. While embryonic TEC differentiate from a cTEC-like progenitors, post-natal TEC rather differentiate from a TEC^{lo} population substantially composed of mTEC^{lo}. Scenith assay showed that cTEC and mTEC have very different bioenergetic profiles, with a higher dependence on OXPHOS for cTEC and a higher dependence on glycolysis for mTEC. Then, with a prenatal progenitor population being composed of cTEC and a postnatal progenitor population being composed of TEC^{lo} (mainly mTEC^{lo}), energy metabolism profiles may be so different between these 2 subsets that the absence of AK2 would impact more severely prenatal progenitors than postnatal

progenitors. Alternatively, but not mutually exclusive, there may be differential dependence on AK2's catalytic activity that changes during the life course of mice. At the foetal stage, TEC display a high proliferation and differentiation rate and may thus have higher energy needs when compared TEC at 4-weeks of age when epithelial cells are most numerous. Hence, the catalytic role of AK2 providing energy substrates is more critical at a stage in life when TEC rapidly expand in number and undergo the stress of expeditious differentiation. Differential need on AK2's activity for cells undergoing or not undergoing the stress of differentiation was already observed with human B cells with hypomorphic variants in AK2[70]. Indeed, AK2-deficient B cells showed similar proliferation and survival than control B cells at basal level. But after stimulation with anti-CD40 and IL-21, proliferation of AK2-deficient B cells was enhanced but not as much as control B cells and their survival was also reduced. Analysis of energy requirements for TEC differentiation was therefore investigated and is discussed later in the manuscript.

The transcription factor FOXN1 is essential for the differentiation, maintenance and function of TEC and thus the thymus[106,159]. As early as E18.5, cTEC from TEC^{AK2KO} embryos express in comparison to their wild type controls lower concentrations of FOXN1. At the same time, the surface detection of the cortical lineage marker Ly51 is also reduced in knockout embryos. Overtime, Ly51 expression at cTEC cell surface diminishes as well as FOXN1 expression which also decreases with age[107], suggesting that Ly51 expression is linked to some extent to FOXN1 expression. Higher expression of *Foxn1* at transcript levels observed in $cTEC^{hi}$ in comparison to $cTEC^{lo}$ [160] support this hypothesis as $cTEC^{hi}$ express also Ly51 at a higher level. Based on these findings, it can be hypothesized that the emergence of $TEC^{Ly51low}$ in mutant mice is subsequent to the reduction of FOXN1 expression observed in these cells.

Unmet energy needs as a result of a loss of AK2 expression may result in an early adoption of a cTEC phenotype that is characteristically only observed later in life. Indeed, we observed in 1-week-old TEC^{AK2KO} mice that cTEC with a low MHC class II but high Sca1 positivity (collectively representing the $cTEC^{lo}$ and $TEC^{Ly51low}$ populations) are already present in abundance (±50% of total cortical epithelium). Normally, cells with this phenotype appear at the onset of puberty in wild type mice[102]. Hence, the absence of AK2 may trigger early postnatally cTEC developmental pathway ordinarily occurring later in life.

As mentioned previously, TEC^{lo}, either in knockout or wild-type mice[160], display a lower FOXN1 expression in comparison to $cTEC^{hi}$. Despite the absence of link in the literature between FOXN1 and the energy metabolism, one can wonder if the reduction of FOXN1 with

age[107] and the emergence of TEC^{lo} are linked, to some extent, to a decrease of energy metabolism. Indeed, in addition to the reduction of FOXN1 in TEC, aging has been associated with a reduction in and/or impairment of in energy metabolism[108–110] although it remains to be demonstrated for TEC. While the loss of AK2 expression results in a decrease in FOXN1 expression in cTEC and the subsequent reduced detection of surface Ly51, it remains to be directly probed how these changes link to a change in TEC differentiation secondary to a senescence-related alteration in metabolism.

AK2 is a key factor of energy metabolism through its regulation of adenine nucleotide pool homeostasis and the renewal of ADP necessary for the production of ATP by oxidative phosphorylation in the mitochondria[161]. Because AK2 has an essential role in the mitochondrial function, TECs' mitochondria were investigated. Flow cytometric analysis of TEC revealed in AK2-deficient cTEC and mTEC^{lo} an increased mass of active mitochondria concurrent with an increased copy number of mitochondrial genome. Analysis of mitochondria by electron microscopy (EM) suggests that this increased mitochondrial mass is due to a higher number of mitochondria rather than an enlargement. However, we should note that sections in EM provide only 2D information and may not faithfully reflect the real 3D organization. For that purpose, the acquisition by fluorescent microscopy of cells incubated with mitochondrial probes would be more appropriate[127,131,162]. This method has been tried with sorted TEC but without success as we could not clearly distinct mitochondrial network due to a lack of details (data not shown).

Fibroblasts of RD patients, similarly to cTEC and mTEC^{lo} from TEC^{AK2KO} mice, show an increase of mitochondrial mass[86]. This common feature between 2 different AK2-deficient cell types suggest that AK2-deficiency can lead, in some cases, to an increase of mitochondrial biogenesis as compensatory mechanism. In TEC from mutant mice, it is likely the activation of AMPK that causes the increase of mitochondrial biogenesis although it remains unclear why cTEC^{lo} from mutant mice show increased mitochondrial mass and mitochondrial genome copy number while activation of AMPK and TFAM expression are not affected. A possibility would be that AK2-deficient cTEC^{hi} increase their number of mitochondria which remains high after cTEC^{hi} differentiated into cTEC^{lo}. However, the observation that the mass of active mitochondria, probed by Mitotracker Deep Red, is even higher in cTEC^{lo} than in cTEC^{hi} does not support this hypothesis. Additional AMPK-independent factors may be involved in mitochondrial biogenesis of TEC but it remains to be demonstrated. Sirt1, the second main biosensor with AMPK, has been investigated too, but its circumscribed expression in mTEC^{hi}

subpopulation suggest its deacetylase's activity remain, in TEC, limited to the deacetylation of AIRE[36].

The activation of AMPK is likely due to observed decreased ATP/ADP ratio or increased ROS production since both can activate AMPK[136]. Further experiments dissecting their individual contribution are needed to elucidate the cause of enhancement of mitochondrial biogenesis in TEC^{AK2KO} mice.

In addition to the number, AK2-deficiency can alter other mitochondrial characteristics[70,77,84,86]. Similarly to fibroblasts from RD patient[86], AK2-deficiency leads to a hyperpolarization of mitochondrial membrane potential in cTEC and $mTEC^{lo}$ which then produce more superoxide. The most probable cause of this hyperpolarization is the activity of ATP synthase that is limited by the decreased renewal of ADP, resulting in a reduced backflow of protons in the mitochondrial matrix. Protons accumulated in the intermembrane then generate more reactive oxygen species in the mitochondria. In transgenic mice with ATP synthase inhibited by overexpression of ATPase Inhibitory Factor 1 (IF1) in brain, colon or liver[130], similar phenotype was observed, namely an increased mitochondrial membrane potential, ROS production and activation of AMPK. Although not direct evidence, the similarity between IF1 transgenic mice and TEC^{AK2KO} mice supports the hypothesis of an analogous partial block of oxidative phosphorylation by AK2-deficiency. For a direct confirmation of OXPHOS' deterioration, metabolic measurement method such as Seahorse[163] would be necessary. Unfortunately, due to technical issues such as the limited number of TEC per mouse or the paucity of culture conditions that support the functional assessment of adult TEC[103], this assay could not be achieved.

The increased ROS production is partially responsible of the reduction of mTEC in TEC^{AK2KO} mice. Indeed, treatment of TEC^{AK2KO} lobes with the reducing molecule NAC partially reversed the mTEC reduction. Furthermore, the real impact of NAC on AK2-deficient TEC may be even underestimated as NAC treatment induces an indirect reduction of mature mTEC via the inhibition of αß T cell development by NAC[141,142]. In our experimental FTOC setting, this effect led to a ±40% reduction of most mature mTEC in wild-type lobes in presence or in absence of RANK-L. These data corroborate findings by Rissone et al.[84] who observed in hematopoietic tissue from *ak2* knockout zebrafish an increased levels of reactive oxygen species and apoptosis that could partially be rescued by treatments with antioxidant molecules such as NAC or glutathione (GSH). However, ROS are unlikely the main cause that prevents mTEC development. Indeed, NAC treatment recovers mTEC cellularity of mutant mice but

only partially (mTECs from TEC^{AK2KO} mice remain 5x less numerous than wild-type) and does not provide any supplemental improvement when mTEC differentiation is boosted with RANK ligand. These findings indicate that another factor, probably the diminished OXPHOS' capacity hypothesized earlier, is the principal cause behind the reduction of mTEC in TEC^{AK2KO} mice although we cannot neglect the role of ROS in this diminution.

cTEC mainly rely on oxidative phosphorylation to produce ATP while mTEC mainly rely on glycolysis. However, loss of AK2, which activity mediates OXPHOS, highly reduces the number of mTECs rather than cTECs. This paradox can be explained by the role of OXPHOS in differentiation. Indeed, cells with low energy demands like hematopoïetic stem cells preferentially use glycolysis and switch to OXPHOS to supply enough energy for their differentiation[105,156]. Importance of OXPHOS in mTEC differentiation was confirmed in FTOC experiments where RANK-induced mTEC differentiation was decreased in the presence of oligomycin. Thus, OXPHOS in AK2-deficient cTEC is likely insufficient to respond to the greater energy demand needed for the differentiation into mTEC, favouring glycolysis to supply their needs in energy as observed in Scenith assay. Findings reported by Six et al[77] on HL60 cells support this hypothesis: AK2-deficiency impaired the mitochondrial metabolism of HL60 cells that could no longer differentiate into neutrophils. However, more direct evidences from techniques such as Seahorse are required to fully estimate the role of OXPHOS on TEC development.

Taken together, AK2-deficiency enhances ROS production and impairs oxidative phosphorylation. These factors are likely co-responsible of the severe reduction of mTEC in TEC^{AK2KO} mice, but further experiments dissecting the impairment of OXPHOS in AK2-deficient TEC and its contribution to the differentiation process would be important for a better understanding of the relationship between energy balance and TEC differentiation, but also as insight for the development of treatments regarding thymus in RD context or for similar endotypes.

TEC from mutant mice multiply the number of mitochondria as compensatory mechanism to make up the absence of AK2. To probe additional means of compensation, several key-enzymes of metabolic pathways involved in energy metabolism potentially affected by the absence of AK2 were investigated by flow cytometry[138]. Among other pathways, glycolysis in mutant TEC subpopulations is likely enhanced through the increased expression of Hexokinase 1. Absence of AK2 has already been reported to increase glycolysis in HL60 cells after induction of neutrophile differentiation[77] and in myocardial cells of adult

mice[87]. As probable compensatory mechanism for impaired OXPHOS, in addition to higher number of mitochondria, key enzymes of pathways upstream of OXPHOS are increased in mutant mice. Increase of CPT1A in AK2-deficient cTEC and mTEC^{lo} likely enhance fatty-acid oxidation, increase of ASS1 in AK2-deficient mTEC^{lo} and mTEC^{hi} likely enhance fumarate production as intermediate of TCA cycle and increased IDH2 in AK2-deficient cTEC and mTEC likely enhance TCA cycle. Yet, increase of IDH2 could also be linked to the increased ROS production since IDH2 is also involved in antioxidant response[164]. However, reduced contribution of OXPHOS in total ATP production in AK2-deficient cTEC infers that the enhancements of OXPHOS-associated metabolic pathways are not sufficient to compensate the absence of AK2. Development and adaptation of metabolic phenotyping methods, such as Seahorse, are required for in-depth analysis and confirmation of our observations.

TEC^{AK2KO} mice show hypoplastic thymi with a reduction of overall cellularity. Since the bulk of thymic cellularity is composed of DP thymocytes, the reduction of cellularity in TEC^{AK2KO} mice can be attributed to a lower recruitment of lymphoid progenitors and diminished development of thymocytes.

The decreased attraction of progenitors is explained by a lower number of CCL21-expressing TEC and a decreased expression of CCL25, these two chemokines orchestrating the thymic seeding of lymphoid progenitors[47]. The input of other chemokines (e.g. CCL19, CXCL12), not investigated in this work, cannot be excluded.

In addition to the recruitment of progenitors, several steps of maturational progression of thymocytes are also impaired in TEC^{AK2KO} mice. First, signal provided by AK2-deficient cTEC and TEC^{Ly51low} to pass the beta selection checkpoint is less efficient and thymocytes are partially blocked at DN3a stage. Then, the differentiation of DP thymocytes into SP4 or SP8 is partially blocked due to the lower positive selection induced by AK2-deficient cTEC and TEC^{Ly51low}. Because these two processes of selection relying on signal provided by TEC in the cortex, it can be concluded that the quality of interactions between cTEC/TEC^{Ly51low} and thymocytes is diminished in absence of AK2. Since half of energy produced by mammalian cells is consumed by protein synthesis machinery[91,165], it would be plausible that the impairment of energy metabolism caused by the absence of AK2 impacts the synthesis of proteins, notably those involved in TEC:thymocyte interactions. Finally, SP4 and SP8 thymocytes are partially blocked at M1 stage. Since the developmental transition from M1 to M2 is occurring in the medulla, it is likely the disruption of medulla and/or reduction of mTEC that cause this block. However, a reduction in the quality of interactions between mTEC and

thymocytes, similarly to those observed between thymocytes and cTEC/TEC^{Ly51low}, cannot be excluded.

Taken together, these results indicate than the hypoplasia of the thymus is due to a lower attraction of progenitors and a diminished thymopoïetic function. Further experiments are indispensable to identify weakened molecular interactions between thymocyte and AK2-deficient TEC underlying impaired TEC support to thymocyte development.

Furthermore, it is worth noting that while the number of lymphoid progenitors at E16.5 remained the same among TEC^{AK2KO} and TEC^{AK2WT} mice, mutant mice displayed fewer mature thymocytes. This finding indicate that thymic hypoplasia is chronologically first caused by a partial block in thymocyte development. But later on, with the increasing presence of CCL21-expressing mTEC^{lo} in TEC^{AK2WT} mice, a TEC subset almost completely absent in TEC^{AK2KO} mice, the gap of cellularity between knockout and wild-type mice has worsened.

T cell lymphopenia observed in the peripheral tissues of TEC^{AK2KO} mice is the consequence of the decreased thymic production of mature CD4 and CD8 T cells. If a similar decrease of T cell pool would occur in human, RD patients may be more prone to life-threatening infections. Fortunately, it has been reported by Hoenig et al.[68] and Bertand et al.[148] that patients that achieve durable T cell repletion after successful hematopoietic stem cell transplantation show normal T cell counts. The *de novo* generation of immune cells from donors' bone marrow seems to durably prevent patients to develop serious or life-threatening infections. However, the quality of their immune response mounted after exposition to pathogens or after vaccination has not been investigated in details. Further experimental investigations could be conducted in TEC^{AK2KO} mice to assess the quality of the T cell compartment to mount a regular immune response.

Moreover, in the peripheral tissues, TEC^{AK2KO} mice show higher proportion of effector cells in both SP4 and SP8 lineages as well as an increased frequency of activated Tregs. These observations can be explained by the lymphopenic environment in peripheral tissues of TEC^{AK2KO} mice. Indeed, in lymphopenic environment, naïve T cells undergo rapid proliferation and acquire characteristics of effector cells[98] while Treg activation is enhanced[166]. Activated Tregs are endowed with a stronger suppressive function[167] that can prevent the onset or restrain the progression of autoimmune and allergic diseases. This increased frequency of activated Treg is presumably one of the immune mechanisms to prevent the emergence of autoimmune disorders in TEC^{AK2KO} mice despite the reduction of negative selection.

In both cortex and medulla, negative selection is decreased in mutant mice. The defective interactions between thymocytes and TEC, likely responsible of diminished positive selection in TEC^{AK2KO} mice, are also probably accountable for the decreased negative selection taking place in the cortex. Indeed, a reduction of TCR signalling leads to a decrease of both positive and negative selection[28,168]. An additional consequence of the reduction of interactions between thymocytes and TEC is the diminished generation of thymic Tregs since thymic Treg generation results from high intensity interactions between stromal cells and thymocytes[64,169]. It remains to be verified whether the diminution of interactions between thymocytes and TEC may not be caused by the downregulation of cell-cell junctions and cell-extracellular matrix adhesion pathways in AK2-deficient subtypes since proteins of these pathways are directly involved in cell contacts.

Decreased negative selection in the medulla can be attributed to the diminution of mTECs as well as the disruption of medullary architecture. With an impaired negative selection, TEC^{AK2KO} mice eliminate deleterious T cells less efficiently and could have been more prone to autoimmunity. However, TEC^{AK2KO} mice do not show more signs of autoimmunity than their wild-type counterparts: severity of cell infiltration as well as the presence of autoantibodies in the serum remain similar between mutant and control mice.

This last observation might be related to the augmentation of several cell populations refraining the emergence and the development of autoimmune reactions as well as immune mechanisms involved in the prevention of autoimmunity in TEC^{AK2KO} mice. In the thymus of TEC^{AK2KO} mice, medullary fibroblasts are increased and occupy the space left empty by mTEC to serve as self-antigen producers in the induction of immune tolerance[120] as mentioned above. In peripheral tissue of AK2-deficient mice, the proportion of anergic T cells is increased. The induction of anergy serves to decrease the proliferative responsiveness of potentially dangerous self-reactive CD4 T cells and generate progenitor cells that can differentiate into Treg[99], a T cell population preventing autoimmune diseases by maintaining self-tolerance. In addition, the frequency of activated Treg, more repressive, among CD4 T cells of TEC^{AK2KO} mice is increased too. The accumulation of all these cellular changes may explain why TEC^{AK2KO} mice are not more prone to autoimmunity despite the reduction of negative selection.

Analysis of autoimmunity is particularly clinically relevant for patients suffering from Reticular Dysgenesis. Among the cases reported in the literature, Hoening et al.[68] and Henderson et al.[170] reported RD patients with Omenn syndrome, a severe combined immunodeficiency that presents autoimmune and allergic disorders[171]. Besides that, Chou et al. reported a patient with hypomorphic variant in *AK2* which presents autoimmune hemolytic

anemia[70]. Taken as a whole, RD patients presenting additional autoimmune disorders represent a minority among the cases reported (3/40)[5,31,67]. This finding accords with our observation that AK2-deficient mice do not show signs of autoimmunity.

Taken together, the findings presented in this thesis demonstrate the crucial role of AK2 in thymus development and function to support T cell development, and are the first ones that provide insights regarding the role of TEC in Reticular Dysgenesis. Moreover, this work is the first publicly available work where energy metabolism of TEC, a field of research almost unexplored, is investigated that extensively.

Insight gained from this work may therefore advance our efforts to provide new strategies of therapy, not only for Reticular Dysgenesis, but also for other thymic disorders related to deficient energy production in TEC.

7. References

1. Flajnik, M. F. & Kasahara, M. Origin and evolution of the adaptive immune system: genetic events and selective pressures. *Nat. Rev. Genet.* **11**, 47–59 (2010).
2. Shah, J. & Shahidullah, A. Ascaris lumbricoides: A Startling Discovery during Screening Colonoscopy. *Case Rep. Gastroenterol.* **12**, 224–229 (2018).
3. Davies, M. G. & Hagen, P.-O. Systemic inflammatory response syndrome. *Br. J. Surg.* **84**, 920–935 (1997).
4. Ejaz, H. *et al.* COVID-19 and comorbidities: Deleterious impact on infected patients. *J. Infect. Public Health* **13**, 1833–1839 (2020).
5. Uthaisangsook, S., Day, N. K., Bahna, S. L., Good, R. A. & Haraguchi, S. Innate immunity and its role against infections. *Ann. Allergy, Asthma Immunol.* **88**, 253–265 (2002).
6. Dunkelberger, J. R. & Song, W. C. Complement and its role in innate and adaptive immune responses. *Cell Res.* **20**, 34–50 (2010).
7. Bonilla, F. A. & Oettgen, H. C. Adaptive immunity. *J. Allergy Clin. Immunol.* **125**, S33–S40 (2010).
8. Dopfer, E. P. *et al.* The CD3 conformational change in the γδ T cell receptor is not triggered by antigens but can be enforced to enhance tumor killing. *Cell Rep.* **7**, 1704–1715 (2014).
9. Porritt, H. E., Gordon, K. & Petrie, H. T. Kinetics of steady-state differentiation and mapping of intrathymic-signaling environments by stem cell transplantation in nonirradiated mice. *J. Exp. Med.* **198**, 957–962 (2003).
10. Zdrojewicz, Z., Pachura, E. & Pachura, P. The thymus: A forgotten, but very important organ. *Adv. Clin. Exp. Med.* **25**, 369–375 (2016).
11. Irla, M. *et al.* Three-Dimensional Visualization of the Mouse Thymus Organization in Health and Immunodeficiency. *J. Immunol.* **190**, 586–596 (2013).
12. Nitta, T. & Takayanagi, H. Non-Epithelial Thymic Stromal Cells: Unsung Heroes in Thymus Organogenesis and T Cell Development. *Front. Immunol.* **11**, 1–11 (2021).
13. Holländer, G. A. *et al.* Developmental control point in induction of thymic cortex regulated by a subpopulation of prothymocytes. *Nature* **373**, 350–353 (1995).
14. Hikosaka, Y. *et al.* The Cytokine RANKL Produced by Positively Selected Thymocytes Fosters Medullary Thymic Epithelial Cells that Express Autoimmune

Regulator. *Immunity* **29**, 438–450 (2008).

15. Hamazaki, Y., Sekai, M. & Minato, N. Medullary thymic epithelial stem cells: Role in thymic epithelial cell maintenance and thymic involution. *Immunol. Rev.* **271**, 38–55 (2016).
16. Linden, M., Ward, J. M. & Cherian, S. Hematopoietic and Lymphoid Tissues. in *Comparative Anatomy and Histology* 309–338 (Elsevier, 2012). doi:10.1016/B978-0-12-381361-9.00019-6
17. Nitta, T., Ota, A., Iguchi, T., Muro, R. & Takayanagi, H. The fibroblast: An emerging key player in thymic T cell selection. *Immunol. Rev.* **302**, 68–85 (2021).
18. Gordon, J. & Manley, N. R. Mechanisms of thymus organogenesis and morphogenesis. *Development* **138**, 3865–3878 (2011).
19. Masuda, K. *et al.* Thymic Anlage Is Colonized by Progenitors Restricted to T, NK, and Dendritic Cell Lineages. *J. Immunol.* **174**, 2525–2532 (2005).
20. Douagi, I., Andre, I., Ferraz, J. C. & Cumano, A. Characterization of T cell precursor activity in the murine fetal thymus: Evidence for an input of T cell precursors between days 12 and 14 of gestation. *Eur. J. Immunol.* **30**, 2201–2210 (2000).
21. Van Ewijk, W., Holländer, G., Terhorst, C. & Wang, B. Stepwise development of thymic microenvironments in vivo is regulated by thymocyte subsets. *Development* **127**, 1583–1591 (2000).
22. Kernfeld, E. M. *et al.* A Single-Cell Transcriptomic Atlas of Thymus Organogenesis Resolves Cell Types and Developmental Maturation. *Immunity* **48**, 1258-1270.e6 (2018).
23. Akiyama, N. *et al.* Identification of embryonic precursor cells that differentiate into thymic epithelial cells expressing autoimmune regulator. *J. Exp. Med.* **213**, 1441–1458 (2016).
24. Rossi, S. W. *et al.* RANK signals from CD4+3- inducer cells regulate development of Aire-expressing epithelial cells in the thymic medulla. *J. Exp. Med.* **204**, 1267–1272 (2007).
25. Akiyama, T. *et al.* The Tumor Necrosis Factor Family Receptors RANK and CD40 Cooperatively Establish the Thymic Medullary Microenvironment and Self-Tolerance. *Immunity* **29**, 423–437 (2008).
26. Mouri, Y. *et al.* Lymphotoxin Signal Promotes Thymic Organogenesis by Eliciting RANK Expression in the Embryonic Thymic Stroma. *J. Immunol.* **186**, 5047–5057 (2011).

27. Shakib, S. *et al.* Checkpoints in the Development of Thymic Cortical Epithelial Cells. *J. Immunol.* **182**, 130–137 (2009).
28. Kim, S. *et al.* Regulation of positive and negative selection and TCR signaling during thymic T cell development by capicua. *Elife* **10**, 1–25 (2021).
29. Klein, L., Kyewski, B., Allen, P. M. & Hogquist, K. a. Positive and negative selection of the T cell repertoire: what thymocytes see (and don't see). *Nat. Rev. Immunol.* **14**, 377–91 (2014).
30. Kaya, V. The role of Lin28a in thymic epithelial cell development and function. (University of Basel, 2021).
31. Rane, S., Hogan, T., Seddon, B. & Yates, A. J. Age is not just a number: Naive T cells increase their ability to persist in the circulation over time. *PLoS Biol.* **16**, 1–20 (2018).
32. Dhalla, F. *et al.* Biologically indeterminate yet ordered promiscuous gene expression in single medullary thymic epithelial cells. *EMBO J.* **39**, 1–18 (2020).
33. Baran-Gale, J. *et al.* Ageing compromises mouse thymus function and remodels epithelial cell differentiation. *Elife* **9**, 1–71 (2020).
34. Anderson, M. S. *et al.* Projection of an immunological self shadow within the thymus by the aire protein. *Science (80-.).* **298**, 1395–1401 (2002).
35. Org, T. *et al.* The autoimmune regulator PHD finger binds to non-methylated histone H3K4 to activate gene expression. *EMBO Rep.* **9**, 370–376 (2008).
36. Chuprin, A. *et al.* The deacetylase Sirt1 is an essential regulator of Aire-mediated induction of central immunological tolerance. *Nat. Immunol.* **16**, 737–745 (2015).
37. Daley, S. R., Hu, D. Y. & Goodnow, C. C. Helios marks strongly autoreactive CD4 + T cells in two major waves of thymic deletion distinguished by induction of PD-1 or NF-κB . *J. Exp. Med.* **210**, 269–285 (2013).
38. Sawicka, M. *et al.* From pre-DP, post-DP, SP4, and SP8 thymocyte cell counts to a dynamical model of cortical and medullary selection. *Front. Immunol.* **5**, 1–14 (2014).
39. Abramson, J. & Anderson, G. Thymic Epithelial Cells. *Annu. Rev. Immunol.* **35**, 85–118 (2017).
40. Mayer, C. E. *et al.* Dynamic spatio-temporal contribution of single β5t+ cortical epithelial precursors to the thymus medulla. *Eur. J. Immunol.* **46**, 846–856 (2016).
41. Baik, S., Jenkinson, E. J., Lane, P. J. L., Anderson, G. & Jenkinson, W. E. Generation of both cortical and Aire+ medullary thymic epithelial compartments from CD205+ progenitors. *Eur. J. Immunol.* **43**, 589–594 (2013).
42. Ohigashi, I. *et al.* Aire-expressing thymic medullary epithelial cells originate from β5t-

expressing progenitor cells. *Proc. Natl. Acad. Sci. U. S. A.* **110**, 9885–9890 (2013).

43. Wagner, D. E. & Klein, A. M. Lineage tracing meets single-cell omics: opportunities and challenges. *Nat. Rev. Genet.* **21**, 410–427 (2020).
44. Nusser, A. *et al.* Developmental dynamics of two bipotent thymic epithelial progenitor types. *Nature* **606**, 165–171 (2022).
45. Kawakami, N. *et al.* Roles of integrins and CD44 on the adhesion and migration of fetal liver cells to the fetal thymus. *J. Immunol.* **163**, (1999).
46. Holländer, G. *et al.* Cellular and molecular events during early thymus development. *Immunol. Rev.* **209**, 28–46 (2006).
47. Liu, C. *et al.* Coordination between CCR7- and CCR9-mediated chemokine signals in prevascular fetal thymus colonization. *Blood* **108**, 2531–2539 (2006).
48. Krueger, A., Willenzon, S., Łyszkiewicz, M., Kremmer, E. & Förster, R. CC chemokine receptor 7 and 9 double-deficient hematopoietic progenitors are severely impaired in seeding the adult thymus. *Blood* **115**, 1906–1912 (2010).
49. Liu, C. *et al.* The role of CCL21 in recruitment of T-precursor cells to fetal thymi. *Blood* **105**, 31–39 (2005).
50. Taghon, T., Yui, M. A., Pant, R., Diamond, R. A. & Rothenberg, E. V. Developmental and molecular characterization of emerging β- and γδ-selected pre-T cells in the adult mouse thymus. *Immunity* **24**, 53–64 (2006).
51. Kelly, A. P. *et al.* Notch-induced T cell development requires phosphoinositide-dependent kinase 1. *EMBO J.* **26**, 3441–3450 (2007).
52. Radtke, F., MacDonald, H. R. & Tacchini-Cottier, F. Regulation of innate and adaptive immunity by Notch. *Nat. Rev. Immunol.* **13**, 427–437 (2013).
53. Ostmeyer, J., Cowell, L., Greenberg, B. & Christley, S. Reconstituting T cell receptor selection in-silico. *Genes Immun.* **22**, 187–193 (2021).
54. McDonald, B. D., Bunker, J. J., Erickson, S. A., Oh-Hora, M. & Bendelac, A. Crossreactive αβ T Cell Receptors Are the Predominant Targets of Thymocyte Negative Selection. *Immunity* **43**, 859–869 (2015).
55. Ohashi, P. S. Negative selection and autoimmunity. *Curr. Opin. Immunol.* **15**, 668–676 (2003).
56. Yamashita, I., Nagata, T., Tada, T. & Nakayama, T. CD69 cell surface expression identifies developing thymocytes which audition for T cell antigen receptor-mediated positive selection. *Int. Immunol.* **5**, 1139–1150 (1993).
57. Barthlott, T., Kohler, H. & Eichmann, K. Asynchronous coreceptor downregulation

after positive thymic selection: Prolonged maintenance of the double positive state in CD8 lineage differentiation due to sustained biosynthesis of the CD4 coreceptor. *J. Exp. Med.* **185**, 357–362 (1997).

58. Singer, A., Adoro, S. & Park, J. H. Lineage fate and intense debate: Myths, models and mechanisms of CD4- versus CD8-lineage choice. *Nat. Rev. Immunol.* **8**, 788–801 (2008).
59. Xing, Y., Wang, X., Jameson, S. C. & Hogquist, K. A. Late stages of T cell maturation in the thymus involve NF-κB and tonic type i interferon signaling. *Nat. Immunol.* **17**, 565–573 (2016).
60. Kurd, N. & Robey, E. A. T-cell selection in the thymus: A spatial and temporal perspective. *Immunol. Rev.* **271**, 114–126 (2016).
61. Lancaster, J. N. *et al.* Live-cell imaging reveals the relative contributions of antigen-presenting cell subsets to thymic central tolerance. *Nat. Commun.* **10**, (2019).
62. Hadeiba, H. *et al.* Plasmacytoid Dendritic Cells Transport Peripheral Antigens to the Thymus to Promote Central Tolerance. *Immunity* **36**, 438–450 (2012).
63. Yamano, T. *et al.* Thymic B Cells Are Licensed to Present Self Antigens for Central T Cell Tolerance Induction. *Immunity* **42**, 1048–1061 (2015).
64. Lee, H. M., Bautista, J. L. & Hsieh, C. S. *Thymic and Peripheral Differentiation of Regulatory T Cells*. *Advances in Immunology* **112**, (Elsevier Inc., 2011).
65. Hoenig, M., Pannicke, U., Gaspar, H. B. & Schwarz, K. Recent advances in understanding the pathogenesis and management of reticular dysgenesis. *Br. J. Haematol.* **180**, 644–653 (2018).
66. Oshima, K. *et al.* Human AK2 links intracellular bioenergetic redistribution to the fate of hematopoietic progenitors. *Biochem. Biophys. Res. Commun.* **497**, 719–725 (2018).
67. Pannicke, U. *et al.* Reticular dysgenesis (aleukocytosis) is caused by mutations in the gene encoding mitochondrial adenylate kinase 2. *Nat. Genet.* **41**, 101–105 (2009).
68. Hoenig, M. *et al.* Reticular dysgenesis: International survey on clinical presentation, transplantation, and outcome. *Blood* **129**, 2928–2938 (2017).
69. Santagata, S., Villa, A., Sobacchi, C., Cortes, P. & Vezzoni, P. The genetic and biochemical basis of Omenn syndrome. *Immunol. Rev.* **178**, 64–74 (2000).
70. Chou, J., Alazami, A. M., Jaber, F., Hoyos-bachiloglu, R. & Jones, J. Hypomorphic variants in AK2 reveal the contribution of mitochondrial function to B-cell activation. *J. Allergy Clin. Immunol.* **146**, 192–202 (2020).
71. Lagresle-Peyrou, C. *et al.* Human adenylate kinase 2 deficiency causes a profound

hematopoietic defect associated with sensorineural deafness. *Nat. Genet.* **41**, 106–11 (2009).

72. Seifert, O. *et al.* Identification of unique gene expression patterns within different lesional sites of keloids. *Wound Repair Regen.* **16**, 254–265 (2008).
73. Noma, T. Dynamics of nucleotide metabolism as a supporter of life phenomena. *J. Med. Invest.* **52**, 127–136 (2005).
74. Rigoulet, M. *et al.* Cell energy metabolism: An update. *Biochim. Biophys. Acta - Bioenerg.* **1861**, (2020).
75. Hüttemann, M. *et al.* Regulation of mitochondrial respiration and apoptosis through cell signaling: Cytochrome c oxidase and cytochrome c in ischemia/reperfusion injury and inflammation. *Biochim. Biophys. Acta - Bioenerg.* **1817**, 598–609 (2012).
76. Lancaster, G., Suprunenko, Y. F., Jenkins, K. & Stefanovska, A. Modelling chronotaxicity of cellular energy metabolism to facilitate the identification of altered metabolic states. *Sci. Rep.* **6**, 1–12 (2016).
77. Six, E. *et al.* AK2 deficiency compromises the mitochondrial energy metabolism required for differentiation of human neutrophil and lymphoid lineages. *Cell Death Dis.* **6**, (2015).
78. Burkart, A., Shi, X., Chouinard, M. & Corvera, S. Adenylate kinase 2 links mitochondrial energy metabolism to the induction of the unfolded protein response. *J. Biol. Chem.* **286**, 4081–4089 (2011).
79. Villa, H. *et al.* Molecular and functional characterization of adenylate kinase 2 gene from Leishmania donovani. *Eur. J. Biochem.* **270**, 4339–4347 (2003).
80. Lee, H. J. *et al.* AK2 activates a novel apoptotic pathway through formation of a complex with FADD and caspase-10. *Nat. Cell Biol.* **9**, 1303–1310 (2007).
81. Kim, H. *et al.* The DUSP26 phosphatase activator adenylate kinase 2 regulates FADD phosphorylation and cell growth. *Nat. Commun.* **5**, 1–11 (2014).
82. Fujisawa, K., Murakami, R., Horiguchi, T. & Noma, T. Adenylate kinase isozyme 2 is essential for growth and development of Drosophila melanogaster. *Comp. Biochem. Physiol. - B Biochem. Mol. Biol.* **153**, 29–38 (2009).
83. Chen, R. P. *et al.* Adenylate kinase 2 (AK2) promotes cell proliferation in insect development. *BMC Mol. Biol.* **13**, 1 (2012).
84. Rissone, A. *et al.* Reticular dysgenesis–associated AK2 protects hematopoietic stem and progenitor cell development from oxidative stress. *J. Exp. Med.* **212**, 1185–1202 (2015).

85. Rissone, A. *et al. A model for reticular dysgenesis shows impaired sensory organ development and hair cell regeneration linked to cellular stress*. *DMM Disease Models and Mechanisms* **12**, (2019).
86. Ghaloul-Gonzalez, L. *et al.* Reticular Dysgenesis and Mitochondriopathy Induced by Adenylate Kinase 2 Deficiency with Atypical Presentation. *Sci. Rep.* **9**, 1–8 (2019).
87. Zhang, S. *et al.* Adenylate kinase AK2 isoform integral in embryo and adult heart homeostasis. *Biochem. Biophys. Res. Commun.* **546**, 59–64 (2021).
88. Waldmann, R. Dissertation: Investigations on the Molecular Biology of Human Adenylate Kinase 2 Deficiency (Reticular Dysgenesis) and the Establishment and Characterisation of an Adenylate Kinase 2-deficient Mouse Model. (Ulm University, 2017).
89. Zuklys, S. *et al.* Stabilized ß-Catenin in Thymic Epithelial Cells Blocks Thymus Development and Function. *J. Immunol.* **182**, 2997–3007 (2009).
90. Abdelmageed, M. E., El-Awady, M. S. & Suddek, G. M. Apocynin ameliorates endotoxin-induced acute lung injury in rats. *Int. Immunopharmacol.* **30**, 163–170 (2016).
91. Argüello, R. J. *et al.* SCENITH: A Flow Cytometry-Based Method to Functionally Profile Energy Metabolism with Single-Cell Resolution. *Cell Metab.* **32**, 1063-1075.e7 (2020).
92. Porritt, H. E. *et al.* Heterogeneity among DN1 prothymocytes reveals multiple progenitors with different capacities to generate T cell and non-T cell lineages. *Immunity* **20**, 735–745 (2004).
93. Tai, X. *et al.* Foxp3 Transcription Factor Is Proapoptotic and Lethal to Developing Regulatory T Cells unless Counterbalanced by Cytokine Survival Signals. *Immunity* **38**, 1116–1128 (2013).
94. Kirberg, J., Bosco, N., Deloulme, J.-C., Ceredig, R. & Agenès, F. Peripheral T Lymphocytes Recirculating Back into the Thymus Can Mediate Thymocyte Positive Selection. *J. Immunol.* **181**, 1207–1214 (2008).
95. Hale, J. S. & Fink, P. J. Back to the thymus: peripheral T cells come home. *Immunol. Cell Biol.* **87**, 58–64 (2009).
96. Cowan, J. E., McCarthy, N. I. & Anderson, G. CCR7 Controls Thymus Recirculation, but Not Production and Emigration, of Foxp3+ T Cells. *Cell Rep.* **14**, 1041–1048 (2016).
97. Thiault, N. *et al.* Peripheral regulatory T lymphocytes recirculating to the thymus

suppress the development of their precursors. *Nat. Immunol.* **16**, 628–634 (2015).

98. Surh, C. D. & Sprent, J. Homeostasis of Naive and Memory T Cells. *Immunity* **29**, 848–862 (2008).
99. Kalekar, L. A. *et al.* CD4+ T cell anergy prevents autoimmunity and generates regulatory T cell precursors. *Nat. Immunol.* **17**, 304–314 (2016).
100. Hayashi, Y., Utsuyama, M., Kurashima, C. & Hirokawa, K. Spontaneous development of organ-specific autoimmune lesions in aged C57BL/6 mice. *Clin. Exp. Immunol.* **78**, 120–6 (1989).
101. Takahama, Y., Ohigashi, I., Baik, S. & Anderson, G. Generation of diversity in thymic epithelial cells. *Nat. Rev. Immunol.* (2017). doi:10.1038/nri.2017.12
102. Lepletier, A. *et al.* Interplay between Follistatin, Activin A, and BMP4 Signaling Regulates Postnatal Thymic Epithelial Progenitor Cell Differentiation during Aging. *Cell Rep.* **27**, 3887-3901.e4 (2019).
103. Wong, K. *et al.* Multilineage potential and self-renewal define an epithelial progenitor cell population in the adult thymus. *Cell Rep.* **8**, 1198–1209 (2014).
104. Walker, L. S. Folate receptor 4: a new handle on regulation and memory? *Immunol. Cell Biol.* **85**, 506–507 (2007).
105. Ito, K. & Suda, T. Metabolic requirements for the maintenance of self-renewing stem cells. *Nat. Rev. Mol. Cell Biol.* **15**, 243–256 (2014).
106. Žuklys, S. *et al.* Foxn1 regulates key target genes essential for T cell development in postnatal thymic epithelial cells. *Nat. Immunol.* **17**, 1206–1215 (2016).
107. Rode, I. *et al.* Foxn1 Protein Expression in the Developing, Aging, and Regenerating Thymus. *J. Immunol.* **195**, 5678–5687 (2015).
108. Duchen, M. R. Mitochondria in health and disease: Perspectives on a new mitochondrial biology. *Mol. Aspects Med.* **25**, 365–451 (2004).
109. Liesa, M. & Shirihai, O. S. Mitochondrial dynamics in the regulation of nutrient utilization and energy expenditure. *Cell Metab.* **17**, 491–506 (2013).
110. Sun, N., Youle, R. J. & Finkel, T. The Mitochondrial Basis of Aging. *Mol. Cell* **61**, 654–666 (2016).
111. Liang, L. *et al.* Meta-analysis of EMT datasets reveals different types of EMT. *PLoS One* **11**, 1–22 (2016).
112. Gordon, J., Patel, S. R., Mishina, Y. & Manley, N. R. Evidence for an early role for BMP4 signaling in thymus and parathyroid morphogenesis. *Dev. Biol.* **339**, 141–154 (2010).

113. Zuklys, S. *et al.* MicroRNAs Control the Maintenance of Thymic Epithelia and Their Competence for T Lineage Commitment and Thymocyte Selection. *J. Immunol.* **189**, 3894–3904 (2012).
114. Žalac, T. The Role of the Transcription Factor Sox9 for Thymic Epithelial Cell Differentiation and Function. (University of Basel, 2011).
115. Emre, Y. *et al.* Thymic epithelial cell expansion through matricellular protein CYR61 boosts progenitor homing and T-cell output. *Nat. Commun.* **4**, 1–11 (2013).
116. Lamouille, S., Xu, J. & Derynck, R. Molecular mechanisms of epithelial–mesenchymal transition. *Nat. Rev. Mol. Cell Biol.* **15**, 178–196 (2014).
117. Espinosa Neira, R. & Salazar, E. P. Native type IV collagen induces an epithelial to mesenchymal transition-like process in mammary epithelial cells MCF10A. *Int. J. Biochem. Cell Biol.* **44**, 2194–2203 (2012).
118. Wu, X. *et al.* USP3 promotes gastric cancer progression and metastasis by deubiquitination-dependent COL9A3/COL6A5 stabilisation. *Cell Death Dis.* **13**, (2022).
119. Shin, S. *et al.* CD200 Induces Epithelial-to-Mesenchymal Transition in Head and Neck Squamous Cell Carcinoma via β-Catenin-Mediated Nuclear Translocation. *Cancers (Basel).* **11**, 1583 (2019).
120. Nitta, T. *et al.* Fibroblasts as a source of self-antigens for central immune tolerance. *Nat. Immunol.* **21**, 1172–1180 (2020).
121. Sun, L. *et al.* FSP1+ fibroblast subpopulation is essential for the maintenance and regeneration of medullary thymic epithelial cells. *Sci. Rep.* **5**, 1–16 (2015).
122. Attwell, D., Mishra, A., Hall, C. N., O'Farrell, F. M. & Dalkara, T. What is a pericyte? *J. Cereb. Blood Flow Metab.* **36**, 451–455 (2016).
123. Zachariah, M. A. & Cyster, J. G. Neural crest-derived pericytes promote egress of mature thymocytes at the corticomedullary junction. *Science (80-.).* **328**, 1129–1135 (2010).
124. Acton, S. E., Onder, L., Novkovic, M., Martinez, V. G. & Ludewig, B. Communication, construction, and fluid control: lymphoid organ fibroblastic reticular cell and conduit networks. *Trends Immunol.* **42**, 782–794 (2021).
125. Textor, J., Mandl, J. N. & de Boer, R. J. The Reticular Cell Network: A Robust Backbone for Immune Responses. *PLoS Biol.* **14**, 1–6 (2016).
126. Krüger-Genge, A., Blocki, A., Franke, R. P. & Jung, F. Vascular endothelial cell biology: An update. *Int. J. Mol. Sci.* **20**, (2019).

127. Cottet-Rousselle, C., Ronot, X., Leverve, X. & Mayol, J. F. Cytometric assessment of mitochondria using fluorescent probes. *Cytom. Part A* **79 A**, 405–425 (2011).
128. Cossarizza, A. *et al.* Guidelines for the use of flow cytometry and cell sorting in immunological studies (second edition). *Eur. J. Immunol.* **49**, 1457–1973 (2019).
129. Perelman, A. *et al.* JC-1: Alternative excitation wavelengths facilitate mitochondrial membrane potential cytometry. *Cell Death Dis.* **3**, 1–7 (2012).
130. García-Aguilar, A. & Cuezva, J. M. A review of the inhibition of the mitochondrial ATP synthase by IF1 in vivo: Reprogramming energy metabolism and inducing mitohormesis. *Front. Physiol.* **9**, 1–10 (2018).
131. Liesa, M. & Shirihai, O. S. Mitochondrial Dynamics in the Regulation of Nutrient Utilization and Energy Expenditure. *Cell Metab.* **17**, 491–506 (2013).
132. Chen, Y., Liu, K., Shi, Y. & Shao, C. The tango of ROS and p53 in tissue stem cells. *Cell Death Differ.* **25**, 637–639 (2018).
133. Quiros, P. M., Goyal, A., Jha, P. & Auwerx, J. Analysis of mtDNA/nDNA Ratio in Mice. *Curr. Protoc. Mouse Biol.* **7**, 47–54 (2017).
134. Nirwane, A. & Majumdar, A. Understanding mitochondrial biogenesis through energy sensing pathways and its translation in cardio-metabolic health. *Arch. Physiol. Biochem.* **124**, 194–206 (2018).
135. Kozhukhar, N. & Alexeyev, M. F. Mitochondrion Limited predictive value of TFAM in mitochondrial biogenesis. *Mitochondrion* **49**, 156–165 (2019).
136. Hardie, D. G., Ross, F. A. & Hawley, S. A. AMPK: A nutrient and energy sensor that maintains energy homeostasis. *Nat. Rev. Mol. Cell Biol.* **13**, 251–262 (2012).
137. Aviner, R. The science of puromycin: From studies of ribosome function to applications in biotechnology. *Comput. Struct. Biotechnol. J.* **18**, 1074–1083 (2020).
138. Ahl, P. J. *et al.* Met-Flow, a stra tegy for single-cell metabolic analysis highlights dynamic changes in immune subpopulations. *Commun. Biol.* **3**, (2020).
139. Martínez-Reyes, I. & Chandel, N. S. Mitochondrial TCA cycle metabolites control physiology and disease. *Nat. Commun.* **11**, 1–11 (2020).
140. Flick, F. & Lüscher, B. Regulation of sirtuin function by posttranslational modifications. *Front. Pharmacol.* **3 FEB**, 1–13 (2012).
141. Ivanov, V., Merkenschlager, M. & Ceredig, R. Antioxidant treatment of thymic organ cultures decreases NF-kappa B and TCF1(alpha) transcription factor activities and inhibits alpha beta T cell development. *J. Immunol.* **151**, 4694–4704 (1993).
142. Anderson, G. *et al.* Mechanisms of Thymus Medulla Development and Function. in

Current Topics in Microbiology and Immunology **351**, 19–47 (2013).

143. Lancaster, J. N., Li, Y. & Ehrlich, L. I. R. Chemokine-Mediated Choreography of Thymocyte Development and Selection. *Trends Immunol.* **39**, 86–98 (2018).
144. Goldfarb, Y. *et al.* HDAC3 Is a Master Regulator of mTEC Development. *Cell Rep.* **15**, 651–665 (2016).
145. Turrens, J. F. Mitochondrial formation of reactive oxygen species. *J. Physiol.* **552**, 335–344 (2003).
146. Bosticardo, M. *et al.* Artificial thymic organoids represent a reliable tool to study T-cell differentiation in patients with severe T-cell lymphopenia. *Blood Adv.* **4**, 2611–2616 (2020).
147. Poliani, P. L. *et al.* Early defects in human T-cell development severely affect distribution and maturation of thymic stromal cells: Possible implications for the pathophysiology of Omenn syndrome. *Blood* **114**, 105–108 (2009).
148. Bertrand, Y. *et al.* Reticular dysgenesis: HLA non-identical bone marrow transplants in a series of 10 patients. *Bone Marrow Transplant.* **29**, 759–762 (2002).
149. Derbinski, J., Schulte, A., Kyewski, B. & Klein, L. Promiscuous gene expression in medullary thymic epithelial cells mirrors the peripheral self. *J. Immunol.* **196**, 2915–2922 (2016).
150. Perry, J. S. A. *et al.* Distinct Contributions of Aire and Antigen-Presenting-Cell Subsets to the Generation of Self-Tolerance in the Thymus. *Immunity* **41**, 414–426 (2014).
151. Shafritz, A. B. *et al.* Overexpression of an Osteogenic Morphogen in Fibrodysplasia Ossificans Progressiva. *N. Engl. J. Med.* **335**, 555–561 (1996).
152. Ohnemus, S. *et al.* Aortic arch and pharyngeal phenotype in the absence of BMP-dependent neural crest in the mouse. *Mech. Dev.* **119**, 127–135 (2002).
153. Bleul, C. C. & Boehm, T. BMP Signaling Is Required for Normal Thymus Development. *J. Immunol.* **175**, 5213–5221 (2005).
154. Montero-Herradón, S. & Zapata, A. G. Delayed maturation of thymic epithelium in mice with specific deletion of β-catenin gene in FoxN1 positive cells. *Histochem. Cell Biol.* **156**, 315–332 (2021).
155. Miragaia, R. J. *et al.* Single-cell RNA-sequencing resolves self-antigen expression during mTEC development. *Sci. Rep.* **8**, 1–13 (2018).
156. Suda, T., Takubo, K. & Semenza, G. L. Metabolic regulation of hematopoietic stem cells in the hypoxic niche. *Cell Stem Cell* **9**, 298–310 (2011).

157. Parrott, D. M. V. & De Sousa, M. A. B. The Persistence of Donor-Derived Cells in Thymus Grafts, Lymph Nodes and Spleens of Recipient Mice. (1967).
158. Tan, J., Wang, Y., Zhang, N. & Zhu, X. Induction of epithelial to mesenchymal transition (EMT) and inhibition on adipogenesis: Two different sides of the same coin? Feasible roles and mechanisms of transforming growth factor β1 (TGF-β1) in age-related thymic involution. *Cell Biol. Int.* **40**, 842–846 (2016).
159. Blackburn, C. C. *et al.* The nu gene acts cell-autonomously and is required for differentiation of thymic epithelial progenitors. *Proc. Natl. Acad. Sci. U. S. A.* **93**, 5742–5746 (1996).
160. Nowell, C. S. *et al.* Foxn1 regulates lineage progression in cortical and medullary thymic epithelial cells but is dispensable for medullary sublineage divergence. *PLoS Genet.* **7**, (2011).
161. Dzeja, P. & Terzic, A. Adenylate kinase and AMP signaling networks: metabolic monitoring, signal communication and body energy sensing. *Int. J. Mol. Sci.* **10**, 1729–1772 (2009).
162. Graves, J. A. *et al.* Mitochondrial structure, function and dynamics are temporally controlled by c-Myc. *PLoS One* **7**, (2012).
163. van der Windt, G. J. W., Chang, C. & Pearce, E. L. Measuring Bioenergetics in T Cells Using a Seahorse Extracellular Flux Analyzer. *Curr. Protoc. Immunol.* **113**, 139–148 (2016).
164. Ku, H. J. & Park, J. W. Downregulation of IDH2 exacerbates H2O2-mediated cell death and hypertrophy. *Redox Rep.* **22**, 35–41 (2017).
165. Buttgereit, F. & Brand, M. D. A hierarchy of ATP-consuming processes in mammalian cells. *Biochem. J.* **312**, 163–167 (1995).
166. Kornete, M., Sgouroudis, E. & Piccirillo, C. A. ICOS-Dependent Homeostasis and Function of Foxp3 + Regulatory T Cells in Islets of Nonobese Diabetic Mice . *J. Immunol.* **188**, 1064–1074 (2012).
167. Li, D. Y. & Xiong, X. Z. ICOS+ Tregs: A Functional Subset of Tregs in Immune Diseases. *Front. Immunol.* **11**, (2020).
168. Delaney, J. R., Sykulev, Y., Eisen, H. N. & Tonegawa, S. Differences in the level of expression of class I major histocompatibility complex proteins on thymic epithelial and dendritic cells influence the decision of immature thymocytes between positive and negative selection. *Proc. Natl. Acad. Sci. U. S. A.* **95**, 5235–5240 (1998).
169. Sakaguchi, S., Yamaguchi, T., Nomura, T. & Ono, M. Regulatory T Cells and Immune

Tolerance. *Cell* **133**, 775–787 (2008).

170. Henderson, L. A. *et al.* First reported case of Omenn syndrome in a patient with reticular dysgenesis. *J. Allergy Clin. Immunol.* **131**, 1227–1230 (2013).

171. Villa, A., Notarangelo, L. D. & Roifman, C. M. Omenn syndrome: Inflammation in leaky severe combined immunodeficiency. *J. Allergy Clin. Immunol.* **122**, 1082–1086 (2008).